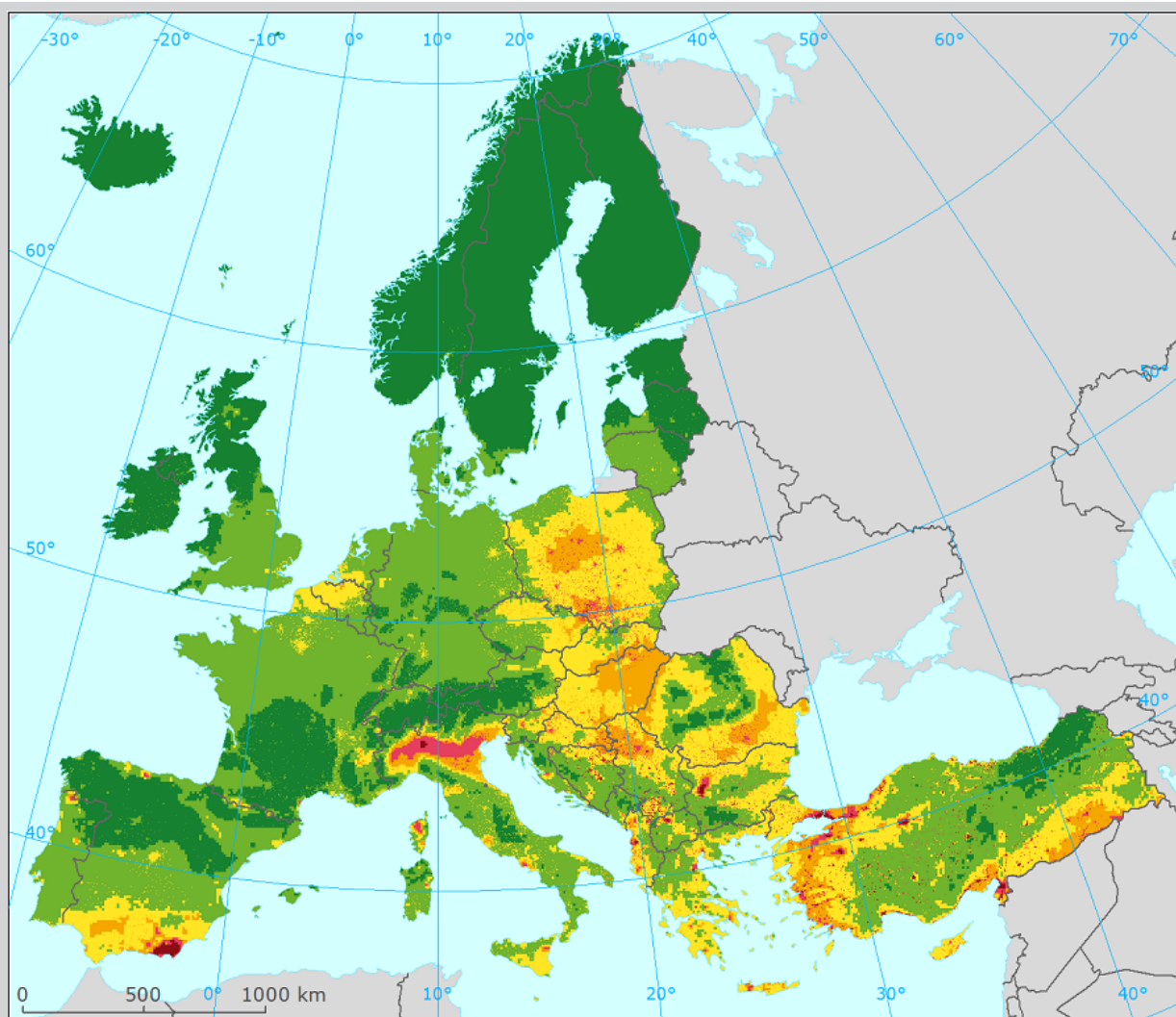


# European air quality maps for 2016

PM<sub>10</sub>, PM<sub>2.5</sub>, Ozone, NO<sub>2</sub> and NO<sub>x</sub>  
spatial estimates and their uncertainties

April 2019



Authors:

Jan Horálek, Markéta Schreiberová, Frank de Leeuw,  
Pavel Kurfürst, Peter de Smet, Jana Schovánková

ETC/ACM consortium partners: National Institute for Public Health and the Environment (RIVM), Aether, Czech Hydrometeorological Institute (CHMI), Institute of Environmental Assessment and Water Research (CSIC/IDAEA), EMISIA, Institut National de l'Environnement Industriel et des Risques (INERIS), Norwegian Institute for Air Research (NILU), Öko-Institute, Öko-Recherche, Netherlands Environmental Assessment Agency (PBL), Universitat Autònoma de Barcelona (UAB), Umweltbundesamt Wien (UBA-V), Vlaamse Instelling voor Technologisch Onderzoek (VITO), 4sfera Innova

European Environment Agency  
European Topic Centre on Air Pollution and  
Climate Change Mitigation



**Cover photo** – Concentration map of  $PM_{10}$  indicator 90.4 percentile of daily means for the year 2016. Spatially interpolated concentration field. Units:  $\mu g \cdot m^{-3}$ . (Map 2.2 of this paper.)

#### **Legal notice**

The contents of this publication do not necessarily reflect the official opinions of the European Commission or other institutions of the European Union. Neither the European Environment Agency, the European Topic Centre on Air Pollution and Climate Change Mitigation nor any person or company acting on behalf of the Agency or the Topic Centre is responsible for the use that may be made of the information contained in this report.

#### **Copyright notice**

© European Topic Centre on Air Pollution and Climate Change Mitigation (2018)  
Reproduction is authorized provided the source is acknowledged.

More information on the European Union is available on the Internet (<http://europa.eu>).

#### **Authors**

Jan Horálek, Markéta Schreiberová, Pavel Kurfürst, Jana Schováňková: Czech Hydrometeorological Institute (CHMI, CZ)  
Peter de Smet, Frank de Leeuw: National Institute for Public Health and the Environment (RIVM, NL)

European Topic Centre on Air Pollution  
and Climate Change Mitigation  
PO Box 1  
3720 BA Bilthoven  
The Netherlands  
Tel.: +31 30 274 8562  
Fax: +31 30 274 4433  
Web: <http://acm.eionet.europa.eu>  
Email: [etcacm@rivm.nl](mailto:etcacm@rivm.nl)

## Contents

Executive summary .....	5
1 Introduction.....	9
2 PM <sub>10</sub> .....	11
2.1 PM <sub>10</sub> annual average .....	11
2.1.1 Concentration map.....	11
2.1.1 Population exposure.....	12
2.2 PM <sub>10</sub> – 90.4 percentile of daily means .....	14
2.2.1 Concentration map.....	15
2.2.2 Population exposure.....	15
3 PM <sub>2.5</sub> .....	19
3.1 PM <sub>2.5</sub> annual average.....	19
3.1.1 Concentration map.....	19
3.2.2 Population exposure.....	20
4 Ozone.....	23
4.1 Ozone – 93.2 percentile of maximum daily 8-hour means .....	23
4.1.1 Concentration map.....	23
4.1.2 Population exposure.....	24
4.2 Ozone – SOMO35 .....	26
4.2.1 Concentration map.....	27
4.2.2 Population exposure.....	27
4.3 Ozone – AOT40 vegetation and AOT40 forests.....	29
4.3.1 Concentration maps .....	30
4.3.2 Vegetation exposure .....	32
5 NO <sub>2</sub> and NO <sub>x</sub> .....	35
5.1 NO <sub>2</sub> – Annual mean .....	35
5.1.1 Concentration maps .....	35
5.1.2 Population exposure.....	36
5.2 NO <sub>x</sub> – Annual mean .....	38
5.2.1 Concentration maps .....	38
6 Exposure trend estimates.....	41
6.1 Mapping and exposure results.....	41
6.1.1 Human health PM <sub>10</sub> indicators .....	41
6.2.1 Human health PM <sub>2.5</sub> indicator .....	42
6.3.1 Human health ozone indicators .....	43
6.4.1 Vegetation and forest ozone indicators .....	44
6.5.1 Human health NO <sub>2</sub> indicators.....	45

References .....	47
Annex 1 – Methodology .....	51
A1.1 Mapping method .....	51
A1.2 Calculation of population and vegetation exposure .....	53
A1.3 Methods for uncertainty analysis.....	55
Annex 2 – Input data .....	59
A2.1 Air quality monitoring data .....	59
A2.2 EMEP MSC-W model output .....	61
A3.3 Other supplementary data .....	62
Annex 3 – Technical details and mapping uncertainties.....	65
A3.1 PM <sub>10</sub> .....	65
A3.2 PM <sub>2.5</sub> .....	70
A3.3 Ozone .....	74
A3.4 NO <sub>2</sub> and NO <sub>x</sub> .....	80
Annex 4 – Inter-annual changes.....	83
A4.1 PM <sub>10</sub> .....	83
A4.2 PM <sub>2.5</sub> .....	87
A4.3 Ozone .....	90
A4.4 NO <sub>2</sub> and NO <sub>x</sub> .....	98
Annex 5 – Concentration maps including station points .....	101



## Executive summary

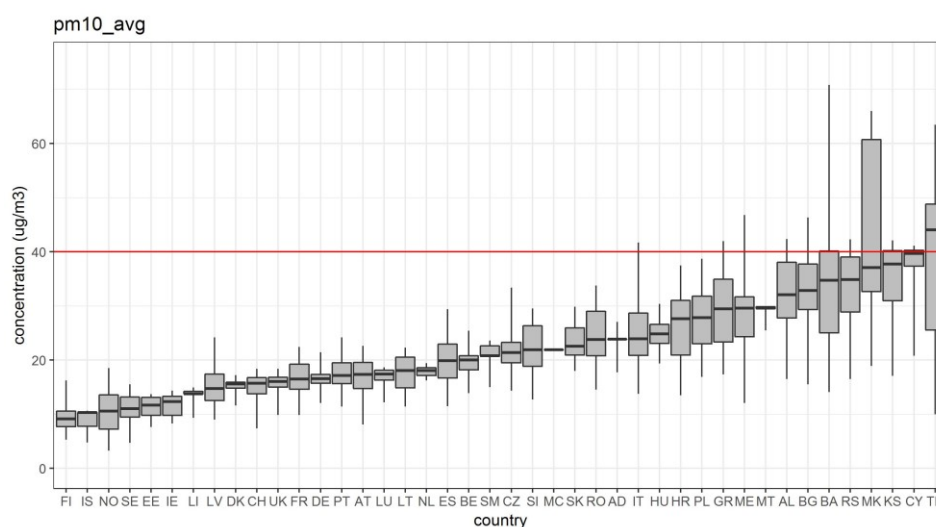
European air quality concentrations maps have been prepared for the year 2016. The maps are based on air quality data as reported under the air quality directive by EEA member and cooperating countries. Concentration maps have been produced to assess the situation with respect to the most stringent air quality limit values and indicators most relevant for the assessment of impacts on human health and vegetation.

The mapping method follows the methodology developed earlier (Horálek et al, 2018a, 2018b, and reference cited therein); it combines the monitoring data with supplementary data (such as the results from a chemical dispersion model, land cover, meteorological and geographical data). The method ('residual kriging') is a linear regression model followed by kriging of the residuals produced from that model. This methodology has been applied systematically during the past 12 years, which enables the evaluation of changes in exposure over time.

### Population exposure

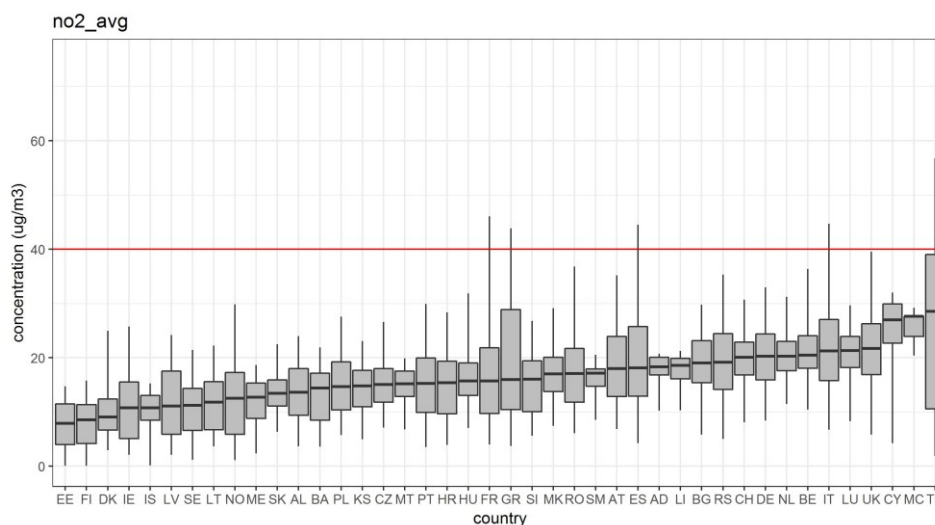
Concentrations of particulate matter continued to exceed the EU and WHO standards in large parts of Europe. 5.4% of the European population is exposed to levels above the EU  $PM_{2.5}$  limit value of  $25 \mu g \cdot m^{-3}$ ; 75.4% of the European population is exposed to levels above the WHO  $PM_{2.5}$  Air Quality Guideline of  $10 \mu g \cdot m^{-3}$  (Table 3.1). Table 2.2 shows that in 9 (eastern European) countries more than 50% of the population is exposed to concentrations above the  $PM_{10}$  daily limit value. Figure ES.1 shows that the countries with the highest values of  $PM_{10}$  annual average are located in the eastern parts of Europe as well. The concentrations of  $PM_{2.5}$  and  $PM_{10}$  are often highly correlated, the highest  $PM_{2.5}$  exposures are also found in the eastern parts.

*Figure ES.1  $PM_{10}$  concentrations to which the population per country was exposed in 2016, in relation to the annual limit value ( $40 \mu g \cdot m^{-3}$ ). The box plots show for each country, the concentration to which 2, 25, 75 and 98% of the population was exposed. The marker corresponds to the concentration to which 50% of the population was exposed.*



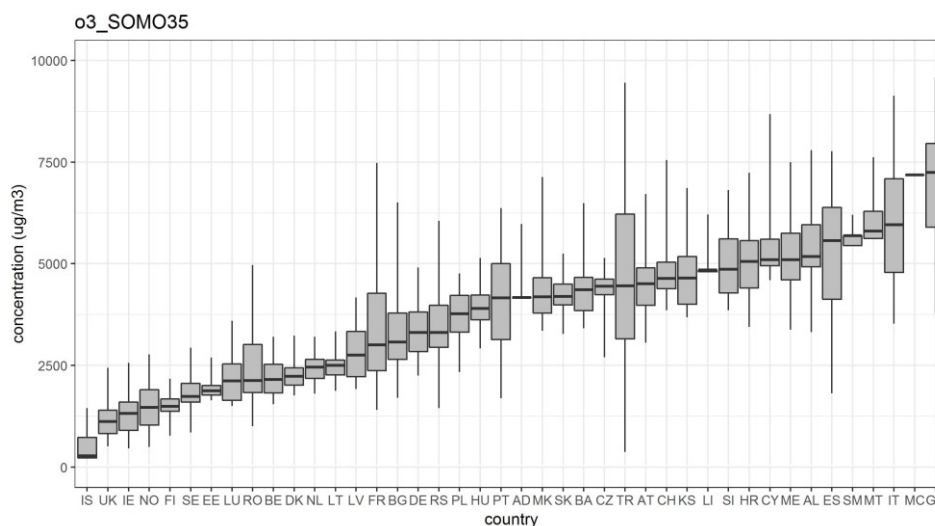
The  $NO_2$  annual mean concentration map shows a different spatial distribution than the PM maps. Table 5.1 indicates that in 21 countries a limited fraction of the population (5.2% in total) is exposed to concentrations above the annual limit value of  $40 \mu g \cdot m^{-3}$ . Figure ES.2 shows that in all countries, the majority of population lives well below the limit value. High exposures are observed in the larger conurbations (e.g. greater London, the Benelux-Ruhr area, Po valley, Naples, Paris, Madrid, and Istanbul).

*Figure ES.2 NO<sub>2</sub> concentrations to which the population per country was exposed in 2016, in relation to the annual limit value (40 µg·m<sup>-3</sup>). The box plots show for each country, the concentration to which 2, 25, 75 and 98% of the population was exposed. The marker corresponds to the concentration to which 50% of the population was exposed.*



Exposure to ozone concentrations above the EU target value (a maximum daily 8-hour average value of 120 µg·m<sup>-3</sup> not to be exceeded on more than 25 days per year) occurs in large parts of southern Europe. 8.5 % of the Europeans live in areas where the ozone TV is exceeded (Table 4.1). Figure ES.3 shows that the countries with the highest values of SOMO35 are located in the southern parts of Europe.

*Figure ES.3 Ozone concentrations to which the population per country was exposed in relation to the indicator SOMO35 in 2016. The box plots show for each country, the concentration to which 2, 25, 75 and 98% of the population was exposed. The marker corresponds to the concentration to which 50% of the population was exposed.*



## Accumulated risks

Although the spatial distributions of PM, NO<sub>2</sub> and ozone concentrations differ widely, the possibility of an accumulation of risk resulting from high exposures to all three pollutants cannot be excluded. Combining the maps of the three most frequently exceeded standards (PM<sub>10</sub> daily limit value, NO<sub>2</sub> annual limit value and ozone target value) shows that out of the total population of 538 million in the model area<sup>1</sup> 3.3% (17.9

<sup>1</sup> Turkey has not been included in these calculations.

million) lives in areas where 2 or 3 air quality standards are exceeded; 2.5 million people live in areas where all three standards are exceeded. The worst situation is observed in Greece: 5.4% of the population lives in areas where all three standards are exceeded; followed by Italy (in particular the Po valley): 3.3% (2.0 million inhabitants) live in areas where the three standards are breached.

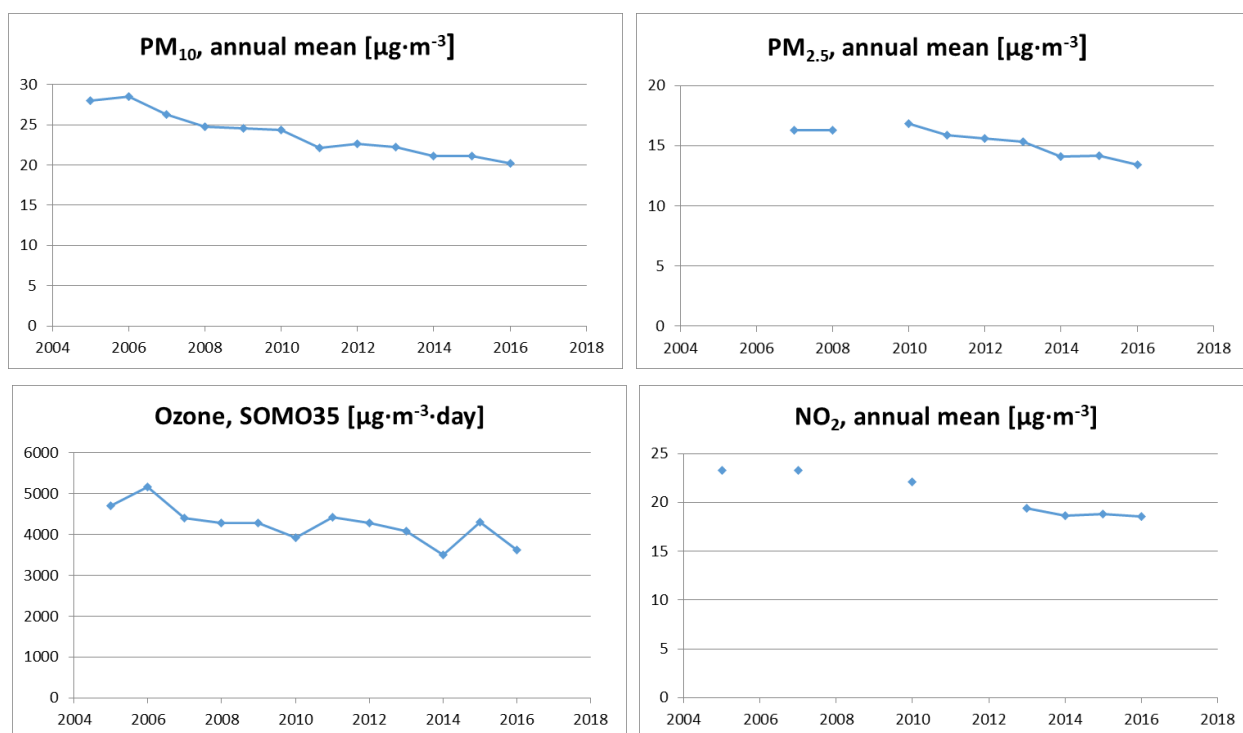
## Vegetation exposure

Standards for the protection of vegetation have been set, among others, for  $\text{NO}_x$  and ozone. In a limited number of cases, the  $\text{NO}_x$  critical level has been exceeded, though this is relevant only if there is vegetation in those areas. A larger impact on vegetation can be expected from the direct exposure to ozone. The target value for the protection of vegetation (AOT40) is exceeded in about 19% of the agricultural areas. The long-term objective is exceeded in 77% of the agricultural areas.

## Changes over time

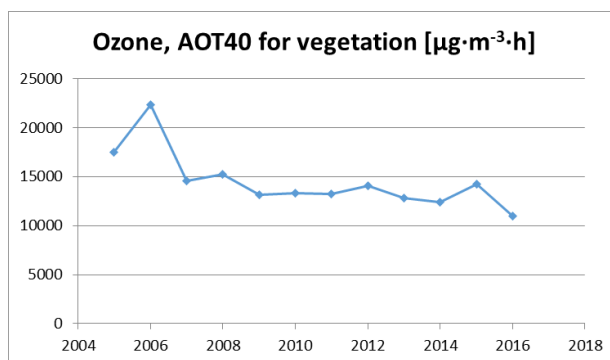
Since 2005 (resp. since 2007 in the case of  $\text{PM}_{2.5}$ ), the maps have been prepared in a consistent way. This enables an analysis of changes in exposure over time. The PM concentrations show a steady decrease of about  $0.7 \mu\text{g}\cdot\text{m}^{-3}$  per year ( $\text{PM}_{10}$  annual average) resp.  $0.4 \mu\text{g}\cdot\text{m}^{-3}$  per year ( $\text{PM}_{2.5}$  annual average). For the ozone concentration (expressed as SOMO35) a small decreasing trend is observed, in spite of the year-to-year variability. For changes in population-weighted concentrations, see Figure ES.4. The population-weighted concentration is calculated for the area of all countries considered in the report, except Turkey, for the comparability reasons, because the area of Turkey has not been mapped until 2016.

Figure ES.4 Changes in population-weighted concentrations of  $\text{PM}_{10}$  (annual mean),  $\text{PM}_{2.5}$  (annual mean), ozone (SOMO35), and  $\text{NO}_2$  (annual mean).



The agricultural-weighted concentration tends to decrease by about  $450 \mu\text{g}\cdot\text{m}^{-3}\cdot\text{h}$  per year over the period 2005–2016. For changes in agricultural-weighted concentrations, see Figure ES.5. Again, the agricultural-weighted concentration is calculated for the area of all countries considered in the report, except Turkey.

Figure ES.5 *Changes in agricultural-weighted concentrations of ozone indicator AOT40 for vegetation.*



# 1 Introduction

This paper provides an update of European air quality concentration maps, population exposure and vegetation exposure estimates and probabilities of exceeding relevant thresholds for 2016. The analysis is based on interpolation of annual statistics of monitoring data from 2016, reported by EEA member and cooperating countries by 2017. The paper presents mapping results and includes an uncertainty analysis of the interpolated maps, adopting the latest methodological developments, see Horálek et al. (2018a, 2018b) and reference cited therein. The mapping area covers all EEA and cooperating countries, i.e. whole Europe apart from Belarus, Moldova, Ukraine and the European parts of Russia and Kazakhstan. For the first time, Turkey is included in the mapping area for all pollutants except PM<sub>2.5</sub>, due to the availability of the measurement data from Turkish stations for 2016 in the AQ e-reporting database (EEA, 2018a).

We consider in this paper PM<sub>10</sub>, PM<sub>2.5</sub>, ozone, NO<sub>2</sub> and NO<sub>x</sub> for 2016, being the most relevant pollutants for annual updating due to their potential impacts on health or ecosystems. The analysis method applied is similar to that of previous years. Another potentially relevant pollutant, benzo[a]pyrene (BaP), is not presented, as the station coverage is not dense enough for enabling the regular mapping. The current status of mapping the BaP concentrations in Europe was discussed by Guerreiro et al. (2016) and Horálek et al. (2017a).

The mapping method is based primarily on air quality measurements. It combines monitoring data, chemical transport model results and other supplementary data (such as altitude and meteorology). The method is a linear regression model followed by kriging of the residuals produced from that model ('residual kriging'). It should be noted that the applied methodology does not allow for formal compliance checking with limit or target values in line with the air quality directive.

The maps of health related indicators of PM<sub>10</sub>, PM<sub>2.5</sub>, and ozone are created for the rural and urban (including suburban) background areas separately on a grid at 10x10 km resolution. Subsequently, the rural and urban background maps are merged into one final combined air quality indicator map using a 1x1 km population density grid, following a weighting criterion applied per grid cell. This fine resolution takes into account the smaller urbanisations in the European context that are not resolved at the 10x10 km grid resolution. The map of health related indicator of NO<sub>2</sub> is constructed by improved methodology developed in Horálek et al. (2017c): next to the rural and urban background map layers, the urban traffic map layer is constructed and incorporated into the final merged map using the road data; all separate map layers are created just at 1x1 km resolution; land cover and road data are included in the mapping process as supplementary data. The maps of ozone and NO<sub>x</sub> vegetation-related indicators are at a grid resolution of 2x2 km and based on rural background measurements; in the case of ozone they serve as input to the EEA's core set indicator CSI005 (EEA, 2018d).

Next to the annual indicator maps, we present in tables the population exposure to PM<sub>10</sub>, PM<sub>2.5</sub>, ozone, and NO<sub>2</sub>, and the exposure of vegetation to ozone. Tables of population exposure are prepared using the final combined maps and the population density map of 1x1 km grid resolution. For NO<sub>2</sub>, the population exposure in each grid cell is calculated separately for urban areas directly influenced by traffic and for the background (both rural and urban) areas, in order to better reflect the population exposed to traffic emissions. The tables of the vegetation exposure are prepared with a 2x2 km grid resolution based on the Corine Land Cover 2012.

Chapters 2, 3, 4 and 5 present the concentration maps and exposure estimates for PM<sub>10</sub>, PM<sub>2.5</sub>, ozone and NO<sub>2</sub>, respectively. Chapter 5 presents the concentration map for NO<sub>x</sub>; exceedances of the critical level for the protection of vegetation occur in very limited areas and, as such, it is considered not to provide

relevant information from the European scale perspective. Chapter 6 summarizes the trends in exposure estimates in the period 2005 – 2016 (2007 – 2016 for PM<sub>2.5</sub>).

Annex 1 describes briefly the different methodological aspects. Annex 2 documents the input data applied in the 2016 mapping and exposure analysis. Annex 3 presents the technical details of the maps and their uncertainty analysis including the cross-validation results and the maps of probability of exceedance of limit/target values. Annex 4 shows the inter-annual changes including the inter-annual difference maps between 2015 and 2016 and the variations in population exposure in the period 2005 – 2016 for PM<sub>10</sub> and ozone, resp. 2007 – 2016 for PM<sub>2.5</sub> and 2013 – 2016 for NO<sub>2</sub>. Annex 5 presents the concentration maps including the station points, in order to provide more complete information of the air quality in 2016 across Europe.

## 2 PM<sub>10</sub>

The Ambient Air Quality Directive (EU, 2008) sets limit values for long-term and for short-term PM<sub>10</sub> concentrations. The long-term annual PM<sub>10</sub> limit value is set at 40  $\mu\text{g}\cdot\text{m}^{-3}$ . The short-term limit value is that the daily average PM<sub>10</sub> concentration should not exceed 50  $\mu\text{g}\cdot\text{m}^{-3}$  during more than 35 days per year. This daily limit value is most frequently exceeded in Europe. It corresponds to the 90.4 percentile of daily PM<sub>10</sub> concentrations in one year. The Air Quality Guideline recommended by the World Health Organization (WHO, 2005) for the PM<sub>10</sub> annual average is 20  $\mu\text{g}\cdot\text{m}^{-3}$ .

This chapter presents the 2016 updates of the two PM<sub>10</sub> indicators: annual average and the 90.4 percentile of the daily averages. The latter is a more relevant indicator in the context of the AQ Directive (EU, 2008) than the formerly used 36<sup>th</sup> highest daily mean (Horálek et al., 2016b). The separate rural and urban background concentration maps are calculated on the 10x10 km resolution grid and the subsequent final combined concentration map is based on the 1x1 km gridded population density map. All maps here are presented in this 1x1 km grid resolution. The population exposure tables are calculated based on these maps in this resolution.

### 2.1 PM<sub>10</sub> annual average

#### 2.1.1 Concentration map

Map 2.1 presents the final combined concentration map for the 2016 PM<sub>10</sub> annual average as the result of interpolation and merging of the separate maps as described in Annex 1 (for a more detailed description see Horálek et al., 2007, and De Smet et al 2011). Red and purple areas indicate exceedances of the limit value (LV) of 40  $\mu\text{g}\cdot\text{m}^{-3}$ .

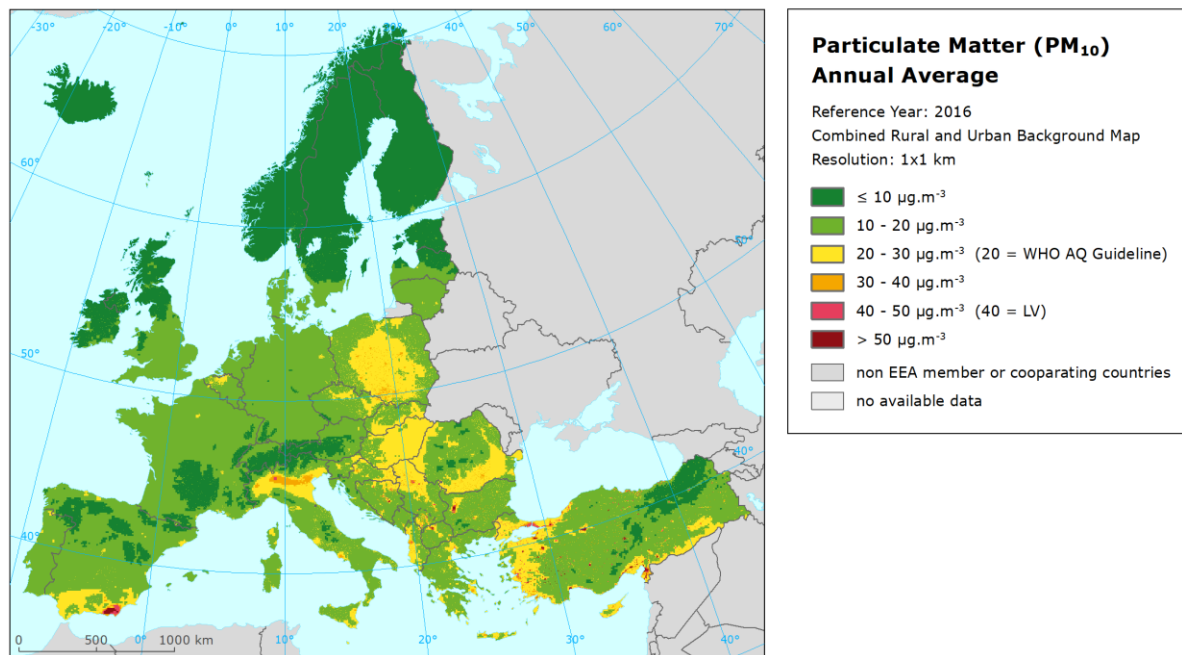
The most relevant linear regression submodel for the use of the PM<sub>10</sub> mapping has been identified earlier in Horálek et al. (2008) and De Smet et al. (2009, 2010, and 2011). Supplementary data used in the linear regression for rural areas consisted of EMEP model output, altitude, wind speed and surface solar radiation and for urban background areas it was EMEP model output only (Annex 3, Section A3.1). The linear regression and ordinary kriging on its residuals is applied on the logarithmically transformed data of both measurement and modelled PM<sub>10</sub> values.

The final combined concentration map presented in Map 2.1 is presented on a 1x1 km grid resolution (Annex 1). The station points are not presented in the map, in order to better visualise the urban areas. However, concentration values from measurements at the station points used in the kriging interpolation methodology (Annex 3) are considered to provide relevant information. In Map A5.1 of Annex 5 these point values are presented on top of Map 2.1 and illustrate the smoothing effect the interpolation methodology can have on the gridded concentration fields.

Map 2.1 shows LV exceedances in southern Spain near Almeria, in northern Italy near Milan, in some urban areas of Bulgaria with high concentrations at Sofia, in urban areas of North Macedonia, Serbia and Turkey. The extent of the exceeded area near Almeria is larger in 2016 compared to 2015. Overall, there are slight improvements in the central and eastern Europe, in the Po Valley and in southern France, slight increases in Bosnia, south Italy and Greece, and rather similar patterns in western, south-western, and northern Europe (Annex 4). Concerning the estimated exceedances in the Almeria area, it should be noted that they are based on the chemical transport modelling, not on measurements.

The uncertainty of the concentration map can be expressed in relative terms of the absolute Root Mean Square Error (RMSE) uncertainty related to the mean air pollution indicator value for all stations (see Annex 1). This *relative mean uncertainty* (RRMSE) of the final combined map of PM<sub>10</sub> annual average is 19.4 % for rural areas and 20.0 % for urban areas without Turkish stations (i.e. quite similar to the last years), resp. 22.7 % for rural areas and 30.6 % for urban areas including Turkish stations (Annex 3). The main reason for presenting the results without Turkish stations is to enable the comparison with previous years.

Map 2.1 Concentration map of PM<sub>10</sub> annual average, 2016



### 2.1.1 Population exposure

Table 2.1 gives the population frequency distribution for a limited number of exposure classes, as well as the population-weighted concentration for individual countries and for Europe as a whole according to Equation A1.7. Annex 4 shows details on the twelve years evolution of population exposure.

About 44 % of the European population and 38 % of the EU-28 population has been exposed to annual average concentrations above the Air Quality Guideline of 20 µg.m<sup>-3</sup> recommended by the World Health Organization (WHO, 2005). CSI004 (EEA, 2018c) estimates that about 42 % of the population in urban agglomerations in the EU-28 was exposed in 2016 to levels above the WHO guideline. The latter estimate accounts for the urban population of the EU-28. It therefore represents areas where, in general, somewhat higher PM<sub>10</sub> concentrations occur. The estimates in Table 2.1 account for the total European and EU-28 population, *including* the population in rural areas, smaller cities and villages that are in general exposed to lower levels of PM<sub>10</sub>. Next to this, it should be mentioned that CSI004 refers to the population in cities for which PM<sub>10</sub> data is available.



Table 2.1 Population exposure and population-weighted concentration, PM<sub>10</sub> annual average, 2016

Country		Population [inhbs . 1000]	PM <sub>10</sub> annual average, exposed population [%]						Population weighted conc. [µg.m <sup>-3</sup> ]
			< LV				> LV		
			< 10 µg.m <sup>-3</sup>	10 - 20 µg.m <sup>-3</sup>	20 - 30 µg.m <sup>-3</sup>	30 - 40 µg.m <sup>-3</sup>	40 - 45 µg.m <sup>-3</sup>	> 45 µg.m <sup>-3</sup>	
Albania	AL	2 876		7.2	32.3	54.8	5.1	0.6	31.6
Andorra	AD	72	0.2	1.6	98.2				23.8
Austria	AT	8 700	5.1	74.2	20.7				16.7
Belgium	BE	11 311		50.3	49.7				19.7
Bosnia & Herzegovina	BA	3 516		13.6	22.8	36.9	16.0	10.8	35.1
Bulgaria	BG	7 154	0.0	9.7	22.7	48.3	17.4	1.8	33.2
Croatia	HR	4 191	0.1	16.7	47.2	36.0	0.0	0.0	26.3
Cyprus	CY	1 184		1.0	15.6	56.3	27.2		36.6
Czechia	CZ	10 554	0.1	29.6	63.7	6.6			21.9
Denmark	DK	5 707	0.2	99.8					15.1
Estonia	EE	1 316	26.9	73.1					11.2
Finland	FI	5 487	66.8	33.2					9.4
France (metropolitan)	FR	64 561	2.2	79.7	18.1	0.0			16.8
Germany	DE	82 176	0.3	94.8	4.9				16.5
Greece	GR	10 784		8.0	42.7	42.0	6.6	0.7	29.3
Hungary	HU	9 830		3.5	94.2	2.2			24.7
Iceland	IS	333	47.1	52.9					9.1
Ireland	IE	4 726	27.7	72.3					11.7
Italy	IT	60 666	0.3	18.7	60.2	17.4	3.4		25.2
Latvia	LV	1 969	7.4	73.9	18.7				15.8
Liechtenstein	LI	38	1.8	98.2					13.7
Lithuania	LT	2 889		68.9	31.1				17.6
Luxembourg	LU	576		100					16.9
Malta	MT	450			100				29.5
Monaco	MC	38			100				21.9
Montenegro	ME	622		19.2	33.5	44.1	3.1		27.0
Netherlands	NL	16 979		99.4	0.6				17.9
North Macedonia	MK	2 071		2.4	11.1	47.4	12.1	26.9	42.4
Norway	NO	5 211	45.0	55.0					10.5
Poland	PL	37 967		9.9	53.7	36.4			27.6
Portugal (excl. Az., Mad.)	PT	9 839	0.5	81.8	17.7				17.5
Romania	RO	19 760	0.0	19.2	58.1	22.6			24.7
San Marino	SM	33		15.9	84.1				21.0
Serbia (incl. Kosovo*)	RS	8 848		6.2	21.9	49.8	22.2	0.0	33.8
Slovakia	SK	5 426		13.8	84.3	1.9			23.4
Slovenia	SI	2 064	0.0	32.4	67.6				22.3
Spain (excl. Canarias)	ES	44 305	0.6	49.8	48.0	0.9	0.6	0.1	20.2
Sweden	SE	9 851	28.7	71.3					11.1
Switzerland	CH	8 327	6.9	92.5	0.6				15.0
Turkey	TR	78 741	2.0	16.7	9.9	11.5	36.7	23.2	39.6
United Kingdom (& dep.)	UK	65 383	2.3	97.6	0.0				15.5
Total		616 531	2.7	52.9	26.2	9.5	5.6	3.0	22.5
			55.7				8.6		
Total without Turkey		537 790	2.8	57.9	28.4	9.3	1.4	0.2	20.2
			60.7				1.7		
EU-28		505 806	2.4	59.2	29.3	8.1	0.9	0.1	19.9
			61.6				1.0		
Kosovo*	KS	1 772		6.3	17.3	49.4	27.0	0.0	34.7
Serbia (excl. Kosovo*)	RS	7 076		6.1	23.0	49.9	21.0		33.5

(\*) under the UN Security Council Resolution 1244/99

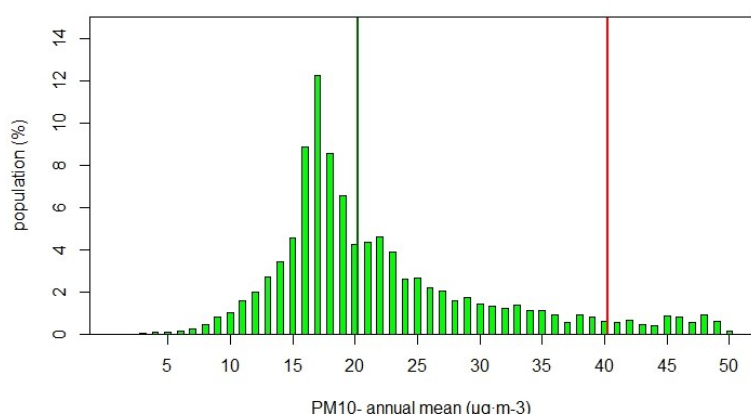
Note: The percentage value "0.0" indicates that an exposed population exists, but it is small and estimated lesser than 0.05 %. Empty cells mean no population in exposure.

The population exposure exceeding the EU annual limit value (ALV) of  $40 \mu\text{g}\cdot\text{m}^{-3}$  is about 9 % for the population of the total of European area (including Turkey) considered and about 1 % for the population of the EU-28. In Bosnia & Herzegovina, Serbia including Kosovo<sup>2</sup>, Bulgaria, North Macedonia, Cyprus and Turkey more than 10 % of the population is exposed to concentrations above the ALV. A limited fraction of the population (0.5 – 7.5 %) is exposed to concentrations above the ALV in Albania, Greece, Italy, Montenegro, and Spain. However, as the current mapping methodology tends to underestimate high values (see Annex 3, Section A3.1), the exceedance percentage will most likely be underestimated. Additional exceedances could therefore be expected in countries like Albania or Cyprus where a relatively large fraction of the population lives in areas with concentration levels above  $30 \mu\text{g}\cdot\text{m}^{-3}$ .

The European-wide population-weighted concentration of the annual average for 2016 is estimated to be about  $23 \mu\text{g}\cdot\text{m}^{-3}$  including Turkey, and  $20 \mu\text{g}\cdot\text{m}^{-3}$  without Turkey, and for the EU-28 only. This is the lowest level of the twelve years period 2005 – 2016 (Tables 6.1 and A4.1).

Figure 2.1 shows, for the whole mapped area, the population frequency distribution for exposure classes of  $1 \mu\text{g}\cdot\text{m}^{-3}$ . One can see the highest population frequency for classes between 16 and 20  $\mu\text{g}\cdot\text{m}^{-3}$ . And continuous decline of population frequency for classes between 20 and 40  $\mu\text{g}\cdot\text{m}^{-3}$ .

Figure 2.1 Population frequency distribution,  $\text{PM}_{10}$  annual average, 2016



## 2.2 $\text{PM}_{10}$ – 90.4 percentile of daily means

The AQ Directive (EU, 2008) describes the  $\text{PM}_{10}$  daily limit value (DLV) as “daily average  $50 \mu\text{g}\cdot\text{m}^{-3}$  not to be exceeded more than 35 times a calendar year”. This requirement can be evaluated by the indicator 36<sup>th</sup> highest daily mean, which is in principle equivalent to the indicator 90.4 percentile of daily means. However, for measurement data these two indicators are equivalent only if no data is missing, which is in general not the case. As shown in de Leeuw (2012), the additional uncertainty related to incomplete time series is substantially smaller when using percentile values instead of the x-th highest value. Furthermore, the AQ Directive requires the use of the 90.4 percentile when random measurements are used to assess the requirements of the  $\text{PM}_{10}$  DLV. As in the previous reports with 2014 and 2015 maps, we express the  $\text{PM}_{10}$  daily means as the 90.4 percentile instead of the formerly used 36<sup>th</sup> highest daily mean.

<sup>2</sup> In this paper, references to Kosovo shall be understood to be in the context of UN Security Council Resolution 1244/99.

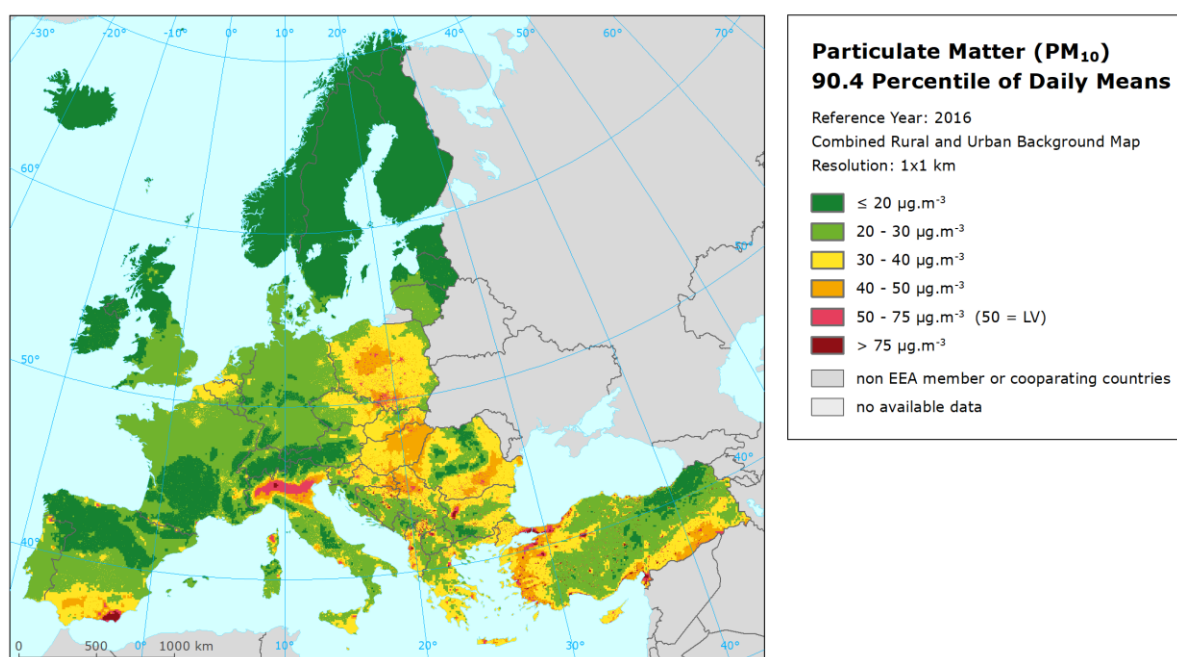
### 2.2.1 Concentration map

Map 2.2 presents the final combined map, where red and purple marked areas indicate exceedances of the DLV of  $50 \mu\text{g}\cdot\text{m}^{-3}$  on more than 35 measurement days. The similar mapping procedure as in the case of the annual average is used. The mapping details and the uncertainty analysis are presented in Annex 3. Large areas above the DLV are observed in northern Italy (i.e. the Po Valley) with elevated values in the region around Milan, in the region with the agglomerations Ostrava – Katowice - Krakow, the Almeria region in Spain, western parts of Turkey. Urban areas with concentrations above the DLV are observed in Poland, southern and eastern Romania, Bulgaria, Turkey, Croatia, Slovenia, Bosnia & Herzegovina, Greece, Albania, North Macedonia, and Serbia including Kosovo. In general, the central and the eastern parts of Europe appear with higher concentrations than the western and the northern parts. As for the  $\text{PM}_{10}$  annual averages, the estimated exceedances in the Almeria area are based on the chemical transport modelling, not on measurements.

The relative mean uncertainty (relative RMSE) of the final combined map of the 90.4 percentile of  $\text{PM}_{10}$  daily means is 22.3 % for rural areas and 24.2 % for urban areas without Turkish stations, resp. 26.5 % for rural areas and 34.2 % for urban areas including Turkish stations (Annex 3).

The final combined map *including* the indicator 90.4 percentile of daily means based on the actual measurement data at station points is presented in Map A5.2 of Annex 5.

Map 2.2 Concentration map of  $\text{PM}_{10}$  indicator 90.4 percentile of daily means, 2016



### 2.2.2 Population exposure

Table 2.2 gives the population frequency distribution for a limited number of exposure classes calculated at 1x1 km grid resolution, as well as the population-weighted concentration for individual countries and for Europe as a whole. Annex 4 shows details on the twelve years evolution of population exposure.

Table 2.2 Population exposure and population-weighted concentrations, PM<sub>10</sub> indicator 90.4 percentile of daily means, 2016

Country		Population  [inhbs . 1000]	PM <sub>10</sub> , 90.4 percentile of daily means, exposed population [%]						Pop. weighted conc. [µg.m <sup>-3</sup> ]
			< LV				> LV		
			< 20 µg.m <sup>-3</sup>	20 - 30 µg.m <sup>-3</sup>	30 - 40 µg.m <sup>-3</sup>	40 - 50 µg.m <sup>-3</sup>	50 - 75 µg.m <sup>-3</sup>	> 75 µg.m <sup>-3</sup>	
Albania	AL	2 876	0.0	3.0	10.8	10.4	49.7	26.1	62.2
Andorra	AD	72	0.1	0.1	2.1	88.0	9.7		47.2
Austria	AT	8 700	6.8	39.0	50.0	4.1	0.0		30.1
Belgium	BE	11 311	0.2	7.8	83.7	8.3			34.4
Bosnia & Herzegovina	BA	3 516	0.1	7.0	10.7	7.7	16.8	57.7	81.2
Bulgaria	BG	7 154	0.2	3.5	8.4	8.4	55.3	24.1	63.4
Croatia	HR	4 191	0.3	6.8	19.9	11.9	55.1	6.0	54.3
Cyprus	CY	1 184			11.8	7.0	81.3		54.0
Czechia	CZ	10 554	0.2	9.4	60.1	21.9	8.4		38.9
Denmark	DK	5 707	2.4	96.9	0.7				24.7
Estonia	EE	1 316	45.1	54.9					19.7
Finland	FI	5 487	85.5	14.5					16.1
France (metropolitan)	FR	64 561	5.7	50.5	43.6	0.2	0.1		28.9
Germany	DE	82 176	0.9	83.6	15.4	0.1			27.9
Greece	GR	10 784		1.7	19.1	32.4	38.7	8.2	51.7
Hungary	HU	9 830		0.0	14.5	72.3	13.2		46.0
Iceland	IS	333	98.7	1.3					16.8
Ireland	IE	4 726	35.4	64.6					21.4
Italy	IT	60 666	0.4	9.6	38.6	23.2	24.3	3.9	44.4
Latvia	LV	1 969	17.3	58.8	23.9				27.2
Liechtenstein	LI	38	4.1	95.9					25.8
Lithuania	LT	2 889	2.9	38.0	59.0				30.1
Luxembourg	LU	576	0.0	82.9	17.1				28.1
Malta	MT	450			2.5	97			44.7
Monaco	MC	38			100				36.3
Montenegro	ME	622	0.9	12.6	8.6	11.0	59.3	7.6	54.9
Netherlands	NL	16 979		55.2	44.8				29.7
North Macedonia	MK	2 071	0.0	1.3	2.0	1.6	29.0	66.1	93.0
Norway	NO	5 211	53.5	40.0	6.5				19.3
Poland	PL	37 967	0.0	2.7	24.0	25.7	46.3	1.3	49.5
Portugal (excl. Az., Mad.)	PT	9 839	2.6	62.4	34.3	0.6	0.1		28.6
Romania	RO	19 760	0.4	6.8	32.3	33.0	27.4		43.9
San Marino	SM	33		4.5	63.4	32			39.2
Serbia (incl. Kosovo*)	RS	8 848	0.0	3.1	6.9	8.8	47.4	33.8	66.3
Slovakia	SK	5 426	0.0	0.8	50.2	25.9	23.0		43.3
Slovenia	SI	2 064	0.1	10.1	34.6	24.1	31.2		43.4
Spain (excl. Canarias)	ES	44 305	3.0	37.0	45.9	12.4	1.0	0.7	32.8
Sweden	SE	9 851	45.2	54.8	0.0				19.6
Switzerland	CH	8 327	8.6	59.3	31.5	0.6			27.4
Turkey	TR	78 741	1.5	10.2	8.4	6.2	14.9	58.8	73.9
United Kingdom (& dep.)	UK	65 383	9.0	80.7	10.3				27.1
Total		616 531	4.8	38.0	26.1	9.9	11.9	9.3	40.2
			78.8				21.2		
Total without Turkey		537 790	5.3	41.8	28.5	10.4	11.5	2.5	35.7
			86.0				14.0		
EU-28		505 806	4.9	42.9	29.5	10.8	10.8	1.2	34.7
			88.0				12.0		
Kosovo*	KS	1 772	0.0	2.3	8.0	6.0	15.7	68.0	73.9
Serbia (excl. Kosovo*)	RS	7 076	0.0	3.3	6.7	9.5	55.1	25.4	64.4

(\*) under the UN Security Council Resolution 1244/99

Note: The percentage value "0.0" indicates that an exposed population exists, but it is small and estimated lesser than 0.05 %. Empty cells mean no population in exposure.

It has been estimated that in 2016 about 21 % of the European population lived in areas where the 90.4 percentile of the PM<sub>10</sub> daily means exceeded the EU limit value of 50 µg·m<sup>-3</sup>. In Albania, Bosnia & Herzegovina, Bulgaria, Croatia, Cyprus, Montenegro, North Macedonia, Serbia (including Kosovo) and Turkey more than half of the population was exposed to concentrations exceeding the DLV. In Greece, Italy, Poland, Romania and Slovenia the portion of the population living in areas with concentrations above the DLV was between 25 and 50 percent.

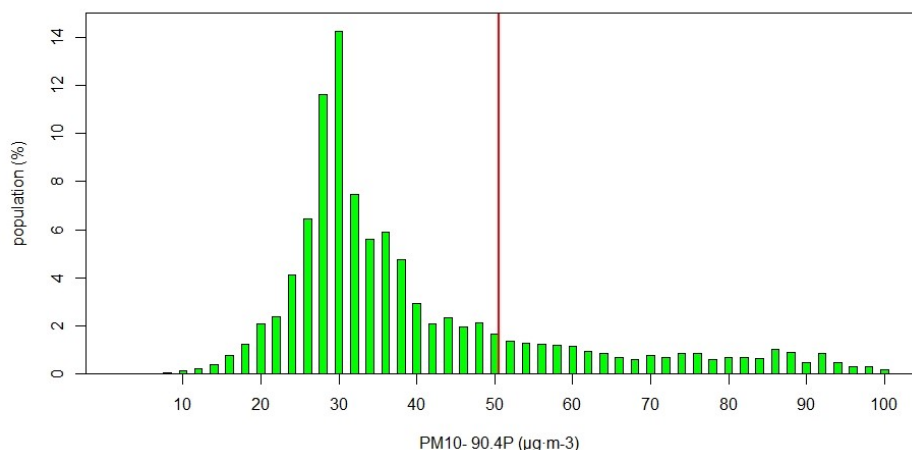
For the EU-28 around 12 % lived in areas where the 90.4 percentile of the PM<sub>10</sub> daily mean exceeded the EU limit value of 50 µg·m<sup>-3</sup>. According to CSI004 (EEA, 2017c), in 2016 about 13 % of the urban population in the EU-28 was exposed to PM<sub>10</sub> above this limit value. The slight difference between the two estimates is influenced by the fact that the EEA accounts for the urban population only, while Table 2.2 provides estimates also including inhabitants in rural areas, smaller cities and villages.

The European-wide population-weighted concentration of the 90.4 percentile of PM<sub>10</sub> daily means is estimated for 2016 at about 40 µg·m<sup>-3</sup> (including Turkey), resp. 36 µg·m<sup>-3</sup> (without Turkey), and 35 µg·m<sup>-3</sup> for the EU-28. This is the lowest level of the twelve years period 2005 – 2016 (Tables 6.1 and A4.2).

Figure 2.2 shows, for the whole mapped area, the population frequency distribution for exposure classes of 2 µg·m<sup>-3</sup>. One can see the highest population frequency for classes between cc. 25 and 35 µg·m<sup>-3</sup>, and continuous decline of population frequency for classes between cc. 35 and 55 µg·m<sup>-3</sup>.

Like in previous years, also in 2016 the daily limit value is more widely exceeded than the annual limit value.

*Figure 2.2 Population frequency distribution, PM<sub>10</sub> indicator 90.4 percentile of daily means, 2016*





### 3 PM<sub>2.5</sub>

In the Ambient Air Quality Directive (EU, 2008), the limit value (LV) for the annual average PM<sub>2.5</sub> concentrations was set at 25 µg·m<sup>-3</sup>. In the AQ directive there is also an indicative LV of 20 µg·m<sup>-3</sup> defined as Stage 2 that should become potentially into force in 2020. The Air Quality Guideline recommended by the World Health Organization (WHO, 2005) for the PM<sub>2.5</sub> annual average is 10 µg·m<sup>-3</sup>.

The current number of PM<sub>2.5</sub> measurement stations is yet limited and its spatial distribution is irregular over Europe. Deriving a reasonably reliable European wide spatially interpolated PM<sub>2.5</sub> annual average map on the basis of these PM<sub>2.5</sub> measurement data alone is not feasible. The resulting map would not be suitable for being used in population exposure assessments.

Therefore, in this paper the mapping of the health-related indicator PM<sub>2.5</sub> annual average is based on a mapping methodology developed in Denby et al. (2011a, 2011b). This methodology derives additional *pseudo* PM<sub>2.5</sub> annual mean concentrations from PM<sub>10</sub> annual mean measurement concentrations. As such, it increases the number and spatial coverage of PM<sub>2.5</sub> 'data points' and these data is used to derive a European wide map of annual mean PM<sub>2.5</sub>. Pseudo PM<sub>2.5</sub> stations data are estimated using PM<sub>10</sub> measurement data, surface solar radiation, latitude and longitude. Separate urban and rural background concentration maps are calculated on a grid of 10x10 km resolution and the subsequent final combined concentration map is based on the 1x1 km gridded population density map. The final PM<sub>2.5</sub> map is presented in this 1x1 km grid resolution. The population exposure table is calculated on basis of this map resolution.

Annex 3 provides details on the regression and kriging parameters applied for deriving the PM<sub>2.5</sub> annual average map, as well as the uncertainty analysis of the map. Annex 4 discusses briefly the inter-annual changes observed in the concentration maps and the relevant population exposure.

#### 3.1 PM<sub>2.5</sub> annual average

##### 3.1.1 Concentration map

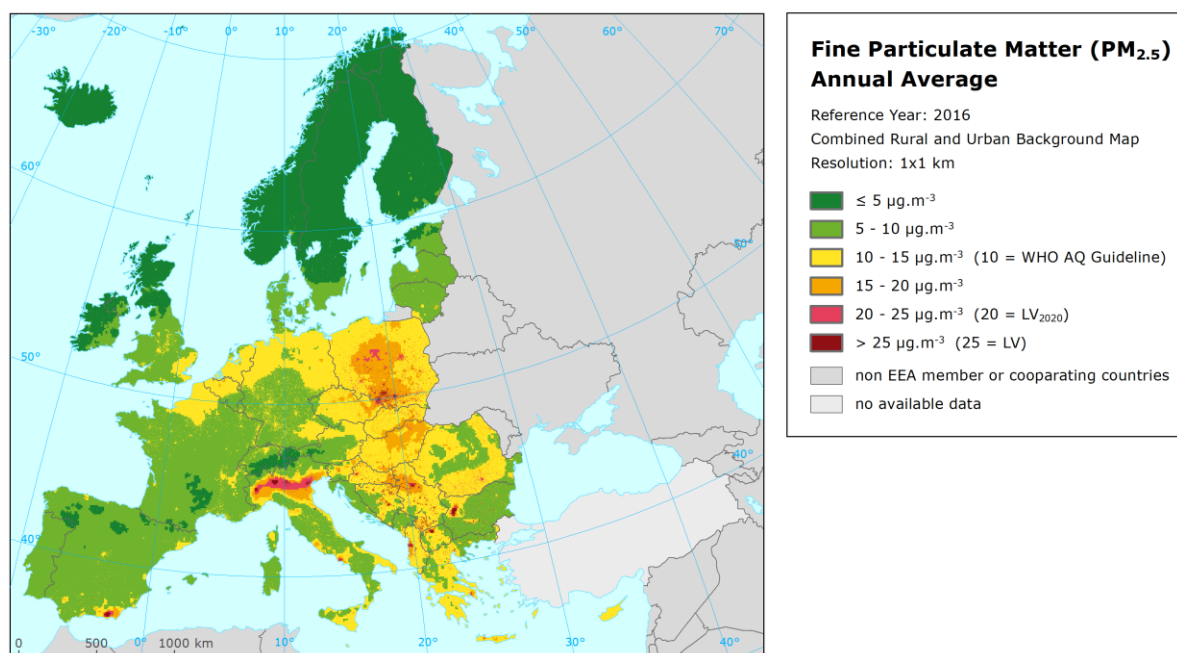
Map 3.1 presents the final combined map for the 2016 PM<sub>2.5</sub> annual average as a result of the interpolation and merging of the separate rural and urban map layers. The dark red areas exceed the ALV of 25 µg·m<sup>-3</sup>. Red areas show exceedances of the indicative LV of 20 µg·m<sup>-3</sup> defined as Stage 2 (LV<sub>2020</sub>).

Due to the lack of rural stations in Turkey for PM<sub>2.5</sub>, no proper interpolation results could be presented for this country in a rural map. Therefore, we do not present the estimated PM<sub>2.5</sub> values for Turkey in the final map.

According to Map 3.1, the areas with the highest PM<sub>2.5</sub> concentrations seem the Po Valley in Northern Italy, the areas around the Balkan cities of Sofia, Tirana, Skopje and Belgrade, and the Krakow – Katowice (PL) – Ostrava (CZ) industrial region. Several other smaller cities in Bulgaria, Serbia, Kosovo, North Macedonia, Bosnia & Herzegovina and Poland also show elevated PM<sub>2.5</sub> annual average concentrations. Like in the case of PM<sub>10</sub>, the central and the eastern parts of Europe show higher concentrations than the western and the northern parts.

The *relative mean uncertainty* of the final combined map of PM<sub>2.5</sub> annual average is 27 % for rural areas and 21 % for urban areas and determined exclusively on the actual PM<sub>2.5</sub> measurement data points, i.e. not on the pseudo stations (Annex 3).

Map 3.1 Concentration map of PM<sub>2.5</sub> annual average, 2016



In order to provide more complete information of the air quality across Europe, the final combined map including the measurement data at station points is presented in Map A5.3 of Annex 5.

### 3.2.2 Population exposure

Table 3.1 gives the population frequency distribution for a limited number of exposure classes calculated on a grid of 1x1 km resolution, as well as the population-weighted concentration for individual countries and for Europe as a whole according to Equation A1.7 of Annex 1. Annex 4 shows details on the ten year evolution of population exposure.

In 2016, 75 % of the European and the EU28 population has been exposed to PM<sub>2.5</sub> annual mean concentrations above the Air Quality Guideline of 10 µg.m<sup>-3</sup> as defined by the World Health Organization (WHO, 2005). The European wide, resp. EU-28, population exposure exceeding the EU limit value (LV) of 25 µg.m<sup>-3</sup> is about 5 %, resp. 4 %. In Albania, Bosnia & Herzegovina, Bulgaria, North Macedonia, and Serbia (including Kosovo) more than 25 % of the population suffers from exposures above this limit value; in Croatia, Greece, Italy, Montenegro and Poland it is between 5 to 25 %. The indicative Stage 2 limit value LV<sub>2020</sub> of 20 µg.m<sup>-3</sup> is exceeded for about 13 % (European wide) resp. 11 % (EU-28) of the population. In Albania, Bosnia & Herzegovina, Bulgaria, Croatia, Greece, Italy, Montenegro, North Macedonia, Poland, Serbia and Slovakia a quarter or more of the population is exposed to concentrations above the LV<sub>2020</sub>. As the current mapping methodology tends to underestimate high values (Annex 3), the exceedance percentages and/or the number of countries with population exposed to concentrations above both the current ALV and the indicative LV<sub>2020</sub> will most likely be higher.



Table 3.1 Population exposure and population-weighted concentration, PM<sub>2.5</sub> annual average 2016

Country		Population  [inhbs . 1000]	PM <sub>2.5</sub> annual average, exposed population [%]						Population weighted conc. [µg.m <sup>-3</sup> ]
			< LV <sub>2020</sub>				> LV <sub>2020</sub>		
			< LV				> LV		
			< 5 µg.m <sup>-3</sup>	5 - 10 µg.m <sup>-3</sup>	10 - 15 µg.m <sup>-3</sup>	15 - 20 µg.m <sup>-3</sup>	20 - 25 µg.m <sup>-3</sup>	> 25 µg.m <sup>-3</sup>	
Albania	AL	2 876		0.4	14.9	17.2	30.1	37.4	22.3
Andorra	AD	72		1.8	98.2				12.1
Austria	AT	8 700	0.6	18.7	76.6	4.1			12.0
Belgium	BE	11 311		4.9	86.8	8.3			12.7
Bosnia & Herzegovina	BA	3 516		2.6	15.5	10.5	11.6	59.8	28.7
Bulgaria	BG	7 154		6.9	7.8	17.8	34.5	33.0	22.3
Croatia	HR	4 191		6.3	24.1	23.4	24.0	22.2	19.4
Cyprus	CY	1 184			100.0				13.7
Czechia	CZ	10 554		1.1	23.2	63.2	9.7	2.8	16.6
Denmark	DK	5 707	0.8	81.0	18.3				9.2
Estonia	EE	1 316	13.3	86.7					5.9
Finland	FI	5 487	49.4	50.6					5.1
France (metropolitan)	FR	64 561	0.3	33.0	66.7				10.9
Germany	DE	82 176	0.0	9.5	86.7	3.7			11.6
Greece	GR	10 784		1.2	17.8	39.6	25.5	15.9	19.6
Hungary	HU	9 830			13.7	76.5	9.8		17.5
Iceland	IS	333	39.4	60.6					4.8
Ireland	IE	4 726	20.9	77.4	1.7				6.8
Italy	IT	60 666	0.0	6.6	39.8	28.2	15.5	9.9	16.6
Latvia	LV	1 969		45.0	36.4	18.7			10.9
Liechtenstein	LI	38		12.2	87.8				10.3
Lithuania	LT	2 889		25.3	57.4	17.3			11.8
Luxembourg	LU	576		14.2	85.8				11.4
Malta	MT	450			100.0				11.1
Monaco	MC	38			100.0				14.3
Montenegro	ME	622		9.3	13.2	25.4	36.9	15.1	20.3
Netherlands	NL	16 979		0.8	99.2				11.3
North Macedonia	MK	2 071		0.5	2.6	2.2	9.8	84.9	34.6
Norway	NO	5 211	38.2	55.4	6.4				5.9
Poland	PL	37 967		0.0	15.5	29.5	37.6	17.4	20.6
Portugal (excl. Az., Mad.)	PT	9 839	0.2	88.4	11.3				8.3
Romania	RO	19 760		3.1	33.3	40.5	22.4	0.6	16.8
San Marino	SM	33		1.9	69.8	28			14.3
Serbia (incl. Kosovo*)	RS	8 848		0.5	8.5	13.1	17.4	60.5	25.1
Slovakia	SK	5 426		0.0	24.3	50.8	24.1	0.9	17.6
Slovenia	SI	2 064		3.3	39.4	45.7	11.6		16.0
Spain (excl. Canarias)	ES	44 305	0.2	37.0	53.9	8.7	0.1	0.0	11.1
Sweden	SE	9 851	41.9	58.1					5.7
Switzerland	CH	8 327	1.3	33.7	64.5	0.6			10.1
United Kingdom (& dep.)	UK	65 383	1.9	51.1	47.0				9.5
Total		537 790	2.2	22.5	48.6	13.6	7.8	5.4	13.4
			24.6		62.2		13.2		
EU-28		505 806	1.9	22.7	50.2	14.0	7.6	3.6	13.1
			24.6		64.2		11.3		

Kosovo*	KS	1 772		0.0	8.1	9.7	9.2	73.1	27.1
Serbia (excl. Kosovo*)	RS	7 076		0.6	8.7	13.9	19.4	57.5	24.6

(\*) under the UN Security Council Resolution 1244/99

Note 1: Turkey not included due to the lack of the rural stations.

Note 2: The percentage value "0.0" indicates that an exposed population exists, but it is small and estimated lesser than 0.05 %. Empty cells mean no population in exposure.

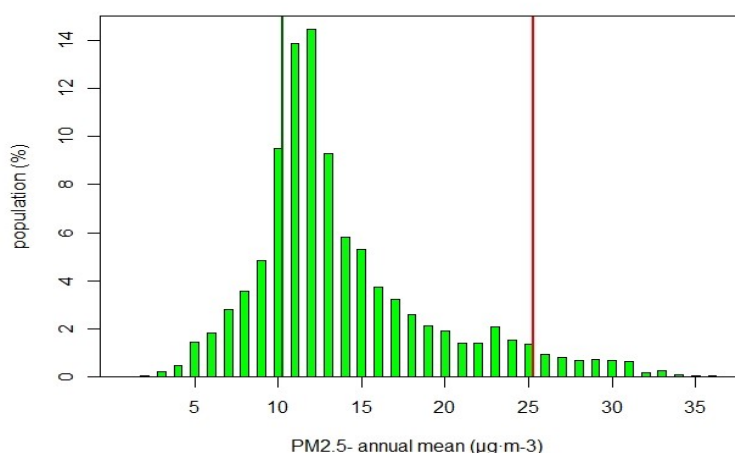
According to EEA CS1004 (EEA, 2018c), about 6 % of the urban population in the EU-28 was exposed to PM<sub>2.5</sub> concentrations above the LV in 2016. The difference with the estimated 3.6 % in Table 3.1 is because

the EEA accounts for the urban population only. Whereas, Table 3.1 provides estimates for the total population, including the population in rural areas, smaller cities and villages. When it comes to the WHO AQ guideline, the urban population exposed to concentrations above its recommended value ( $10 \mu\text{g}\cdot\text{m}^{-3}$ ) in 2016 was estimated at 74 %, which is more in line with the total population estimation of 75 % as presented in Table 3.1.

The European-wide population-weighted concentration of the  $\text{PM}_{2.5}$  annual means is estimated for 2016 at about  $13 \mu\text{g}\cdot\text{m}^{-3}$  for both Europe as a whole and the EU-28. This is the lowest level of the period 2007 – 2016 (data lacking for 2009; Tables 6.2 and A4.4).

Figure 3.1 shows, for the whole mapped area, the population frequency distribution for exposure classes of  $1 \mu\text{g}\cdot\text{m}^{-3}$ . The highest population frequency is found for classes between 10 and 13  $\mu\text{g}\cdot\text{m}^{-3}$ .

*Figure 3.1 Population frequency distribution,  $\text{PM}_{2.5}$  annual average, 2016*



## 4 Ozone

For ozone, the two health-related indicators *93.2 percentile of maximum daily 8-hour means* (see below) and *SOMO35*, and the two vegetation-related indicators *AOT40 for vegetation* and *AOT40 for forests* are considered. For the definition of the SOMO35 and AOT40 indicators, see following sections and Annex 2. The separate rural and urban background health-related indicator fields are calculated at a resolution of 10x10 km. Subsequently, the final health-related indicator maps are created by combining rural and urban areas based on the 1x1 km gridded population density map. We present these maps on this 1x1 km grid resolution. The population exposure tables are calculated on the basis of these health-related indicator maps.

The vegetation-related indicator maps are calculated from observations at rural background stations and are representative for rural areas only (assuming urban areas do not cover vegetation). The maps have a resolution of 2x2 km. This resolution serves the needs of the EEA Core Set Indicator 005 (EEA, 2017d) on ecosystem exposure to ozone.

Annex 3 provides details on the regression and kriging parameters applied for deriving the maps of the ozone indicators, as well as the uncertainty analysis of the maps. Annex 4 discusses briefly the inter-annual changes observed in the concentration maps and the relevant population and vegetation exposure.

### 4.1 Ozone – 93.2 percentile of maximum daily 8-hour means

The AQ Directive (EU, 2008) describes the ozone target value (TV) for the protection of human health as “a maximum daily 8-hour mean of  $120 \mu\text{g}\cdot\text{m}^{-3}$  not to be exceeded on more than 25 times a calendar year, averaged over three years”. On an annual basis, it can be evaluated by the indicator 26<sup>th</sup> highest maximum daily 8-hour mean, which is in principle equivalent to the indicator 93.2 percentile of maximum daily 8-hour means. However, for measurement data these two indicators are equivalent only if no data is missing, which is in general not the case. As shown in de Leeuw (2012), the additional uncertainty related to incomplete time series is substantially smaller when using percentile values instead of the x-th highest value. As in the previous ETC/ACM Technical Papers 2016/6 and 2017/7, we express this ozone indicator as the 93.2 percentile of maximum daily 8-hour means instead of the formerly used 26<sup>th</sup> highest maximum daily 8-hour mean.

#### 4.1.1 Concentration map

Map 4.1 presents the final combined map for 93.2 percentile of the maximum daily 8-hour means as a result of combining the separate rural and urban interpolated maps following the procedures as described in Annex 1 (for a more detailed description, see Horálek et al., 2007, 2010). The supplementary data used are EMEP model output, altitude and surface solar radiation for rural areas and EMEP model output, wind speed and surface solar radiation for urban areas (Annex 3).

In the final combined map the red and dark red areas show values above the TV of  $120 \mu\text{g}\cdot\text{m}^{-3}$  on more than 25 days in 2016. Note that in the AQ Directive (EU, 2008) the target value is actually defined as  $120 \mu\text{g}\cdot\text{m}^{-3}$  not to be exceeded on more than 25 days per calendar year *averaged over three years*. Here only 2016 data are presented, and no three-year average is calculated.

The map shows that in 2016 values above  $120 \mu\text{g}\cdot\text{m}^{-3}$  on more than 25 days occur in the Alpine region, northern and central Italy, southern France, central and south-eastern Spain, Greece, southern Turkey and Cyprus. In general, the southern parts of Europe show higher ozone concentrations than the

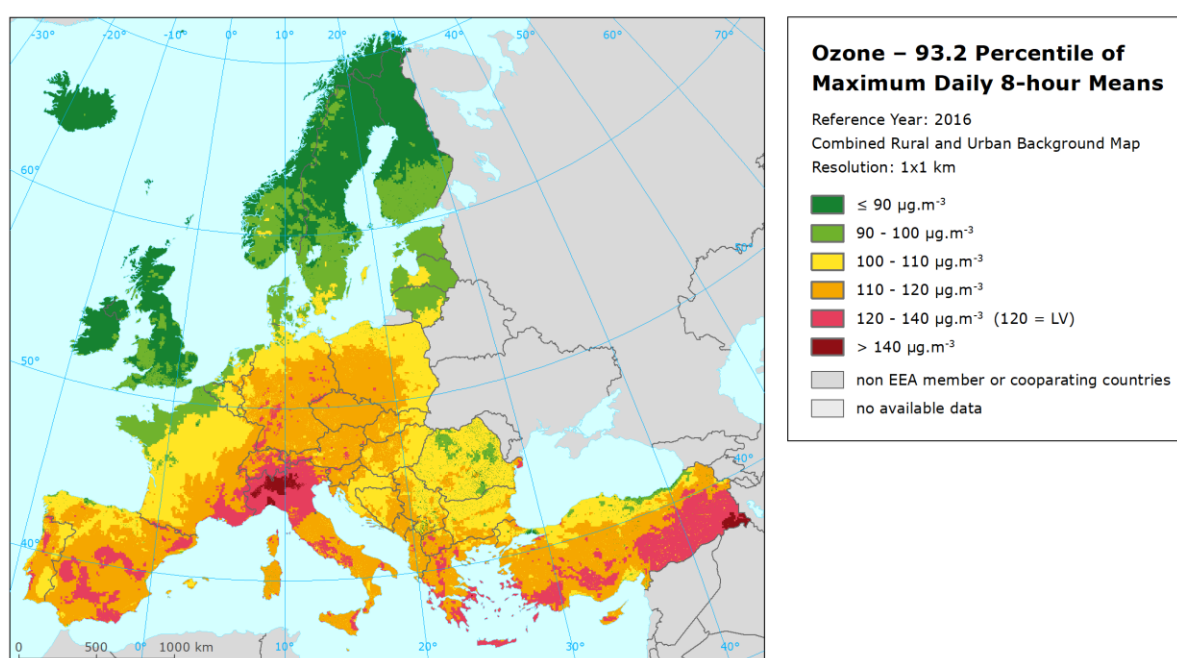
northern parts, which is caused mainly by higher solar radiation and temperature in these areas. An exception is north-eastern Romania where remarkably low values are observed. Furthermore, in general, higher levels of ozone do also occur more frequently in mountainous areas than in lowlands.

Most of the European continent and Iceland show a quite steep decrease from 2015 to 2016, i.e. the opposite of that of the 2015-2014 difference as shown in Horálek et al (2018a). This development is caused by extraordinary high ozone concentrations in 2015 (Annex 4).

The relative mean uncertainty of the 2016 map of the 93.2 percentile of maximum daily 8-h ozone means is about 9 % for both rural and urban areas (Annex 3).

In order to provide more complete information of the air quality across Europe, the final combined map including the measurement data at station points is presented in Map A5.4 of Annex 5.

*Map 4.1 Concentration map of ozone indicator 93.2 percentile of maximum daily 8-hour means, 2016*



#### 4.1.2 Population exposure

Table 4.1 gives, for 93.2 percentile of maximum daily 8-hour means, the population frequency distribution for a limited number of exposure classes, as well as the population-weighted concentration for individual countries and for Europe as a whole. Annex 4 presents the twelve-years evolution of population exposure.

It has been estimated that in 2016 about 9 % of both the European population (including Turkey) and the EU-28 lived in areas where the ozone concentration exceeded the health related target value threshold (TV of  $120 \mu\text{g.m}^{-3}$ ). For European population without Turkey, it is about 8 %. This is the second lowest level of the twelve years period 2005 – 2016 (Table 6.3). According to CSI004 (EEA, 2018c), about 12 % of the urban population in the EU-28 was exposed to ozone above the target value threshold in 2016. It should be mentioned that the CSI004 refers only to the population in cities for which ozone measurement data is available.

Table 4.1 Population exposure and population-weighted concentrations, ozone indicator 93.2 percentile of maximum daily 8-hour means, 2016

Country		Population  [inhbs . 1000]	Ozone, 93.2 percentile of max. daily 8-h means, exposed population [%]						Population- weighted conc.  [µg.m <sup>-3</sup> ]
			< TV				> TV		
			< 90 µg.m <sup>-3</sup>	90 - 100 µg.m <sup>-3</sup>	100 - 110 µg.m <sup>-3</sup>	110 - 120 µg.m <sup>-3</sup>	120 - 140 µg.m <sup>-3</sup>	> 140 µg.m <sup>-3</sup>	
Albania	AL	2 876		9.9	47.9	41.7	0.5		107.7
Andorra	AD	72			76.8	22.7	0.5		109.2
Austria	AT	8 700		0.6	31.1	67.3	1.1		111.8
Belgium	BE	11 311	1.8	46.7	46.4	5.1			100.2
Bosnia & Herzegovina	BA	3 516		4.3	90.2	5.6			105.2
Bulgaria	BG	7 154	8.7	49.2	39.7	2.3	0.0		98.7
Croatia	HR	4 191		0.9	53.5	42.7	3.0		109.5
Cyprus	CY	1 184		3.3	80.1	14.8	1.8		105.0
Czechia	CZ	10 554			9.2	90.5	0.3		114.7
Denmark	DK	5 707	1.0	91.1	7.8	0.0			95.3
Estonia	EE	1 316	16.8	82.7	0.5				92.6
Finland	FI	5 487	54.9	45.1	0.0				88.8
France (metropolitan)	FR	64 561	5.7	27.1	38.8	21.4	7.0	0.0	104.8
Germany	DE	82 176		1.8	37.1	60.1	1.0		110.7
Greece	GR	10 784		5.1	24.1	35.1	35.5	0.3	115.8
Hungary	HU	9 830		1.6	90.9	7.5			106.2
Iceland	IS	333	100						78.3
Ireland	IE	4 726	96	3.9	0.0				84.4
Italy	IT	60 666	0.1	3.3	24.2	24.4	29.7	18.3	122.1
Latvia	LV	1 969		62.8	34.4	2.8			99.0
Liechtenstein	LI	38				93	7.1		117.3
Lithuania	LT	2 889		87.3	12.7	0.0			98.1
Luxembourg	LU	576		52.3	45.1	2.6			99.6
Malta	MT	450			89.9	9.4	0.7		106.5
Monaco	MC	38					100		120.2
Montenegro	ME	622		14.4	65.8	19.8			106.3
Netherlands	NL	16 979	1.2	48.0	44.3	6.5			100.9
North Macedonia	MK	2 071	18.0	61.6	16.5	3.7	0.3		95.2
Norway	NO	5 211	91.6	8.4	0.0				84.0
Poland	PL	37 967	0.3	5.7	42.1	51.8	0.0		109.2
Portugal (excl. Az., Mad.)	PT	9 839	2.5	12.2	53.5	29.6	2.2		107.0
Romania	RO	19 760	46.5	39.2	13.7	0.7	0.0		90.4
San Marino	SM	33				95.5	4.5		118.0
Serbia (incl. Kosovo*)	RS	8 848	29.5	18.3	47.0	5.3	0.0		96.9
Slovakia	SK	5 426		0.1	65.0	34.9			109.0
Slovenia	SI	2 064			41.3	55.9	2.7		111.9
Spain (excl. Canarias)	ES	44 305	3.2	18.4	24.1	41.7	12.7		109.7
Sweden	SE	9 851	37.9	59.2	2.9	0.0			90.7
Switzerland	CH	8 327			4.4	83.0	11.8	0.8	117.3
Turkey	TR	78 741	20.8	13.7	30.6	25.9	8.7	0.2	102.7
United Kingdom (& dep.)	UK	65 383	93.8	6.1	0.1				84.1
Total		616 531	18.2	15.6	29.3	28.5	6.6	1.9	104.5
			33.7		57.8		8.5		
Total without Turkey		537 790	17.8	15.8	29.1	28.9	6.4	2.1	104.8
			33.6		57.9		8.4		
EU-28		505 806	17.4	16.0	28.9	29.0	6.6	2.2	105.0
			33.4		57.9		8.8		
Kosovo*	KS	1 772	64.8	16.9	14.5	3.7	0.0		89.0
Serbia (excl. Kosovo*)	RS	7 076	20.8	18.6	54.9	5.7			98.9

(\*) under the UN Security Council Resolution 1244/99

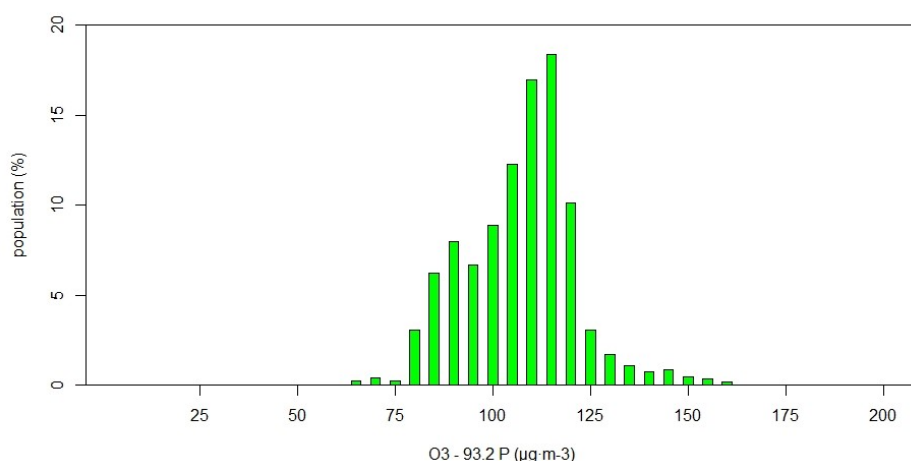
Note: The percentage value "0.0" indicates that an exposed population exists, but it is small and estimated lesser than 0.05 %. Empty cells mean no population in exposure.

In the following countries at least 5 % of the population suffered exposures above the TV: France, Greece, Italy, Liechtenstein, Monaco, Spain, Switzerland and Turkey. As the current mapping methodology tends to underestimate high values due to interpolation smoothing (Annex 3), the exceedance percentage is most likely even somewhat underestimated; additional exceedances might be expected and in additional countries: Austria, Czechia, Germany, Poland, San Marino, and Slovenia. The reason is that in these countries the estimated percentage population exposed to the concentrations above  $110 \mu\text{g}\cdot\text{m}^{-3}$  is considerable.

The overall European and EU-28 population-weighted ozone concentrations in terms of the 93.2 percentile of maximum daily 8-hour means were estimated for 2016 as being  $105 \mu\text{g}\cdot\text{m}^{-3}$ , which is the second lowest of the twelve-years period 2005 – 2016 (Table A4.6).

Figure 4.1 shows, for the whole mapped area, the population frequency distribution for exposure classes of  $5 \mu\text{g}\cdot\text{m}^{-3}$ . The highest population frequency is found for classes between 105 and  $120 \mu\text{g}\cdot\text{m}^{-3}$ .

*Figure 4.1 Population frequency distribution,  $\text{O}_3$  indicator 93.2 percentile of maximum daily 8-hour means, 2016*



## 4.2 Ozone – SOMO35

SOMO35 is the annually accumulated ozone maximum daily 8-hourly means in excess of 35 ppb (i.e.  $70 \mu\text{g}\cdot\text{m}^{-3}$ ). It is not subject to any of the EU air quality directives and there are no limit or target values defined. Comparing the 93.2 percentile of maximum daily 8-hour means versus the SOMO35 for all background stations shows no simple relationship between the two indicators. However, it seems that the target value of the 93.2 percentile of maximum daily 8-hour means (being  $120 \mu\text{g}\cdot\text{m}^{-3}$ ) is related approximately with a SOMO35 value in the range of  $6\,000 - 8\,000 \mu\text{g}\cdot\text{m}^{-3}\cdot\text{d}$ . This comparison motivates a somewhat arbitrarily chosen threshold of  $6\,000 \mu\text{g}\cdot\text{m}^{-3}\cdot\text{d}$ , in order to facilitate the discussion of the observed distributions of SOMO35 levels in their spatial and temporal context. This threshold is used in this and previous papers (Horálek et al. 2017b and the references cited therein) when dealing with the population exposure estimates.

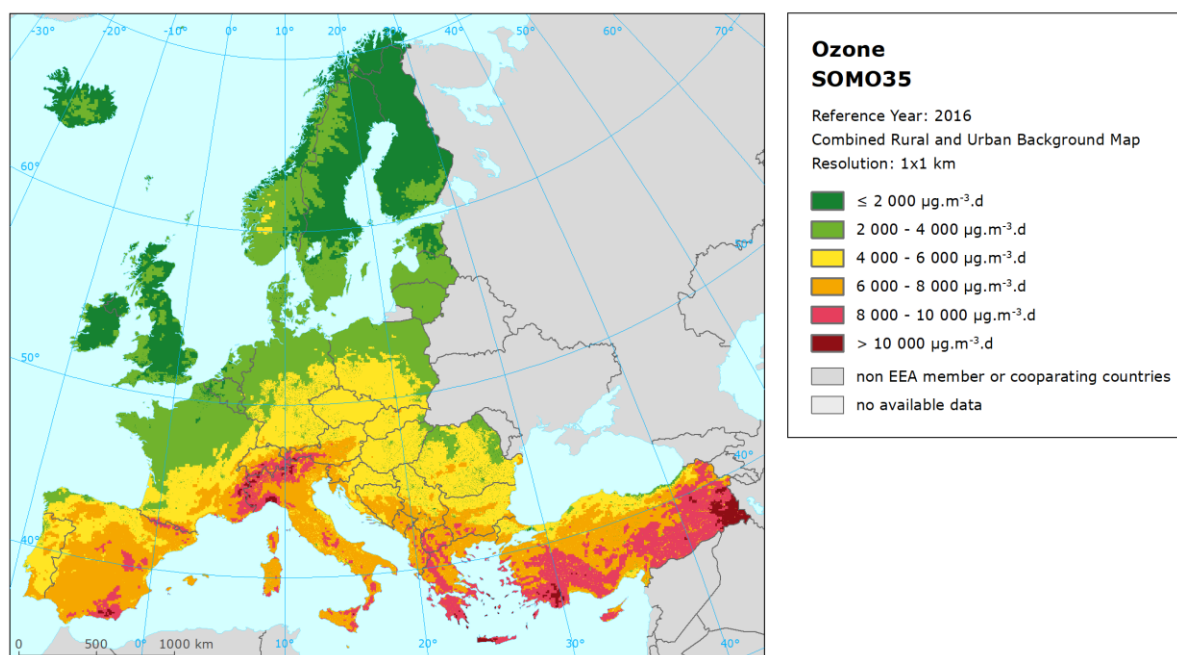
#### 4.2.1 Concentration map

Map 4.2 presents the final combined map for SOMO35 as a result of combining the separate rural and urban interpolated maps following the same procedure as for 93.2 percentile of the maximum daily 8-hour means. The mapping details and the uncertainty analysis are presented in Annex 3. In the final combined map the red and dark red areas show values above 8 000  $\mu\text{g}\cdot\text{m}^{-3}\cdot\text{d}$ , while the orange areas show values above 6 000  $\mu\text{g}\cdot\text{m}^{-3}\cdot\text{d}$ .

Like in the case of the 93.2 percentile of the maximum daily 8-hour means, the southern parts of Europe show higher ozone SOMO35 concentrations than the northern parts. Higher levels of ozone do also occur more frequently in mountainous areas south of 50 degrees latitude than in lowlands. The relative mean uncertainty of the 2016 map of the SOMO35 is about 33 % for both rural and urban areas (Annex 3).

In order to provide more complete information of the air quality across Europe, the final combined map including the ozone indicator values at station points, based on the measurement data is presented in Map A5.5 of Annex 5.

Map 4.2 Concentration map of ozone indicator SOMO35, 2016



#### 4.2.2 Population exposure

Table 4.2 gives for SOMO35 the population frequency distribution for a limited number of exposure classes, as well as the population-weighted concentration for individual countries and for Europe as a whole. Annex 4 shows details on the twelve-year evolution of population exposure.



Table 4.2 Population exposure and population-weighted concentrations, ozone indicator SOMO35, 2016

Country		Population  [inhbs.1000]	Ozone, SOMO35, exposed population [%]						Population- weighted conc.  [µg.m <sup>-3</sup> .d]
			< 2000 µg.m <sup>-3</sup> .d	2000 - 4000 µg.m <sup>-3</sup> .d	4000 - 6000 µg.m <sup>-3</sup> .d	6000 - 8000 µg.m <sup>-3</sup> .d	8000 - 10000 µg.m <sup>-3</sup> .d	> 10000 µg.m <sup>-3</sup> .d	
Albania	AL	2 876		3.5	72.0	23.5	0.9		5 475
Andorra	AD	72			98.2	0.9	1.0		4 423
Austria	AT	8 700		25.3	68.3	6.1	0.3	0.0	4 522
Belgium	BE	11 311	39.5	60.5	0.0				2 203
Bosnia & Herzegovina	BA	3 516		34.3	60.5	5.2			4 409
Bulgaria	BG	7 154	3.5	76.9	15.8	3.8	0.1		3 347
Croatia	HR	4 191		15.4	74.1	10.1	0.4		4 996
Cyprus	CY	1 184			80.0	13.0	7.0		5 612
Czechia	CZ	10 554		15.2	84.8	0.0			4 353
Denmark	DK	5 707	24.7	75.1	0.2				2 293
Estonia	EE	1 316	65.3	34.7					1 949
Finland	FI	5 487	93.2	6.8					1 510
France (metropolitan)	FR	64 561	16.5	53.4	22.0	7.6	0.6	0.0	3 420
Germany	DE	82 176	0.2	80.7	19.0	0.0	0.0		3 368
Greece	GR	10 784		2.3	23.8	49.1	23.7	1.0	6 871
Hungary	HU	9 830		60.6	39.4	0.0			3 952
Iceland	IS	333	100.0	0.0					499
Ireland	IE	4 726	92.8	7.2					1 323
Italy	IT	60 666		8.3	43.4	39.0	8.0	1.3	6 058
Latvia	LV	1 969	4.5	92.5	3.0				2 773
Liechtenstein	LI	38			95.6	4.4			4 945
Lithuania	LT	2 889	10.0	89.9	0.1				2 456
Luxembourg	LU	576	37.4	62.6					2 211
Malta	MT	450			74.2	24.5	1.4		5 985
Monaco	MC	38				100			7 186
Montenegro	ME	622		8.6	69.5	21.7	0.1		5 269
Netherlands	NL	16 979	15.5	84.4	0.2				2 428
North Macedonia	MK	2 071		31.6	63.1	4.8	0.4		4 434
Norway	NO	5 211	79.9	20.1	0.0				1 502
Poland	PL	37 967	1.2	60.0	38.8	0.0			3 699
Portugal (excl. Az., Mad.)	PT	9 839	2.2	44.1	49.1	4.6	0.0		4 074
Romania	RO	19 760	39.2	50.5	10.3	0.0			2 485
San Marino	SM	33			92.8	7.2			5 667
Serbia (incl. Kosovo*)	RS	8 848	3.8	61.4	30.5	4.3	0.0		3 755
Slovakia	SK	5 426		25.9	74.0	0.1			4 232
Slovenia	SI	2 064		11.8	73.9	14.3	0.0		5 007
Spain (excl. Canarias)	ES	44 305	3.4	18.7	43.0	33.8	1.1	0.0	5 212
Sweden	SE	9 851	73.6	26.4	0.0				1 819
Switzerland	CH	8 327		4.4	87.1	7.2	1.4	0.0	4 842
Turkey	TR	78 741	14.4	22.5	35.1	17.0	10.2	0.8	4 673
United Kingdom (& dep.)	UK	65 383	94.3	5.6	0.1				1 168
Total		616 531	20.2	38.1	28.1	10.8	2.6	0.2	3 745
			86.4			13.6			
Total without Turkey		537 790	21.0	40.2	27.1	9.9	1.6	0.2	3 619
			88.3			11.7			
EU-28		505 806	21.4	40.9	25.7	10.1	1.6	0.2	3 598
			88.0			12.0			
Kosovo*	KS	1 772		23.0	64.1	12.7	0.2		4 769
Serbia (excl. Kosovo*)	RS	7 076	4.8	70.8	22.2	2.2	0.0		3 508

(\*) under the UN Security Council Resolution 1244/99

Note: The percentage value "0.0" indicates that an exposed population exists, but it is small and estimated lesser than 0.05 %. Empty cells mean no population in exposure.



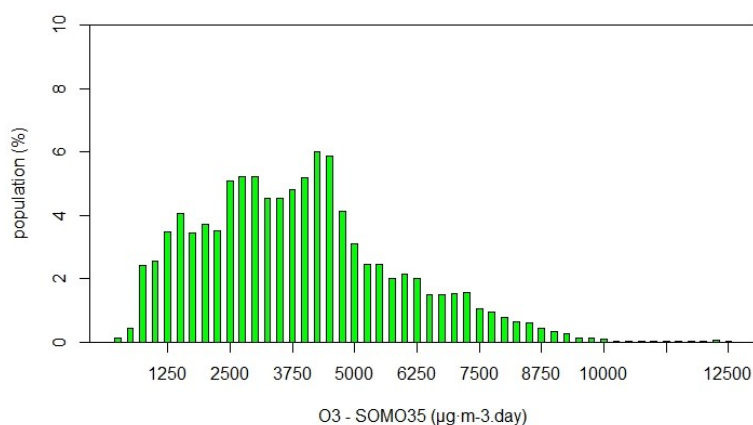
It has been estimated that in 2016 about 14 % of the European population (including Turkey), resp. about 12 % of both European population without Turkey and the EU-28 population, lived in areas with SOMO35 values above 6 000  $\mu\text{g}\cdot\text{m}^{-3}\cdot\text{d}$  (see above on the motivation of this criterion). This is the second lowest level in the twelve years period 2005 – 2016 (Table 6.3).

In 2016, the northern and north-western European countries do not have people exposed to SOMO35 concentrations above 6 000  $\mu\text{g}\cdot\text{m}^{-3}\cdot\text{d}$ , and almost no people above 4 000  $\mu\text{g}\cdot\text{m}^{-3}\cdot\text{d}$ . Most of the countries in southern and south-eastern Europe show exposures above or well above 6 000  $\mu\text{g}\cdot\text{m}^{-3}\cdot\text{d}$ , most notably (at least 20 % of population) Albania, Cyprus, Greece, Italy, Malta, Monaco, Montenegro, Spain, and Turkey. This can also be observed in Map 4.2.

In 2016, the total European, resp. the EU-28, population-weighted ozone concentrations, in terms of SOMO35, were estimated to be around 3 700  $\mu\text{g}\cdot\text{m}^{-3}\cdot\text{d}$ , resp. 3 600  $\mu\text{g}\cdot\text{m}^{-3}\cdot\text{d}$ , which is the second lowest in the twelve years period 2005 – 2016 (Table 6.3).

Figure 4.2 shows, for the whole mapped area, the population frequency distribution for exposure classes of 250  $\mu\text{g}\cdot\text{m}^{-3}\cdot\text{d}$ . Highest frequencies are found for classes between 2500 and 4500  $\mu\text{g}\cdot\text{m}^{-3}\cdot\text{d}$ . For exposure classes above 5000  $\mu\text{g}\cdot\text{m}^{-3}\cdot\text{d}$  a decline is seen.

Figure 4.2 Population frequency distribution, ozone indicator SOMO35, 2016



### 4.3 Ozone – AOT40 vegetation and AOT40 forests

In the Ambient Air Quality Directive (EU, 2008) a target value (TV) and a long-term objective (LTO) for the *protection of vegetation* from high ozone concentrations accumulated during the growing season have been defined. TV and LTO are specified using “accumulated ozone exposure over a threshold of 40 parts per billion” (AOT40). This is calculated as a sum of the difference between hourly concentrations greater than 80  $\mu\text{g}\cdot\text{m}^{-3}$  (i.e. 40 parts per billion) and 80  $\mu\text{g}\cdot\text{m}^{-3}$ , using only observations between 08:00 and 20:00 Central European Time (CET) each day, calculated over three months from 1 May to 31 July. The TV is 18 000  $\mu\text{g}\cdot\text{m}^{-3}\cdot\text{h}$  (averaged over five years) and the LTO is 6 000  $\mu\text{g}\cdot\text{m}^{-3}\cdot\text{h}$ .

Note that the term *vegetation* as used in the Air Quality Directive (EU, 2008) is not further defined. Nevertheless, the target value used in the directive is the same as the critical load used in the Mapping Manual (UNECE, 2004) for “agricultural crops”, so we have interpreted the term *vegetation* in the AQ directive as primarily agricultural crops. Therefore, the exposure of *agricultural crops* has been

evaluated here based on the AOT40 for vegetation as defined in the AQ directive and the agricultural areas, defined as the CORINE Land Cover level-1 class 2 *Agricultural areas* (encompassing the level-2 classes 2.1 *Arable land*, 2.2 *Permanent crops*, 2.3 *Pastures* and 2.4 *Heterogeneous agricultural areas*), see Section 4.3.2. Note that in addition to these agricultural areas there are several other CLC classes that could be considered “vegetation”, namely level-2 classes 1.4 *Artificial, non-agricultural vegetated areas* (encompassing the level-3 classes 1.4.1 *Green urban areas* and 1.4.2 *Sport and leisure facilities*), 2.3 *Forests* (see below) and 2.4 *Scrub and/or herbaceous vegetation associations*.

Next to the AOT40 for vegetation protection, the AQ Directive (EU, 2008) defines also the AOT40 for *forest protection*, which is calculated similarly as the AOT40 for vegetation, but is summed over six months from 1 April to 30 September. For AOT40 for forests there is no TV defined. However, there is a critical level (CL) established by UNECE (2004). This critical level is set at  $10\,000\ \mu\text{g}\cdot\text{m}^{-3}\cdot\text{h}$ .

For the exposure of forests evaluation, the CLC level-2 class 3.1 *Forests* has been used.

The ecosystem based accumulative ozone indicators described in this section are specifically prepared for calculation of the EEA Core Set Indicator 005 (EEA, 2018d). For the estimation of the vegetation and forested area exposure to accumulated ozone, the maps in this section are created on a grid of 2x2 km resolution. The exposure frequency distribution outcomes are based on the overlay with the 100x100 m grid resolution of the CLC2012 land cover classes.

#### 4.3.1 Concentration maps

The interpolated map of AOT40 for vegetation and of AOT40 for forests are created for rural areas only, as urban areas are considered not to represent agricultural or forested areas. These maps are therefore applicable to rural areas only, and as such they are based on AOT40 data derived from rural background station observations only. These AOT40 monitoring data are combined in the mapping with the supplementary data sources EMEP model output, altitude and surface solar radiation. These supplementary data sources are the same as those selected at the human health related ozone indicators.

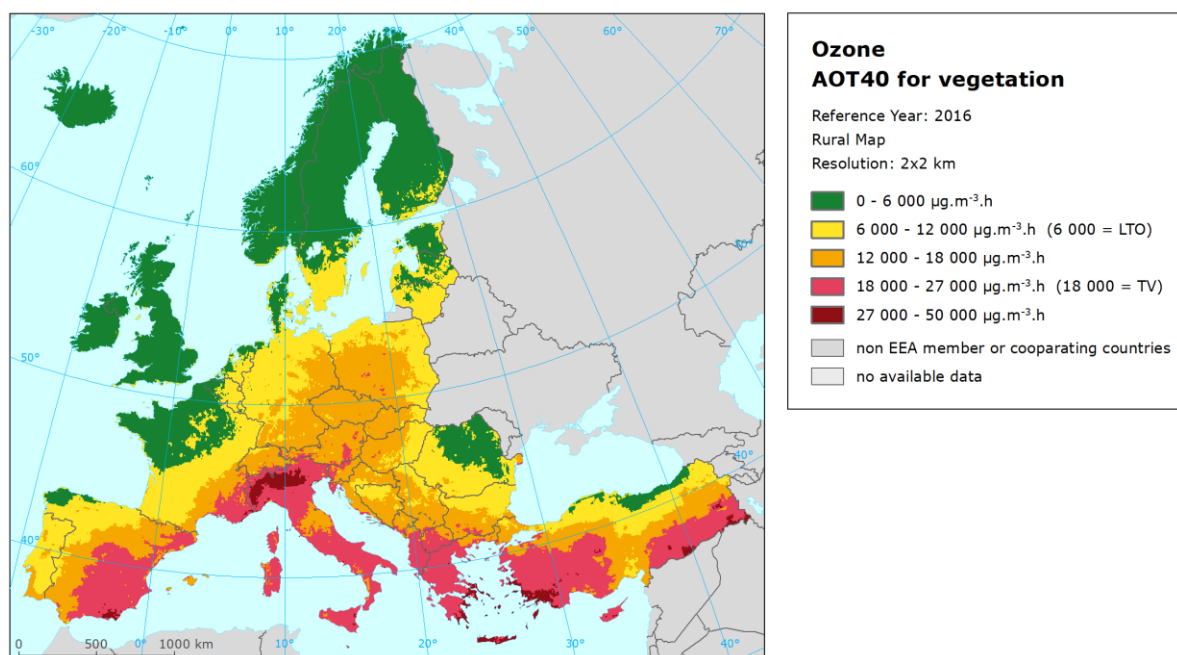
Map 4.3 presents the final map of AOT40 for *vegetation* in 2016. Note that in Directive 2008/50/EC the target value is actually defined as  $18\,000\ \mu\text{g}\cdot\text{m}^{-3}\cdot\text{h}$  *averaged over five years*. Here only 2016 data are presented, and no five-year average is calculated.

The areas in the map with concentrations above the target value (TV) of  $18\,000\ \mu\text{g}\cdot\text{m}^{-3}\cdot\text{h}$ , are marked in red and dark red. The areas below the long term objective (LTO) are marked in green. The high and very high AOT40 levels for vegetation do occur specifically in southern, south-western and south-eastern regions of Europe. The relative mean uncertainty of the 2016 map of the AOT40 for vegetation is about 37 % (Annex 3).

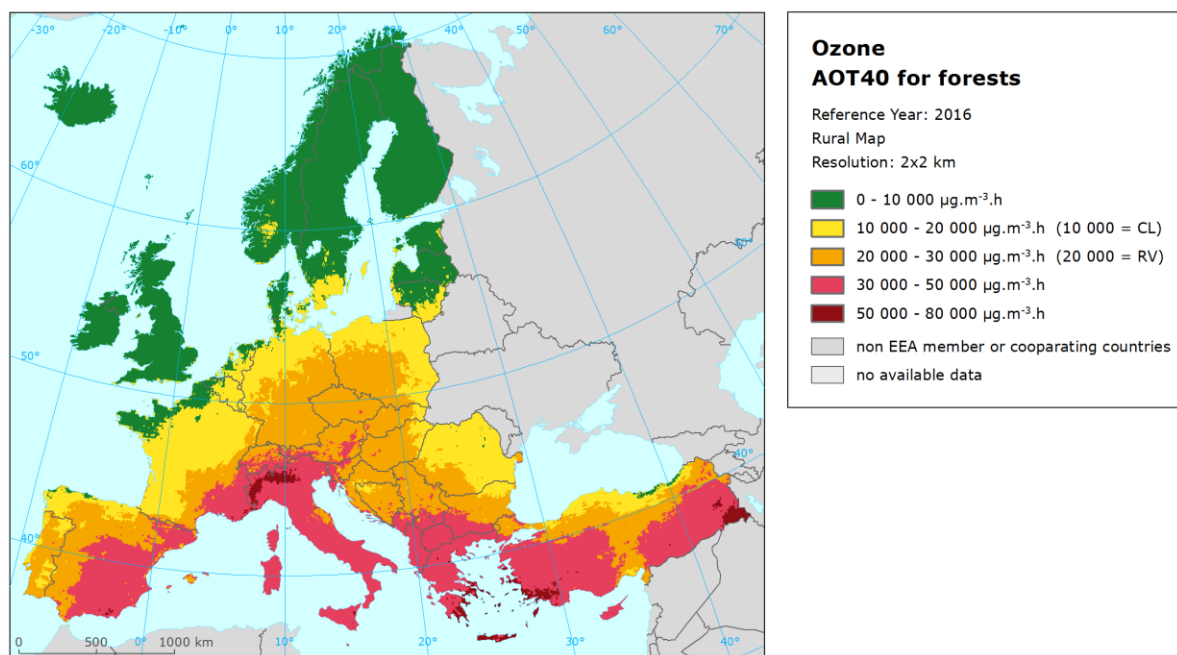
Map 4.4 presents the final map of AOT40 for *forests* in 2016. The areas in the map with concentrations above the critical level (CL) defined by UNECE (2004) are marked in yellow, orange, red and dark red. One can see large European forested areas exceeding this level.

Like for the AOT40 for vegetation indicator, the highest levels of the AOT40 for forests are found in the south-western, southern and south-eastern European region. The relative mean uncertainty of the 2016 map of the AOT40 for forests is about 37 % (Annex 3).

Map 4.3 Concentration map of  $O_3$  indicator AOT40 for vegetation, rural map, 2016



Map 4.4 Concentration map of ozone indicator AOT40 for forests, rural map, 2016



In order to provide more complete information of the air quality across Europe, the AOT40 maps including the AOT40 values based on the actual rural background measurement data at station points are presented in Maps A5.6 and A5.7 of Annex 5.

### 4.3.2 Vegetation exposure

#### **Agricultural crops**

The rural map with ozone indicator AOT40 for vegetation has been combined with the land cover CLC2012 map. Following a similar procedure as described in Horálek et al. (2007), the exposure of agricultural areas (as defined above) has been calculated at the country-level.

Table 4.3 gives the absolute and relative agricultural area for each country and for four European regions where the ozone target value (TV) threshold and long-term objective (LTO) for protection of vegetation as defined in the AQ Directive (EU, 2008) are exceeded. The frequency distribution of the agricultural area over some exposure classes per country is presented as well. The table indicates the country grouping with corresponding colours of the region *Northern Europe*: Denmark, Estonia, Finland, Latvia, Lithuania, Norway, and Sweden. *North-western Europe*: Belgium, France north of 45 degrees latitude, Ireland, Iceland, Luxembourg, the Netherlands, and United Kingdom. *Central and Eastern Europe*: Austria, Bulgaria, Czechia, Germany, Hungary, Liechtenstein, Poland, Romania, Slovakia and Switzerland. *Southern Europe*: Albania, Bosnia-Herzegovina, Croatia, Cyprus, France south of 45 degrees latitude, Greece, Italy, Malta, Monaco, Montenegro, North Macedonia, Portugal, San Marino, Serbia (including Kosovo under the UN Security Council Resolution 1244/99), Slovenia, Spain and Turkey.

Table 4.3 illustrates that in 2016, about 19 % of all European agricultural land was exposed to ozone exceeding the target value (TV) of 18 000  $\mu\text{g}\cdot\text{m}^{-3}\cdot\text{h}$ . For the areas excluding Turkey, it was about 15 %, which is the lowest percentage of the twelve-year period 2005 – 2016, see Table 6.4.

Considering the long-term objective (LTO) of 6 000  $\mu\text{g}\cdot\text{m}^{-3}\cdot\text{h}$  the area in excess is about 77 %. For the areas excluding Turkey, it is 74 %, which is also the lowest for this twelve year period (Table 6.4). Iceland, together with the most of Ireland, the United Kingdom and Norway are the areas with ozone levels not being in excess of the LTO. In Albania, Cyprus, Greece, Italy, Malta, and North Macedonia, more than half of their agricultural area experienced exposures above the TV threshold in 2016.

#### **Forests**

The rural map with ozone indicator AOT40 for forests was combined with the land cover CLC2012 map. Following a similar procedure as described in Horálek et al. (2007), the exposure of forest areas (as defined above) has been calculated for each country, for the same four European regions as for crops and for Europe as a whole.

Table 4.4 gives the absolute and relative forest area where the Critical Level (CL) as defined in UNECE (2004) and the value 20 000  $\mu\text{g}\cdot\text{m}^{-3}\cdot\text{h}$  (which is equal to the earlier used Reporting Value, RV, as was defined in the repealed ozone directive 2002/3/EC) are exceeded. Next to the forest area in exceedance, the table presents the frequency distribution of the forest area over some exposure classes.

The Critical Level was exceeded in 2016 at about 63 % of all European forested area. For the areas excluding Turkey it was at about 60 %, which is the second lowest exceedance observed for the twelve-year period 2005 – 2016 (Table 6.4). As in previous years, most countries continue to have in 2016 considerable forest areas in excess to the CL, with specifically almost all forest area in southern and central & eastern European countries.

In this context, it should be mentioned that the AOT40 indicator probably is not the best proxy for the vegetation damage. E.g., it does not take into account that the Mediterranean vegetation closes its stomata in the warmest and driest season protecting itself from the exposure to ozone. A flux approach – as done e.g. in the EMEP model – taking into account the reduced deposition when stomata are closed would be better. However, there is still a damage to Mediterranean forests – e.g. the Aleppo pine in southern France seems to be quite sensitive to ozone exposure and suffering damage, UNECE (2016).

Table 4.3 Agricultural area exposure and exceedance, ozone indicator AOT40 for vegetation, 2016

Country	Agricultural Area, 2016					Percentage of agricultural area, 2016 [%]				
	Total area [km <sup>2</sup> ]	> LTO (6 000 µg.m <sup>-3</sup> .h)		> TV (18 000 µg.m <sup>-3</sup> .h)		< 6 000 µg.m <sup>-3</sup> .h	6 000 - 12 000 µg.m <sup>-3</sup> .h	12 000 - 18 000 µg.m <sup>-3</sup> .h	18 000 - 27 000 µg.m <sup>-3</sup> .h	> 27 000 µg.m <sup>-3</sup> .h
		[km <sup>2</sup> ]	[%]	[km <sup>2</sup> ]	[%]					
Albania	8041	8041	100	7286	91			9.4	90.6	
Austria	26862	26862	100	1911	7.1		1.0	91.9	7.1	
Belgium	17544	11564	65.9			34.1	65.9			
Bosnia-Herzegovina	17830	17830	100				52.9	47.1		
Bulgaria	57550	57266	99.5	481	0.8	0.5	66.8	31.8	0.8	
Croatia	22535	22535	100	1867	8.3		16.6	75.1	8.3	0.0
Cyprus	4304	4304	100	4193	97			2.6	95.1	2.3
Czechia	44966	44966	100	11	0.0		2.0	98.0	0.0	
Denmark (excl. Faroes)	31924	14660	45.9			54.1	45.8	0.2		
Estonia	14318	2160	15.1			84.9	15.1	0.0		
Finland	28370	2637	9			90.7	9.3			
France (metropolitan)	325895	164460	50.5	10062	3.1	49.5	40.2	7.2	3.1	0.0
Germany	204146	199292	97.6	8	0.0	2.4	64.0	33.6	0.0	
Greece	50469	50469	100	45119	89.4			10.6	74.2	15.2
Hungary	61298	61297	100	89	0.1	0.0	49.5	50.4	0.1	
Iceland	2456					100				
Ireland	46761	274	0.6			99	0.6			
Italy	156406	156406	100	137059	87.6		0.1	12.3	77.6	10.0
Latvia	26873	13263	49.4			50.6	49.4	0.0		
Liechtenstein	39	39	100	7.5	19			80.6	19.4	
Lithuania	39018	32295	82.8			17.2	82.8	0.0		
Luxembourg	1376	1180	86			14.2	86			
Malta	124	124	100	124	100				100.0	
Monaco										
Montenegro	2231	2231	100	302	13.6		1.1	85.3	13.6	
Netherlands	23886	14607	61.2			38.8	61.1	0.0		
North Macedonia	9237	9237	100	5633	61.0			39.0	61.0	0.0
Norway	15669	452	2.9			97.1	2.9			
Poland	186164	186149	100.0	484	0.3	0.0	49.9	49.9	0.3	
Portugal (excl. Az., Mad.)	41515	41515	100.0	4	0.0		87.2	12.8	0.0	
Romania	135971	74505	54.8			45.2	53.7	1.1		
San Marino	41	41	100	33	81			19.5	80.5	
Serbia (incl. Kosovo*)	47350	47350	100	236	0.5		35.7	63.8	0.5	
Slovakia	23234	23234	100.0	2	0.0		21.3	78.7	0.0	
Slovenia	7070	7070	100	1482	21.0		0.6	78.4	21.0	0.0
Spain (excl. Canarias)	236224	229112	97.0	92841	39.3	3.0	21.4	36.3	39.0	0.3
Sweden	38581	16078	41.7			58.3	41.6	0.0		
Switzerland	11795	11790	100	269	2.3	0.0	15.1	82.6	2.2	0.1
Turkey	338487	323807	96	150269	44.4	4.3	20.0	31.3	42.2	2.2
United Kingdom (& dep.)	137243	4891	3.6			96.4	3.6			
<b>Total</b>	<b>2443805</b>	<b>1883995</b>	<b>77.1</b>	<b>459770</b>	<b>18.8</b>	<b>22.9</b>	<b>32.9</b>	<b>25.4</b>	<b>17.5</b>	<b>1.3</b>
<b>Total without Turkey</b>	<b>2105318</b>	<b>1560188</b>	<b>74.1</b>	<b>309501</b>	<b>14.7</b>	<b>25.9</b>	<b>34.9</b>	<b>24.5</b>	<b>13.5</b>	<b>1.2</b>
<b>EU-28</b>	<b>1990139</b>	<b>1462686</b>	<b>73.5</b>	<b>295735</b>	<b>14.9</b>	<b>26.5</b>	<b>35.5</b>	<b>23.2</b>	<b>13.6</b>	<b>1.2</b>
France over 45N	258413	96978	37.5	205	0.1	62.5	33.5	4.0	0.1	
France below 45N	67482	67482	100	9857	14.6		65.8	19.6	14.5	0.1
Kosovo*	4383	4383	100	236	5			94.6	5.4	
Serbia (excl. Kosovo*)	42967	42967	100				39.3	60.7		
Northern	194753	81546	41.9			58.1	41.8	0.0		
North-western	487679	129494	26.6	205	0.0	73.4	24.4	2.1	0.0	
Central & Eastern	752027	685401	91.1	3262	0.4	8.9	49.6	41.1	0.4	0.0
Southern	1009345	987554	97.8	456304	45.2	2.2	22.7	29.9	42.1	3.1

\*) under the UN Security Council Resolution 1244/99

Note 1: Country not included due to the lack of land cover data: Andorra.

Note 2: The percentage value "0.0" indicates an exposed agricultural area exists, but is small and estimated less than 0.05 %. Empty cells mean no agricultural area in exposure.

Table 4.4 Forested area exposure and exceedance, ozone indicator AOT40 for forests, 2016

Country	Forested area, 2016					Percentage of forested area, 2016 [%]				
	Total area [km <sup>2</sup> ]	> CL (10 000 µg.m <sup>-3</sup> .h)		> RV (20 000 µg.m <sup>-3</sup> .h)		< 10 000 µg.m <sup>-3</sup> .h	10 000 - 20 000 µg.m <sup>-3</sup> .h	20 000 - 30 000 µg.m <sup>-3</sup> .h	30 000 - 50 000 µg.m <sup>-3</sup> .h	> 50 000 µg.m <sup>-3</sup> .h
		[km <sup>2</sup> ]	[%]	[km <sup>2</sup> ]	[%]					
Albania	7572	7572	100	7572	100			0.0	100.0	
Austria	36999	36999	100	36988	100		0.0	73.1	26.9	
Belgium	6085	5947	97.7			2.3	97.7			
Bosnia-Herzegovina	23469	23469	100	21860	93		6.9	89.9	3.3	
Bulgaria	34798	34798	100	32466	93.3		6.7	47.3	46.0	
Croatia	19868	19868	100	19407	98		2.3	77.3	20.3	
Cyprus	1524	1524	100	1524	100				99.3	0.7
Czechia	26246	26246	100	26246	100			99.0	1.0	
Denmark (excl. Faroes)	3671	1471	40.1	0	0.0	59.9	40.1	0.0		
Estonia	20952	1322	6.3			93.7	6.3			
Finland	205795	371	0.2			99.8	0.2			
France (metropolitan)	141542	136372	96.3	64618	45.7	3.7	50.7	25.1	20.1	0.4
Germany	108509	108121	99.6	80743	74.4	0.4	25.2	74.2	0.2	
Greece	24957	24957	100	24957	100			0.2	87.8	12.0
Hungary	17185	17185	100	15528	90.4		9.6	89.6	0.8	
Iceland	424					100				
Ireland	3691					100.0				
Italy	79208	79208	100.0	79208	100.0			1.5	89.8	8.7
Latvia	24041	2286	9.5			90.5	9.5			
Liechtenstein	85	85	100	85	100			9.5	90.5	
Lithuania	18871	10679	56.6	25	0.1	43.4	56.5	0.1		
Luxembourg	928	874	94			5.9	94.1			
Malta	2	2	100	2	100				100.0	
Monaco	0.44	0.44	100	0.44	100				84.1	15.9
Montenegro	5832	5832	100	5832	100			20.0	80.0	
Netherlands	3099	2796	90.2			9.8	90.2			
North Macedonia	8216	8216	100	8216	100				100.0	0
Norway	103616	2042	2.0			98.0	2.0			
Poland	96165	96163	100.0	47141	49.0	0.0	51.0	49.0		
Portugal (excl. Az., Mad.)	20116	20116	100.0	16671	82.9		17.1	82.8	0.0	
Romania	71842	71764	100	17033	23.7	0.1	76.2	23.7	0.0	
San Marino	6	6	100	6	100				100.0	
Serbia (incl. Kosovo)	27108	27108	100	27077	100		0.1	60.5	39.3	
Slovakia	19964	19964	100	17224	86.3		13.7	84.5	1.7	
Slovenia	11524	11524	100	11487	100		0.3	44.8	54.8	
Spain (excl. Canarias)	110018	108183	98.3	87674	79.7	1.7	18.6	29.6	50.0	0.1
Sweden	261977	21478	8.2			91.8	8.2			
Switzerland	12401	12401	100	12364	100		0.3	56.9	41.8	1.1
Turkey	115599	113076	98	85391	74	2.2	23.9	26.7	42.5	4.7
United Kingd. (& dep.)	20434	339	1.7			98.3	1.7			
<b>Total</b>	<b>1694337</b>	<b>1060363</b>	<b>62.6</b>	<b>747344</b>	<b>44.1</b>	<b>37.4</b>	<b>18.5</b>	<b>25.4</b>	<b>17.8</b>	<b>1.0</b>
<b>Total without Turkey</b>	<b>1578738</b>	<b>947287</b>	<b>60.0</b>	<b>661953</b>	<b>41.9</b>	<b>40.0</b>	<b>18.1</b>	<b>25.3</b>	<b>16.0</b>	<b>0.7</b>
<b>EU-28</b>	<b>1389969</b>	<b>860541</b>	<b>61.9</b>	<b>578940</b>	<b>41.7</b>	<b>38.1</b>	<b>20.3</b>	<b>25.4</b>	<b>15.5</b>	<b>0.8</b>
France over 45N	89165	83994	94.2	26042	29.2	5.8	65.0	23.2	6.0	
France below 45N	52377	52377	100	38576	73.7		26.3	28.5	44.0	1.1
Kosovo*	4304	4304	100	4304	100			4.0	96.0	
Serbia (excl. Kosovo)*	22804	22804	100	22773	100		0.1	71.2	28.7	
Northern	638922	39649	6.2	26	0.0	93.8	6.2	0.0		
North-western	123826	93950	75.9	26042	21.0	24.1	54.8	16.7	4.3	
Central & Eastern	424194	423725	100	285818	67.4	0.1	32.5	59.8	7.6	0.0
Southern	507395	503038	99.1	435459	85.8	0.9	13.3	30.6	52.0	3.2

\*) under the UN Security Council Resolution 1244/99

Note 1: Country not included due to the lack of land cover data: Andorra.

Note 2: The percentage value "0.0" indicates an exposed forested area exists, but is small and estimated less than 0.05 %. Empty cells mean: no forested area in exposure.



## 5 NO<sub>2</sub> and NO<sub>x</sub>

Annual average maps for NO<sub>2</sub> (related to protection of human health) and for NO<sub>x</sub> (related to protection of vegetation) were produced and presented in the regular mapping report for the first time for year 2014 (Horálek et al., 2017b).

The methodology for creating the concentration maps follows the same principle as for the rest of pollutants: a linear regression model on the basis of European wide station measurement data, followed by kriging of the residuals produced from that regression model (residual kriging).

The map on NO<sub>2</sub> is based on an improved mapping methodology developed in Horálek et al. (2017c, 2018b). The map layers are created for the rural, urban background and urban traffic areas separately on a grid at 1x1 km resolution. Subsequently, the urban background and urban traffic map layers are merged together using the gridded road data into one urban map layer. This urban map layer is further combined with the rural map layer into the final NO<sub>2</sub> map using a population density grid at 1x1 km resolution. We present this final combined map in this 1x1 km grid resolution.

The map of the vegetation-related indicator NO<sub>x</sub> annual average is created on a grid at 2x2 km resolution, based on rural background measurements only, as vegetation is considered not to be extensively present at urban and suburban areas. Hence, this map is applicable to rural areas only. The resolution is chosen equally to the one of the vegetation indicator for ozone.

Annex 3 provides details on the regression and kriging parameters applied for deriving the maps, as well as the uncertainty analysis of the maps.

### 5.1 NO<sub>2</sub> – Annual mean

#### 5.1.1 Concentration maps

The AQ Directive (EU, 2008) sets two limit values (LV) for NO<sub>2</sub> for the human health protection. The first one is an annual LV (ALV) at the level of 40 µg·m<sup>-3</sup>. This is the same concentration level as recommended by the World Health Organization for the NO<sub>2</sub> annual average as the Air Quality Guideline (WHO, 2005). The second one is an hourly LV (HLV, 200 µg·m<sup>-3</sup> not to be exceeded on more than 18 hours per year). The HLV has been exceeded in 2016 at only 1.3 % of all the reporting stations (EEA, 2018b). In view of this low number of exceedances, the short-term LV has not been included in the mapping procedures.

Map 5.1 presents the final combined concentration 1x1 km gridded map for the 2016 NO<sub>2</sub> annual average as the result of interpolation and merging of the separate maps as described in Annex 1.

Supplementary data used in the linear regression are in principle the same as in Horálek et al. (2017c). For rural areas they consist of EMEP model output, altitude, OMI satellite data, wind speed, population density and land cover; for urban background areas these are EMEP model output, altitude, OMI satellite data, wind speed, population density and land cover; for traffic areas the EMEP model output, altitude, and OMI satellite data are used (Annex 3).

According to Map 5.1, the areas where the ALV of 40 µg·m<sup>-3</sup> was exceeded include urbanized parts of some large cities, particularly Milan, Rome, Paris, Turin, Barcelona, Madrid, Naples, Lyon, London, Munich, Athens, Istanbul, Ankara, and some other smaller Turkish cities. Some other cities show NO<sub>2</sub> levels above 30 µg·m<sup>-3</sup>, e.g. in Germany, Italy, the Netherlands, Belgium, United Kingdom, Turkey. The most of the European area shows NO<sub>2</sub> levels below 20 µg·m<sup>-3</sup>, with most of the rural areas below 10 µg·m<sup>-3</sup>. Some

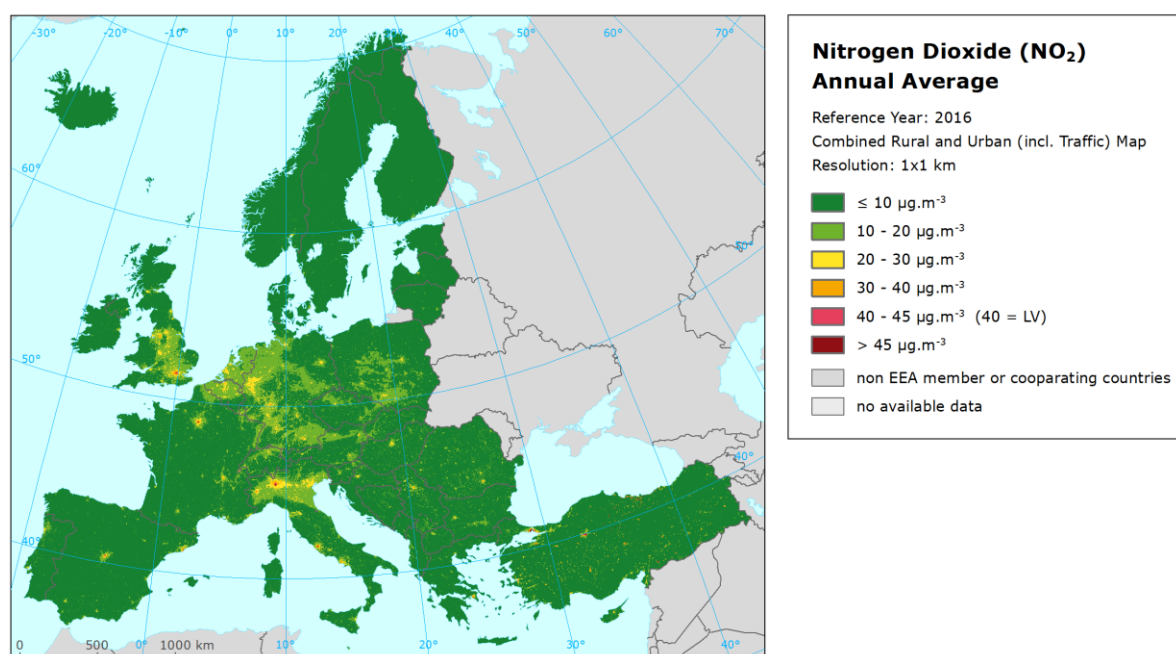
larger areas above  $20 \mu\text{g}\cdot\text{m}^{-3}$  can be found in the Po valley, the Benelux, the German Ruhr region, in central and southern England, in the Île de France and around Rome.

It should be noted that the interpolated map is created at 1x1 km only and as such refers to the rural and urban *background* situations only, while the exceedances of the NO<sub>2</sub> limit values occur mostly at local *hotspots* such as dense traffic locations and densely urbanised and industrialised areas. Although the urban traffic map layer is used in the map creation, the traffic locations are smoothed in the 1x1 km resolution.

The relative mean uncertainty of the NO<sub>2</sub> annual average map is 28 % for rural, 32 % for urban background and 26 % for urban traffic areas (Annex 3).

In order to provide more complete information of the air quality across Europe, the final combined map including the measurement data at station points is presented in Map A5.8 of Annex 5.

*Map 5.1 Concentration map of NO<sub>2</sub> annual average, 2016*



### 5.1.2 Population exposure

Table 5.1 gives the population frequency distribution for a limited number of exposure classes calculated on a grid of 1x1 km resolution, as well as the population-weighted concentration for individual countries and for Europe as a whole according to Equation A1.7 of Annex 1.

The human exposure to NO<sub>2</sub> has been calculated based on the improved methodology as developed in Horálek et al. (2017c). The population exposure is calculated according to Equation A1.6 of Annex I, i.e. it is calculated separately for urban areas directly influenced by traffic and for the background (both rural and urban) areas, in order to better reflect the population exposed to traffic. Based on this, the different concentration levels in urban background and traffic areas inside the 1x1 km grid cells are taken into account.



Table 5.1 Population exposure and population-weighted concentration, NO<sub>2</sub> annual average 2016

Country		Population [inhbs . 1000]	NO <sub>2</sub> annual average, exposed population [%]						Population weighted conc. [µg.m <sup>-3</sup> ]
			< 10 µg.m <sup>-3</sup>	< LV 10 - 20 µg.m <sup>-3</sup>	20 - 30 µg.m <sup>-3</sup>	30 - 40 µg.m <sup>-3</sup>	> LV 40 - 45 µg.m <sup>-3</sup>	> 45 µg.m <sup>-3</sup>	
Albania	AL	2 876	30.7	52.8	13.9	2.6			13.7
Andorra	AD	72	1.0	3.9	94.6	0.1	0.4		18.2
Austria	AT	8 700	12.6	49.2	26.3	10.0	1.3	0.5	18.9
Belgium	BE	11 311	1.8	45.9	39.2	12.0	1.0	0.1	21.7
Bosnia & Herzegovina	BA	3 516	30.6	60.5	8.2	0.7			13.2
Bulgaria	BG	7 154	12.6	46.6	38.1	2.7			18.8
Croatia	HR	4 191	27.1	50.0	21.8	1.1			15.2
Cyprus	CY	1 184	13.4	7.9	67.2	9.2	2.5		24.0
Czechia	CZ	10 554	15.8	68.7	13.6	1.8	0.1		15.2
Denmark	DK	5 707	63.6	26.0	9.4	1.0	0.1		10.4
Estonia	EE	1 316	66.5	30.0	3.4				7.8
Finland	FI	5 487	65.4	32.0	2.6				8.0
France (metropolitan)	FR	64 561	28.1	42.6	18.1	5.9	2.1	3.1	17.3
Germany	DE	82 176	5.4	47.5	39.7	4.8	1.3	1.3	20.2
Greece	GR	10 784	24.0	36.8	16.6	15.1	5.2	2.3	19.6
Hungary	HU	9 830	13.2	64.9	18.2	3.3	0.4		16.6
Iceland	IS	333	44.1	54.0	1.8				10.1
Ireland	IE	4 726	49.0	40.0	9.2	1.8			11.0
Italy	IT	60 666	7.3	37.6	38.0	11.9	2.8	2.3	22.1
Latvia	LV	1 969	44.3	36.8	18.4	0.5			12.0
Liechtenstein	LI	38	1.3	85.3	12.1	1.3			17.8
Lithuania	LT	2 889	39.8	53.8	4.9	1.5			11.7
Luxembourg	LU	576	4.8	40.0	47.6	7.6			20.7
Malta	MT	450	11.6	78.2	5.6	5			14.9
Monaco	MC	38			78	22			26.8
Montenegro	ME	622	30.3	65.4	4.3	0.0			11.9
Netherlands	NL	16 979	0.6	49.2	45.0	4.9	0.3		20.5
North Macedonia	MK	2 071	7.5	64.7	25.5	2.4			17.4
Norway	NO	5 211	42.4	41.6	13.5	1.9	0.6		12.4
Poland	PL	37 967	23.1	55.4	19.8	1.3	0.4	0.1	15.2
Portugal (excl. Az., Mad.)	PT	9 839	25.9	49.3	21.6	3.1	0.1		15.3
Romania	RO	19 760	18.2	49.7	23.7	7.2	0.4	0.7	17.6
San Marino	SM	33	4.7	90.8		5			16.3
Serbia (incl. Kosovo*)	RS	8 848	16.2	45.5	29.6	8.6	0.2		18.4
Slovakia	SK	5 426	18.6	74.7	5.4	1.3			13.5
Slovenia	SI	2 064	24.9	53.7	20.3	1.2			15.4
Spain (excl. Canarias)	ES	44 305	14.5	43.4	25.1	11.2	3.8	1.9	20.0
Sweden	SE	9 851	43.5	51.0	4.6	0.9			10.7
Switzerland	CH	8 327	5.2	51.4	37.1	4.8	1.3	0.1	19.7
Turkey	TR	78 741	24.4	9.6	20.1	22.9	9.7	13.4	26.9
United Kingdom (& dep.)	UK	65 383	6.8	35.5	43.8	10.9	1.2	1.8	21.8
Total		616 531	17.2	41.0	27.9	8.7	2.4	2.7	19.6
			94.8				5.2		
Total without Turkey		537 790	16.2	45.3	29.0	6.8	1.5	1.3	18.6
			97.2				2.8		
EU-28		505 806	15.9	45.0	29.3	7.0	1.5	1.4	18.7
			97.1				2.9		
Kosovo*	KS	1 772	21.0	68.0	11.0	0.0	0.0	0.0	14.4
Serbia (excl. Kosovo*)	RS	7 076	15.0	40.0	34.1	10.7	0.3	0.0	19.4

\*) under the UN Security Council Resolution 1244/99

Note: The percentage value "0.0" indicates that an exposed population exists, but it is small and estimated lesser than 0.05 %. Empty cells mean no population in exposure.

Thus – contrary to other pollutants – the population exposure refer not only to the rural and urban *background* areas, but to the urban *traffic* locations as well. However, it should be mentioned that the

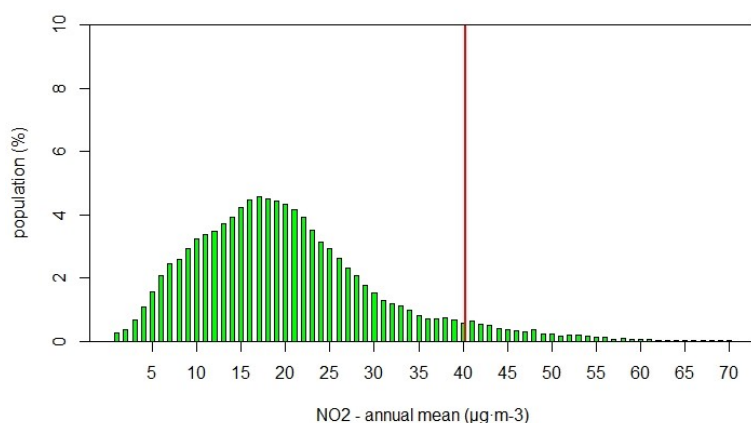
population density data in 1x1 km only is used. It means that contrary to the concentration levels, the population density is constant inside the 1x1 grid cells. This shortcoming can increase the uncertainty of the population exposure results.

It has been estimated that in 2016 about 5 % of the European population and about 3 % of both the total European population without Turkey and the EU-28 population lived in areas with NO<sub>2</sub> annual average concentrations above the EU limit value of 40 µg·m<sup>-3</sup>. CSI004 (EEA, 2017c) estimates that about 7 % of the population in urban agglomerations in the EU-28 was exposed in 2016 to levels above the EU limit value. The difference with the estimated 3 % in Table 5.1 is mainly because the EEA accounts for the urban population in the agglomerations only. Whereas, Table 5.1 provides estimates including the population in rural areas, smaller cities and villages.

The European-wide population-weighted concentration of the NO<sub>2</sub> annual average for 2016 is estimated to be about 20 µg·m<sup>-3</sup>, while for the EU-28 only it is about 19 µg·m<sup>-3</sup>.

Figure 5.1 shows, for the whole mapped area, the population frequency distribution for exposure classes of 1 µg·m<sup>-3</sup>. The frequency distribution is centred around 17-18 µg·m<sup>-3</sup>.

*Figure 5.1 Population frequency distribution, NO<sub>2</sub> annual average, 2016*



## 5.2 NO<sub>x</sub> – Annual mean

### 5.2.1 Concentration maps

The AQ Directive (EU, 2008) sets a Critical Level (CL) for the protection of vegetation for the NO<sub>x</sub> annual mean at 30 µg·m<sup>-3</sup>. According to this directive, the sampling points targeted at the protection of vegetation and natural ecosystems shall be in general sited more than 20 km away from agglomerations or more than 5 km away from other built-up areas. Thus, only the observations at rural background stations are used for the NO<sub>x</sub> mapping and the resulting map is representative for rural areas only.

The number of NO<sub>x</sub> measurement stations is limited. The mapping of the NO<sub>x</sub> annual average is therefore performed on the basis of an approach presented in Horálek et al. (2007). This approach derives additional *pseudo* NO<sub>x</sub> annual mean concentrations from NO<sub>2</sub> annual mean measurement concentrations and increases as such the number and spatial coverage of NO<sub>x</sub> 'data points', and applies these data to the NO<sub>x</sub> mapping. Section A1.1 of Annex 1 provides some details.

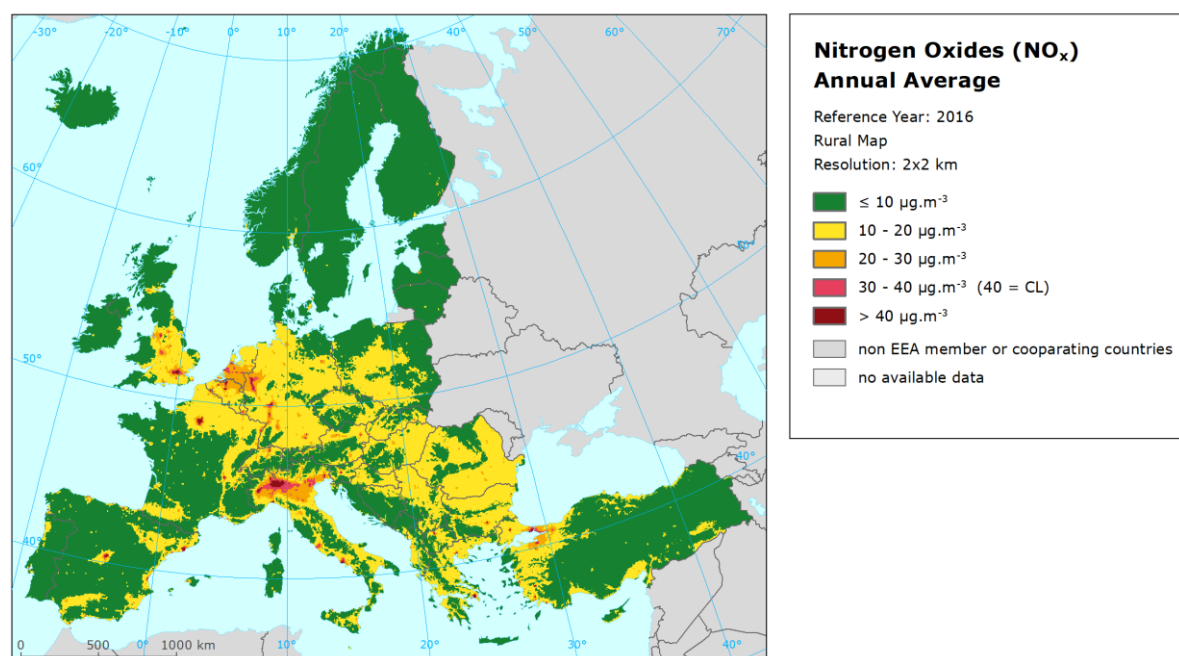
Map 5.2 presents the concentration map of NO<sub>x</sub> annual average. It concerns rural areas only, representing an indicator for vegetation exposure to NO<sub>x</sub>.

Most of the European area shows NO<sub>x</sub> levels below 20 µg·m<sup>-3</sup>. However, at the Po valley, southern part of the Netherlands, northern Belgium, the German Ruhr region and around some larger European cities (typically being the national capitals) elevated NO<sub>x</sub> concentrations above the Critical Level (CL) are observed. Furthermore, around many larger European cities concentrations just below the CL are observed. These concentrations are expected to be the result of large emissions from transport in and around the cities, as well as energy production and industrial facilities taking place at these areas. However, this is relevant only if there is vegetation around those larger cities.

The NO<sub>x</sub> annual average rural map has a relative mean uncertainty of 50 %.

The NO<sub>x</sub> annual average rural map including the data measured at rural background stations is presented in Map A5.9 of Annex 5. The map illustrates the lack of the NO<sub>x</sub> rural stations in the Balkan area.

*Map 5.2 Concentration map of NO<sub>x</sub> annual average, rural map, 2016*



Vegetation exposure is not calculated for NO<sub>x</sub>, as the critical level (CL) applies actually to vegetation only, which is by nature mostly allocated in rural areas where there is limited CL exceedance observed. Therefore, the vegetation exposure exceedance would occur in limited vegetation areas only and, as such, is considered not to provide essential information from the European scale perspective. Furthermore, contrary to vegetation exposure to high ozone concentrations in Europe that leads to considerable damage, vegetation exposure to NO<sub>x</sub> pollution is of minor importance in terms of actual impacts. On the other hand, NO<sub>x</sub> concentrations contribute in part to the total N-deposition, which leads to acidifying and eutrophying effects on vegetation. These effects, especially eutrophication, are still very important in Europe (e.g. De Wit et al., 2016). However, these effects on vegetation cannot be easily expressed by an exposure table.

Concerning the potential exposure estimate of vegetation and natural ecosystems to NO<sub>x</sub> there is an additional dilemma: which receptor types should be selected to estimate the exposure and critical level exceedance of vegetation and natural ecosystems? An option would be the use of CLC classes (e.g. like in Horálek et al., 2008); nevertheless this classification is too general. Other option would be the

NATURA2000 database. However, that source contains a wide series of receptor types, species and classes. It would need serious additional efforts to conclude on the most relevant set of receptors from the NATURA 2000 geographical database.

## 6 Exposure trend estimates

### 6.1 Mapping and exposure results

This paper has presented the interpolated maps for 2016 on the PM<sub>10</sub>, PM<sub>2.5</sub>, ozone and NO<sub>2</sub> *human health* related air pollution indicators. It presents the maps of annual average and the 90.4 percentile of PM<sub>10</sub> daily mean, annual average for PM<sub>2.5</sub>, the 93.2 percentile of maximum daily 8-hour means and the SOMO35 for ozone, and the annual average for NO<sub>2</sub>, together with the tables with the frequency distribution of the estimated population exposures and exceedances per country and as European totals.

Furthermore, interpolated maps on ozone and NO<sub>x</sub> *vegetation* related air pollution indicators have been produced. It involves the map of ozone indicators AOT40 for vegetation and AOT40 for forests, including the tables with the frequency distribution of estimated land area exposures and exceedances per country and the European totals. In addition, the map of the annual average for NO<sub>x</sub> has been produced, but without exposure estimates.

A mapping approach similar to previous years (Horálek et al., 2018a) based primarily on observational data was used. With the interpolated air pollution maps and exposure estimates for the year 2016, a twelve-year (for PM<sub>10</sub> and ozone) resp. nine-year (for PM<sub>2.5</sub>) and four-year (for NO<sub>2</sub>) overview on comparable exposure estimates has been obtained. In this chapter we provide these multi-annual overviews of exposure estimates for each of the indicators of PM<sub>10</sub>, PM<sub>2.5</sub> and ozone, including the trend analysis. Maps for the nitrogen related indicators were not produced on a multi-annual basis so far and therefore only four-time series for NO<sub>2</sub> annual average can be given in this chapter.

For the human health indicators, we express the exposure estimates on the one hand as population-weighted concentration and on the other hand as percentage of population exposed to concentrations above the limit/target value. For the vegetation related indicators, the exposure estimates are expressed as the agricultural or forest areas exposed to concentrations above defined thresholds.

It should be noted that the percentage of population resp. agricultural or forest area exposed is a less robust indicator compared to the population resp. agricultural or forest weighted concentration, as a small concentration increase (or decrease) may lead to a major increase (or decrease) of population resp. agricultural or forest area exposed, whereas that is not the case when taking the population-weighted concentration as indicator. Therefore, the trend analysis is done on basis of the population-weighted concentrations only.

When thinking about a trend, we should take into account (i) the meteorologically induced variations, (ii) the uncertainties involved in the interpolation (Annex 3), and (iii) the station densities and their spatial distributions over the European regions. Next to this, we should be aware that different trends in various parts of Europe may occur. However, bearing in mind these limitations we provide here a trend analysis for the period 2005 – 2016 on the population-weighted concentrations for Europe as a whole.

For comparability reasons, we present in this chapter the results for Europe as a whole without Turkey, because 2016 is the first year for which the area of Turkey has been mapped.

#### 6.1.1 Human health PM<sub>10</sub> indicators

Table 6.1 summarises over the twelve year period 2005 – 2016 for both *human health* PM<sub>10</sub> indicators the average concentration to which the European population has been exposed to, expressed as the population-weighted concentration, and the percentage of population exposed to PM<sub>10</sub> concentrations above the limit values (LV).

For years 2012 and 2013 both the 36<sup>th</sup> highest value and the 90.4 percentile of daily mean(s) have been calculated. Their results demonstrate an underestimation of almost 1  $\mu\text{g}\cdot\text{m}^{-3}$  at the 36<sup>th</sup> highest daily mean. One may conclude that this underestimation has its cause in the fact that when calculating the 36<sup>th</sup> highest daily mean value there is no correction for the missing values at incomplete time series. Whereas the 90.4 percentile of daily mean(s) adjusts for such missing data.

*Table 6.1 Population-weighted concentration and percentage of the European population (without Turkey) exposed to concentrations above the PM<sub>10</sub> limit values (LV) for the protection of health for 2005 to 2016*

PM <sub>10</sub>		2005	2006	2007	2008	2009	2010	2011	2012	2013	2014	2015	2016
<b>Annual average</b>													
Population-weighted concentration	[ $\mu\text{g}\cdot\text{m}^{-3}$ ]	28.0	28.5	26.2	24.8	24.6	24.3	22.1	22.7	22.2	21.1	21.2	20.2
Population exposed > LV (40 $\mu\text{g}\cdot\text{m}^{-3}$ )	[%]	13.3	10.3	6.8	5.8	6.0	5.2	2.5	3.4	2.6	2.0	0.6	1.7
<b>36<sup>th</sup> highest daily mean / 90.4 percentile of daily means</b>													
Population-weighted concentration	[ $\mu\text{g}\cdot\text{m}^{-3}$ ]	36 <sup>th</sup> highest d. m.	46.8	47.8	44.1	41.3	41.2	41.9	39.0	39.7	38.6		
Population-weighted concentration	[ $\mu\text{g}\cdot\text{m}^{-3}$ ]	90.4 perc. of d. m.							40.6	39.4	37.1	36.9	35.7
Population exposed > LV (50 $\mu\text{g}\cdot\text{m}^{-3}$ )	[%]	36 <sup>th</sup> highest d. m.	34.3	35.7	26.2	19.4	16.5	20.6	15.8	16.5	16.4		
Population exposed > LV (50 $\mu\text{g}\cdot\text{m}^{-3}$ )	[%]	90.4 perc. of d. m.							17.7	17.3	13.3	12.9	14.0

In 2016 the population exposed to *annual mean* concentrations of PM<sub>10</sub> above the limit value of 40  $\mu\text{g}\cdot\text{m}^{-3}$  is 1.7 % of the total population, which is the second lowest percentage of the complete time series and somewhat higher compared to the previous year. Furthermore, it is estimated that European inhabitants living in background (neither hot-spot nor industrial) areas – regardless if these areas are urban or rural – are exposed on average to an annual mean PM<sub>10</sub> concentration of 20  $\mu\text{g}\cdot\text{m}^{-3}$ , the least in the twelve years' time series. The comparison of results for 2015 and 2016 illustrates well that a clear decrease in the population-weighted concentrations does not lead necessarily to the decrease in the population exceedance exposure numbers.

In the twelve-year series, the number of people living in areas with concentrations above the LV is the lowest in the latest three years, 2014 – 2016. The overall picture of the population-weighted concentration of the European totals (i.e. totals of 40 European countries considered) demonstrates a downward trend of -0.7  $\mu\text{g}\cdot\text{m}^{-3}\cdot\text{year}^{-1}$  for the years 2005 – 2016 (for methodology, see Annex 1, Section A1.2). This trend is statistically significant (at the strongest level \*\*\*, i.e. 0.001) and expresses a mean decrease of 0.7  $\mu\text{g}\cdot\text{m}^{-3}$  per year.

In 2016 about 14 % of the European population lived in areas where the PM<sub>10</sub> daily limit value (calculated using the *90.4 percentile*) was exceeded, being slightly more than in the previous two years. The overall European population-weighted concentration of the 90.4 percentile of the PM<sub>10</sub> daily means (formerly the 36<sup>th</sup> highest daily mean) for the background areas is estimated to be about 36  $\mu\text{g}\cdot\text{m}^{-3}$  in 2016, which is the lowest of the twelve years considered. This is the case even though possible underestimated data have been used in the 2005 – 2011 calculations. The population-weighted concentration of the European total (i.e. total of 40 European countries considered) demonstrate a statistically significant (at the strongest level \*\*\*, i.e. 0.001) downward trend of -0.9  $\mu\text{g}\cdot\text{m}^{-3}$  per year for the years 2005 – 2016.

### 6.2.1 Human health PM<sub>2.5</sub> indicator

Table 6.2 summarises for *human health PM<sub>2.5</sub> indicator* (annual average) the population-weighted concentration and the percentage of European population exposed to PM<sub>2.5</sub> concentrations above the EU LV for the years 2007 to 2016 (without 2009, for which neither a map nor a population exposure was prepared).

Table 6.2 Population-weighted concentration and percentage of the European population (without Turkey) exposed to concentrations above the PM<sub>2.5</sub> limit value (LV) for the protection of health for 2007 to 2016

PM <sub>2.5</sub>	2007	2008	2009	2010	2011	2012	2013	2014	2015	2016
<b>Annual average</b>										
Population-weighted concentration [µg·m <sup>-3</sup> ]	16.3	16.3	not mapped	16.8	15.9	15.6	15.3	14.1	14.2	13.4
Population exposed > LV (25 µg·m <sup>-3</sup> ) [%]	7.8	7.6	not mapped	8.3	6.2	9.0	5.8	4.2	6.3	5.4

The percentage of population exposed in 2016 to annual mean concentrations of PM<sub>2.5</sub> above the LV of 25 µg·m<sup>-3</sup> is about 5 %, which is second lowest value of the limited time series. Furthermore, it is estimated that European inhabitants living in background (neither hot-spot, nor industrial) areas – regardless if these areas are urban or rural – are exposed on average to an annual mean PM<sub>2.5</sub> concentration of about 13 µg·m<sup>-3</sup>, being the lowest in the time series.

The trend analysis of the population-weighted concentrations across the period 2007 – 2016 for Europe as a whole has been executed. At European scale a statistical significant (at the strongest level \*\*\*, i.e. 0.001) downward trend can be observed, estimated to be -0.4 µg·m<sup>-3</sup> per year.

### 6.3.1 Human health ozone indicators

Table 6.3 summarises for both *human health ozone indicators* the exposure levels of the European inhabitants in terms of population-weighted concentrations. Furthermore, it presents the percentage of European population exposed to concentrations above the target value (TV) and above a level of 6 000 µg·m<sup>-3</sup>·d for the SOMO35 for the years 2005 to 2016.

Table 6.3 Population-weighted concentration and percentage of the European population (without Turkey) exposed to concentrations above the target value (TV) threshold for the protection of health and a SOMO35 threshold of 6 000 µg·m<sup>-3</sup>·d for 2005 to 2016

Ozone	2005	2006	2007	2008	2009	2010	2011	2012	2013	2014	2015	2016
<b>26<sup>th</sup> highest daily max. 8-h mean / 93.2 percentile of daily max. 8-h means</b>												
Popul.-weighted concentr. [µg·m <sup>-3</sup> ]	112.1	118.2	110.7	109.8	108.1	106.8	108.9	107.9	108.3			
Popul.-weighted concentr. [µg·m <sup>-3</sup> ]								108.5	108.9	102.9	110.4	104.8
Popul. exposed > TV (120 µg·m <sup>-3</sup> )	31.6	51.4	27.1	15.0	16.0	16.3	16.5	20.7	15.0			
Popul. exposed > TV (120 µg·m <sup>-3</sup> )								21.9	15.9	5.6	34.0	8.4
<b>SOMO35</b>												
Popul.-weighted concentration [µg·m <sup>-3</sup> ·d]	4706	5167	4411	4275	4275	3917	4414	4279	4088	3500	4312	3619
Popul. exposed > 6000 µg·m <sup>-3</sup> ·d [%]	27.0	29.5	28.1	19.6	24.6	16.6	23.6	24.5	18.8	9.4	22.2	11.7

The table presents the results obtained with the 1x1 km merging resolution as tested on the 2006 data in Horálek et al (2010), then recomputed for 2005 and 2007, and finally implemented fully on the 2008 data and onwards. For 2012 and 2013, both the 26<sup>th</sup> highest value and the 93.2<sup>nd</sup> percentile of maximum daily 8-hour mean(s) have been calculated. It demonstrates an underestimation of about 0.6 µg·m<sup>-3</sup> at the 26<sup>th</sup> maximum daily 8-hour mean, which is caused by the fact that when calculating this indicator there is no correction for the missing values in the incomplete measurement time series.

Using the *93.2 percentile of ozone maximum daily 8-hour means* it is estimated that 8 % of the population lived in 2016 in areas where concentrations were above the ozone target value (TV) of 120 µg·m<sup>-3</sup>, which is the second lowest number of the twelve years period. The overall European population-weighted ozone concentration in terms of the 93.2 percentile maximum daily 8-hour means in the background areas is estimated at about 105 µg·m<sup>-3</sup>, which is also the second lowest value of the whole twelve years period (please be aware that for 2005–2011 the 26<sup>th</sup> highest value of the maximum daily eight-hour mean was considered instead).



Examining the time series 2005 – 2016, it can be concluded that 2006, but also 2005 and 2015 are exceptional years with high ozone concentrations, leading to increased exposure levels compared to the other nine years. The years 2014 and 2016 show the lowest exposure levels in the twelve years' time series.

The trend analysis of the population-weighted concentrations for the 93.2 percentile of the maximum daily 8-hour means across the period 2005 – 2016 for Europe as a whole has been executed. The population-weighted concentration of the European totals (i.e. totals of 40 European countries considered) demonstrates a statistically significant (at the weakest level +, i.e. 0.1) downward trend of  $-0.7 \mu\text{g}\cdot\text{m}^{-3}$  per year.

A similar tendency is observed for the *SOMO35*. In 2006 – 2007 almost one-third of the population lived in areas where a level of  $6\,000 \mu\text{g}\cdot\text{m}^{-3}\cdot\text{d}^3$  was exceeded, with the highest level in 2006. In the period of 2008 – 2016, it fluctuates from about 17 % to 25 % of the population, except 2014 with about 9 % and 2016 with about 12 %.

The population-weighted *SOMO35* concentrations show a quite similar kind of pattern over time. Trend analysis on the population-weighted concentration of the European totals shows a slightly downward trend of about  $-95 \mu\text{g}\cdot\text{m}^{-3}\cdot\text{d}$ , for the period 2005 – 2016, which is statistically significant (at the lowest level +, i.e. 0.1) and expresses a mean decrease of about  $95 \mu\text{g}\cdot\text{m}^{-3}\cdot\text{d}$  per year.

#### 6.4.1 Vegetation and forest ozone indicators

Exposure indicators describing the *agricultural and forest areas exposed to accumulated ozone concentrations above defined thresholds* are summarised in Table 6.4. Those thresholds are the target value (TV) of  $18\,000 \mu\text{g}\cdot\text{m}^{-3}\cdot\text{h}$  and the long-term objective (LTO) of  $6\,000 \mu\text{g}\cdot\text{m}^{-3}\cdot\text{h}$  for the AOT40 for vegetation, and the former Reporting Value (RV) of  $20\,000 \mu\text{g}\cdot\text{m}^{-3}\cdot\text{h}$  and the Critical Level (CL) of  $10\,000 \mu\text{g}\cdot\text{m}^{-3}\cdot\text{h}$  for the AOT40 for forests.

*Table 6.4 Percentages of the European agricultural and forest area (without Turkey) exposed to ozone concentrations above the target value (TV) and the long-term objective (LTO) for AOT40 for vegetation, and above Critical Level (CL) and Reporting Value (RV) for AOT40 for forests and agricultural- and forest-weighted concentrations for 2005 to 2016*

Ozone	2005	2006	2007	2008	2009	2010	2011	2012	2013	2014	2015	2016
<b>AOT40 for vegetation</b>												
Agricultural area % > TV ( $18\,000 \mu\text{g}\cdot\text{m}^{-3}\cdot\text{h}$ ) [%]	48.5	69.1	35.7	37.8	26.0	21.3	19.2	30.0	22.1	17.8	31.4	14.7
Agricultural area % > LTO ( $6\,000 \mu\text{g}\cdot\text{m}^{-3}\cdot\text{h}$ ) [%]	88.8	97.6	77.5	95.5	81.0	85.4	87.9	86.4	81.0	85.5	79.7	74.1
Agricultural-weighted concentration ( $\mu\text{g}\cdot\text{m}^{-3}\cdot\text{h}$ )	17481	22344	14597	15214	13157	13310	13255	14041	12838	12427	14223	10942
<b>AOT40 for forests</b>												
Forest area exposed > RV ( $20\,000 \mu\text{g}\cdot\text{m}^{-3}\cdot\text{h}$ ) [%]	59.1	69.4	48.4	50.2	49.2	49.3	53.0	47.2	44.1	37.7	52.4	41.9
Forest area exposed > CL ( $10\,000 \mu\text{g}\cdot\text{m}^{-3}\cdot\text{h}$ ) [%]	76.4	99.8	62.1	79.6	67.4	63.4	68.6	65.0	67.2	68.2	59.8	60.0
Forest-weighted concentration ( $\mu\text{g}\cdot\text{m}^{-3}\cdot\text{h}$ )	25900	31154	23744	21951	23532	19625	21892	21580	21753	17124	21150	17573

In 2016, some 15 % of all agricultural land (crops) was exposed to accumulated ozone concentrations (AOT40 for vegetation) exceeding the target value (TV), which is the lowest percentage of the twelve years period. About 74 % of all agricultural land was exposed to levels in excess of the long-term objective (LTO), which is the lowest of all twelve years.

The trend analysis of the agricultural-weighted concentrations for the AOT40 for vegetation across the period 2005 – 2016 for Europe as a whole has been executed. The agricultural-weighted concentration

<sup>3</sup> Note that the  $6\,000 \mu\text{g}\cdot\text{m}^{-3}\cdot\text{d}$  does not represent a health-related legally binding 'threshold'. In this and previous papers it concerns a somewhat arbitrarily chosen threshold to facilitate the discussion of the observed distributions of *SOMO35* levels in their spatial and temporal context. For motivation of this choice, see Section 4.2.



of the European totals (i.e. totals of 40 European countries considered) demonstrates a statistically significant (at the level \*\*, i.e. 0.01) downward trend of  $-446 \mu\text{g}\cdot\text{m}^{-3}\cdot\text{h}$  per year.

For the ozone indicator AOT40 for *forests* the level of  $20\,000 \mu\text{g}\cdot\text{m}^{-3}\cdot\text{h}$  (earlier used Reporting Value, RV) was exceeded in about 42 % of the European forest area in 2016, which is the second lowest of the whole time series. The forest area exceeding the Critical Level (CL) was in 2016 about 60 %, which is – together with 2015 – the lowest percentage of the twelve years period.

The temporal pattern of the AOT40 for forests exceedances shows some similarity with those of the AOT40 for vegetation, despite their different definitions and receptors and their natural difference in area type characteristics and occurrence. Their annual variability is, however, heavily dependent on meteorological variability.

The trend analysis of the forest-weighted concentrations for the AOT40 for forests across the period 2005 – 2016 for Europe as a whole has been executed. The forest-weighted concentration of the European totals (i.e. totals of 40 European countries considered) demonstrates a statistically significant (at the level \*\*, i.e. 0.01) downward trend of  $-659 \mu\text{g}\cdot\text{m}^{-3}\cdot\text{h}$  per year.

### 6.5.1 Human health $\text{NO}_2$ indicators

Table 6.5 summarises for the *human health  $\text{NO}_2$  indicator* the exposure levels of the European inhabitants in terms of population-weighted concentrations. Furthermore, it presents the percentage of European population exposed to concentrations above the limit value (LV) of  $40 \mu\text{g}\cdot\text{m}^{-3}$  for the years 2005, 2010 and 2013 to 2016.

*Table 6.5 Population-weighted concentration and percentage of the European population (without Turkey) exposed to concentrations above the  $\text{NO}_2$  limit value (LV) of  $40 \mu\text{g}\cdot\text{m}^{-3}$  for the protection of health for 2005 to 2016*

$\text{NO}_2$	2005	2006	2007	2008	2009	2010	2011	2012	2013	2014	2015	2016
<b>Annual average</b>												
Population-weighted concentration [ $\mu\text{g}\cdot\text{m}^{-3}$ ]	23.3	not	23.3	not	not	22.1	not	not	19.4	18.6	18.8	18.6
Population exposed > LV ( $40 \mu\text{g}\cdot\text{m}^{-3}$ ) [%]	7.9	mapped		mapped	mapped	4.9	mapped	mapped	3.2	2.8	3.2	2.8

In 2016 the population exposed to  $\text{NO}_2$  annual mean concentrations above the limit value of  $40 \mu\text{g}\cdot\text{m}^{-3}$  is 2.8 % of the total population, which is the same as in 2014 and slightly less than in 2013 and 2015. Furthermore, it is estimated that European inhabitants are exposed on average to an annual mean  $\text{NO}_2$  concentration of  $19 \mu\text{g}\cdot\text{m}^{-3}$ , about the same as in the three previous years.



## References

Cressie N (1993). Statistics for spatial data. Wiley series, New York.

Danielson JJ, Gesch DB (2011). Global multi-resolution terrain elevation data 2010 (GMTED2010): U.S. Geological Survey Open-File Report 2011–1073. <https://lta.cr.usgs.gov/GMTED2010>

De Leeuw F (2012). AirBase: a valuable tool in air quality assessments at a European and local level. ETC/ACM Technical Paper 2012/4.

[http://www.eionet.europa.eu/etcs/etc-atni/products/etc-atni-reports/etcacm\\_tp\\_2012\\_4\\_airbase\\_aqassessment](http://www.eionet.europa.eu/etcs/etc-atni/products/etc-atni-reports/etcacm_tp_2012_4_airbase_aqassessment)

Denby B, Schaap M, Segers A, Builtjes P, Horálek J (2008). Comparison of two data assimilation methods for assessing PM<sub>10</sub> exceedances on the European scale. Atmospheric Environment 42, 7122–7134.

Denby B, Gola G, De Leeuw F, De Smet P, Horálek J (2011a). Calculation of pseudo PM<sub>2.5</sub> annual mean concentrations in Europe based on annual mean PM<sub>10</sub> concentrations and other supplementary data.

ETC/ACC Technical Paper 2010/9. [http://www.eionet.europa.eu/etcs/etc-atni/products/etc-atni-reports/etcacc\\_tp\\_2010\\_9\\_pseudo\\_pm2-5\\_stations](http://www.eionet.europa.eu/etcs/etc-atni/products/etc-atni-reports/etcacc_tp_2010_9_pseudo_pm2-5_stations)

Denby B, Horálek J, de Smet P, de Leeuw F (2011b). Mapping annual mean PM<sub>2.5</sub> concentrations in Europe: application of pseudo PM<sub>2.5</sub> station data. ETC/ACM Technical Paper 2011/5.

[http://www.eionet.europa.eu/etcs/etc-atni/products/etc-atni-reports/etcacm\\_tp\\_2011\\_5\\_spatialpm2-5mapping](http://www.eionet.europa.eu/etcs/etc-atni/products/etc-atni-reports/etcacm_tp_2011_5_spatialpm2-5mapping)

De Smet P, Horálek J, Coňková M, Kurfürst P, de Leeuw F, Denby B (2009). European air quality maps of ozone and PM<sub>10</sub> for 2006 and their uncertainty analysis. ETC/ACC Technical Paper 2008/8.

[http://www.eionet.europa.eu/etcs/etc-atni/products/etc-atni-reports/etcacc\\_tp\\_2008\\_8\\_spatagmaps\\_2006](http://www.eionet.europa.eu/etcs/etc-atni/products/etc-atni-reports/etcacc_tp_2008_8_spatagmaps_2006)

De Smet P, Horálek J, Coňková M, Kurfürst P, de Leeuw F, Denby B (2010). European air quality maps of ozone and PM<sub>10</sub> for 2007 and their uncertainty analysis. ETC/ACC Technical Paper 2009/9.

[http://www.eionet.europa.eu/etcs/etc-atni/products/etc-atni-reports/etcacc\\_tp\\_2009\\_9\\_spatagmaps\\_2007](http://www.eionet.europa.eu/etcs/etc-atni/products/etc-atni-reports/etcacc_tp_2009_9_spatagmaps_2007)

De Smet P, Horálek J, Coňková M, Kurfürst P, de Leeuw F, Denby B (2011). European air quality maps of ozone and PM<sub>10</sub> for 2008 and their uncertainty analysis. ETC/ACC Technical Paper 2010/10.

[http://www.eionet.europa.eu/etcs/etc-atni/products/etc-atni-reports/etcacc\\_tp\\_2010\\_10\\_spatagmaps\\_2008](http://www.eionet.europa.eu/etcs/etc-atni/products/etc-atni-reports/etcacc_tp_2010_10_spatagmaps_2008)

De Wit HA, Hettelingh JP, Harmens H (2016). Trends in ecosystem and health responses to long-range transported atmospheric pollutants. ICP Waters Report 125/2015.

[https://www.unece.org/fileadmin/DAM/env/documents/2016/AIR/Publications/Trends\\_in\\_ecosystem\\_and\\_health\\_responses\\_to\\_long-range\\_transported\\_atmospheric\\_pollutants.pdf](https://www.unece.org/fileadmin/DAM/env/documents/2016/AIR/Publications/Trends_in_ecosystem_and_health_responses_to_long-range_transported_atmospheric_pollutants.pdf)

ECMWF: Meteorological Archival and Retrieval System (MARS). <http://www.ecmwf.int/>

EEA (2008). ORNL Landsat 2008 Global Population Data conversion into EEA ETRS89-LAEA5210 1km grid (eea\_r\_3035\_1\_km\_landsat-eurmed\_2008, by Hermann Peifer of EEA).

EEA (2016). Corine land cover 2012 (CLC2012) raster data. 100x100m gridded version 18 (09/2016)

EEA (2018a). Air Quality e-Reporting. Air quality database. <https://www.eea.europa.eu/data-and-maps/data/aqereporting-8>

EEA (2018b). Air quality in Europe – 2018 Report. EEA Report 12/2018. <https://www.eea.europa.eu/publications/air-quality-in-europe-2018>

EEA (2018c). Exceedance of air quality limit values in urban areas. CSI004 indicator assessment. <https://www.eea.europa.eu/data-and-maps/indicators/exceedance-of-air-quality-limit-3/assessment-4>

EEA (2018d). Exposure of ecosystems to acidification, eutrophication and ozone. <https://www.eea.europa.eu/data-and-maps/indicators/exposure-of-ecosystems-to-acidification-14/assessment-1>

EEA (2018e). Guide for EEA map layout. EEA operational guidelines. January 2015, version 5. [https://www.eionet.europa.eu/gis/docs/GISguide\\_v5\\_EEA\\_Layout\\_for\\_map\\_production.pdf](https://www.eionet.europa.eu/gis/docs/GISguide_v5_EEA_Layout_for_map_production.pdf)

EU (2008). Directive 2008/50/EC of the European Parliament and of the Council of 21 May 2008 on ambient air quality and cleaner air for Europe. OJ L 152, 11.06.2008, 1-44. <http://eur-lex.europa.eu/LexUriServ/LexUriServ.do?uri=OJ:L:2008:152:0001:0044:EN:PDF>

Eurostat (2014). GEOSTAT 2011 grid dataset. Population distribution dataset. <http://ec.europa.eu/eurostat/web/gisco/geodata/reference-data/population-distribution-demography>

Eurostat (2018). Total population for European states for 2016. <http://epp.eurostat.ec.europa.eu/tgm/table.do?tab=table&language=en&pcode=tps00001&tableSelecti on=1&footnotes=yes&labeling=labels&plugin=1>

EMEP (2018). Transboundary particular matter, photo-oxidants, acidifying and eutrophying components. EMEP Report 1/2018. [http://emep.int/publ/reports/2018/EMEP\\_Status\\_Report\\_1\\_2018.pdf](http://emep.int/publ/reports/2018/EMEP_Status_Report_1_2018.pdf)

Gilbert, RO (1987). Statistical Methods for Environmental Pollution Monitoring. Van Nostrand Reinhold, New York.

Guerreiro C, Horálek J, de Leeuw F, Couvidat F (2016). Benzo(a)pyrene in Europe: Ambient air concentrations, population exposure and health effects, Environmental Pollution 214, 657–667.

Horálek J, Kurfürst P, Denby B, de Smet P, de Leeuw F, Brabec M, Fiala J (2005). Interpolation and assimilation methods for European scale air quality assessment and mapping. Part II: Development and testing new methodologies. ETC/ACC Technical paper 2005/8. [http://www.eionet.europa.eu/etcs/etc-atni/products/etc-atni-reports/etcacc\\_techpaper\\_2005\\_8\\_spatial\\_aq\\_dev\\_test\\_part\\_ii](http://www.eionet.europa.eu/etcs/etc-atni/products/etc-atni-reports/etcacc_techpaper_2005_8_spatial_aq_dev_test_part_ii)

Horálek J, Denby B, de Smet P, de Leeuw F, Kurfürst P, Swart R, van Noije T (2007). Spatial mapping of air quality for European scale assessment. ETC/ACC Technical paper 2006/6. [http://www.eionet.europa.eu/etcs/etc-atni/products/etc-atni-reports/etcacc\\_techpaper\\_2006\\_6\\_spat\\_aq](http://www.eionet.europa.eu/etcs/etc-atni/products/etc-atni-reports/etcacc_techpaper_2006_6_spat_aq)

Horálek J, de Smet P, de Leeuw F, Denby B, Kurfürst P, Swart R (2008). European air quality maps for 2005 including uncertainty analysis. ETC/ACC Technical paper 2007/7. [http://www.eionet.europa.eu/etcs/etc-atni/products/etc-atni-reports/etcacc\\_tp\\_2007\\_7\\_spatial\\_aq\\_maps\\_ann\\_interpol](http://www.eionet.europa.eu/etcs/etc-atni/products/etc-atni-reports/etcacc_tp_2007_7_spatial_aq_maps_ann_interpol)

Horálek J, de Smet P, de Leeuw F, Coňková M, Denby B, Kurfürst P (2010). Methodological improvements on interpolating European air quality maps. ETC/ACC Technical Paper 2009/16.

[http://www.eionet.europa.eu/etcs/etc-atni/products/etc-atni-reports/etcacc\\_tp\\_2009\\_16\\_improv\\_spatialmapping](http://www.eionet.europa.eu/etcs/etc-atni/products/etc-atni-reports/etcacc_tp_2009_16_improv_spatialmapping)

Horálek J, Kurfürst P, de Smet P (2014). Additional 2011 European air quality maps. ETC/ACM Technical Paper 2014/5. [http://www.eionet.europa.eu/etcs/etc-atni/products/etc-atni-reports/etcacm\\_tp\\_2014\\_5\\_add\\_2011\\_aqmaps](http://www.eionet.europa.eu/etcs/etc-atni/products/etc-atni-reports/etcacm_tp_2014_5_add_2011_aqmaps)

Horálek J, de Smet P, Kurfürst P, de Leeuw F, Benešová N (2015). European air quality maps of PM and ozone for 2012 and their uncertainty. ETC/ACM Technical Paper 2014/4. [http://www.eionet.europa.eu/etcs/etc-atni/products/etc-atni-reports/etcacm\\_tp\\_2014\\_4\\_spatialmaps\\_2012](http://www.eionet.europa.eu/etcs/etc-atni/products/etc-atni-reports/etcacm_tp_2014_4_spatialmaps_2012)

Horálek J, Benešová N, de Smet P (2016a). Application of FAIRMODE Delta tool to evaluate interpolated European air quality maps for 2012. ETC/ACM Technical Paper 2015/2. [http://www.eionet.europa.eu/etcs/etc-atni/products/etc-atni-reports/etcacm\\_tp\\_2015\\_2\\_delta\\_evaluation\\_aqmaps2012](http://www.eionet.europa.eu/etcs/etc-atni/products/etc-atni-reports/etcacm_tp_2015_2_delta_evaluation_aqmaps2012)

Horálek J, de Smet P, Kurfürst P, de Leeuw F, Benešová N (2016b). European air quality maps of PM and ozone for 2013 and their uncertainty. ETC/ACM Technical Paper 2015/5. [http://www.eionet.europa.eu/etcs/etc-atni/products/etc-atni-reports/etcacm\\_tp\\_2015\\_5\\_aqmaps2013](http://www.eionet.europa.eu/etcs/etc-atni/products/etc-atni-reports/etcacm_tp_2015_5_aqmaps2013)

Horálek J, Guerreiro C., de Leeuw, de Smet (2017a). Potential improvements on benzo(a)pyrene (BaP) mapping. ETC/ACM Technical Paper 2016/3. [http://www.eionet.europa.eu/etcs/etc-atni/products/etc-atni-reports/etcacm\\_tp\\_2016\\_3\\_bap\\_improved\\_mapping](http://www.eionet.europa.eu/etcs/etc-atni/products/etc-atni-reports/etcacm_tp_2016_3_bap_improved_mapping)

Horálek J, de Smet P, de Leeuw F, Kurfürst P, Benešová N (2017b). European air quality maps for 2014. ETC/ACM Technical Paper 2016/6. [http://www.eionet.europa.eu/etcs/etc-atni/products/etc-atni-reports/etcacm\\_tp\\_2016\\_6\\_aqmaps2014](http://www.eionet.europa.eu/etcs/etc-atni/products/etc-atni-reports/etcacm_tp_2016_6_aqmaps2014)

Horálek J, de Smet P, Schneider P, Kurfürst P, de Leeuw F (2017c). Inclusion of land cover and traffic data in NO<sub>2</sub> mapping methodology. ETC/ACM Technical Paper 2016/12. [http://www.eionet.europa.eu/etcs/etc-atni/products/etc-atni-reports/etcacm\\_tp\\_2016\\_12\\_lc\\_and\\_traffic\\_data\\_in\\_no2\\_mapping](http://www.eionet.europa.eu/etcs/etc-atni/products/etc-atni-reports/etcacm_tp_2016_12_lc_and_traffic_data_in_no2_mapping)

Horálek J, de Smet P, de Leeuw F, Kurfürst P, Benešová N (2018a). European air quality maps for 2015. ETC/ACM Technical Paper 2017/7. [http://www.eionet.europa.eu/etcs/etc-atni/products/etc-atni-reports/etcacm\\_tp\\_2017\\_7\\_aqmaps2015](http://www.eionet.europa.eu/etcs/etc-atni/products/etc-atni-reports/etcacm_tp_2017_7_aqmaps2015)

Horálek J, de Smet P, Schneider P, Maiheu P, de Leeuw F, Janssen S, Benešová N, Lefebvre W (2018b). Satellite data inclusion and kernel based potential improvements in NO<sub>2</sub> mapping. ETC/ACM Technical Paper 2017/14. [http://www.eionet.europa.eu/etcs/etc-atni/products/etc-atni-reports/etcacm\\_tp\\_2017\\_14\\_improved\\_aq\\_no2mapping](http://www.eionet.europa.eu/etcs/etc-atni/products/etc-atni-reports/etcacm_tp_2017_14_improved_aq_no2mapping)

IPCC (2010). Guidance note for lead authors of the IPCC Fifth Assessment Report on consistent treatment of uncertainties. Jasper Ridge, USA. <http://www.ipcc.ch/pdf/supporting-material/uncertainty-guidance-note.pdf>

JRC (2009). Population density disaggregated with Corine land cover 2000. 100x100 m grid resolution, EEA version popu01clcv5.tif of 24 Sep 2009. <http://www.eea.europa.eu/data-and-maps/data/population-density-disaggregated-with-corine-land-cover-2000-2>

Mareckova K, Pinterits M, Ullrich B, Wankmüller R, Burgstaller J, Tista M (2018). Inventory Review 2018. Review of emission data reported under the LRTAP Convention and NEC Directive. Stage 1 and 2 review

& Status of gridded and LPS data. EEA/CEIP Technical Report 2/2017.

[https://webdab01.umweltbundesamt.at/download/InventoryReport\\_2018\\_v2.pdf](https://webdab01.umweltbundesamt.at/download/InventoryReport_2018_v2.pdf)

NILU (2018). EBAS, database of atmospheric chemical composition and physical properties (NILU, Norway). <http://ebas.nilu.no/>

NMI (2017). EMEP/MSW-W modelled air concentrations and depositions. Gridded data for 2016 (2018 Reporting), EMEP01deg. [http://www.emep.int/mscw/mscw\\_ydata.html](http://www.emep.int/mscw/mscw_ydata.html)

ORNL (2008). ORNL LandScan high resolution global population data set. [http://www.ornl.gov/sci/landscan/landscan\\_documentation.shtml](http://www.ornl.gov/sci/landscan/landscan_documentation.shtml)

Simpson D, Benedictow A, Berge H, Bergström R, Emberson LD, Fagerli H, Hayman GD, Gauss M, Jonson JE, Jenkin ME, Nyíri A, Richter C, Semeena VS, Tsyro S, Tuovinen J-P, Valdebenito A, Wind P (2012). The EMEP MSC-W chemical transport model – technical description. Atmospheric Chemistry and Physics, 12, 7825–7865, doi:10.5194/acp-12-7825-2012. <http://www.atmos-chem-phys.net/12/7825/2012/acp-12-7825-2012.html>

UNECE (2004). Manual on methodologies and criteria for modelling and mapping critical loads and levels and air pollution effects, risks and trends. UNECE Convention on Long-range Transboundary Air Pollution. [http://www.icpmapping.org/Mapping\\_Manual](http://www.icpmapping.org/Mapping_Manual)

UNECE (2016). Forest condition in Europe. 2016 report of ICP Forests. UNECE Convention on Long-range Transboundary Air Pollution. [http://www.wsl.ch/info/mitarbeitende/schaub/ICPF\\_TR\\_2016.pdf](http://www.wsl.ch/info/mitarbeitende/schaub/ICPF_TR_2016.pdf)

WHO (2005). WHO Air quality guidelines for particulate matters, ozone, nitrogen dioxide and sulphur dioxide. Global update 2005. [http://www.who.int/phe/health\\_topics/outdoorair/outdoorair\\_agg/en/index.html](http://www.who.int/phe/health_topics/outdoorair/outdoorair_agg/en/index.html)

## Annex 1 – Methodology

### A1.1 Mapping method

Previous technical papers prepared by Horálek et al. (2005, 2007, 2008, 2010, 2014, 2017c), De Smet et al. (2011), Denby et al. (2011a, 2011b) discuss methodological developments and details on spatial interpolations and their uncertainties. No changes took place in the mapping methodology compared to the preceding report (Horálek et al., 2018a). This annex summarizes the currently applied method for all these indicators. The mapping method has been evaluated with the FAIRMODE Delta tool in Horálek et al. (2016a). The method can be described as the *Regression – Interpolation – Merging Mapping*.

#### Pseudo PM<sub>2.5</sub> and NO<sub>x</sub> station data estimation

To supplement PM<sub>2.5</sub> measurement data, in the mapping procedure we also use data from so-called *pseudo PM<sub>2.5</sub> stations*. These data are the estimates of PM<sub>2.5</sub> concentrations at the locations of PM<sub>10</sub> stations with no PM<sub>2.5</sub> measurement. These estimates are based on PM<sub>10</sub> measurement data and different supplementary data, using linear regression:

$$\hat{Z}_{PM2.5}(s) = c + b \cdot Z_{PM10}(s) + a_1 \cdot X_1(s) + \dots + a_n \cdot X_n(s) \quad (A1.1)$$

where  $\hat{Z}_{PM2.5}(s)$  is the estimated value of PM<sub>2.5</sub> at the station  $s$ ,  
 $Z_{PM10}(s)$  is the measurement value of PM<sub>10</sub> at the station  $s$ ,  
 $X_1(s), \dots, X_n(s)$  are the values of other supplementary variables at the station  $s$ ,  
 $c, b, a_1, \dots, a_n$  are the parameters of the linear regression model calculated based on the data at the points of measuring stations with both PM<sub>2.5</sub> and PM<sub>10</sub> measurements,  
 $n$  is the number of other supplementary variables used in the linear regression model (apart from PM<sub>10</sub>).

When applying this estimation method, all background stations (either classified as rural, urban or suburban) are handled together. For details, see Denby et al. (2011b).

To supplement NO<sub>x</sub> measurement data, we estimate NO<sub>x</sub> values at the locations of NO<sub>2</sub> stations with no NO<sub>x</sub> data. The estimates are calculated similarly as in Horálek et al. (2007), using quadratic regression:

$$\hat{Z}_{NOx}(s) = a \cdot Z_{NO2}(s)^2 + b \cdot Z_{NO2}(s) + c \quad (A1.2)$$

where  $\hat{Z}_{NOx}(s)$  is the estimated value of NO<sub>x</sub> at the station  $s$ ,  
 $Z_{NO2}(s)$  is the measurement value of NO<sub>2</sub> at the station  $s$ ,  
 $a, b, c$  are the parameters of the quadratic regression calculated based on the data at the points of measuring stations with both NO<sub>x</sub> and NO<sub>2</sub> measurements.

#### Interpolation

The mapping method used is a linear regression model followed by kriging of the residuals produced from that model (residual kriging). Interpolation is therefore carried out according to the relation:

$$\hat{Z}(s_0) = c + a_1 \cdot X_1(s_0) + a_2 \cdot X_2(s_0) + \dots + a_n \cdot X_n(s_0) + \eta(s_0) \quad (A1.3)$$



where  $\hat{Z}(s_0)$  is the estimated value of the air pollution indicator at the point  $s_0$ ,  
 $X_1(s_0), X_2(s_0), \dots, X_n(s_0)$  are the  $n$  number of individual supplementary variables at the point  $s_0$   
 $c, a_1, a_2, \dots, a_n$  are the  $n+1$  parameters of the linear regression model calculated based on the data at the points of measurement,  
 $\eta(s_0)$  is the spatial interpolation of the residuals of the linear regression model at the point  $s_0$  calculated based on the residuals at the points of measurement.

For different pollutants and area types (rural, urban background, and in the case of NO<sub>2</sub> also urban traffic), different supplementary data are used, depending on their improvement to the fit of the regression. Ordinary kriging is used to interpolate the residuals:

$$\hat{R}(s_0) = \sum_{i=1}^N \lambda_i R(s_i), \sum_{i=1}^N \lambda_i = 1, \quad (\text{A1.4})$$

where  $R(s_i)$  are the residuals in the points of the measuring stations  $s_i$ ,  
 $\lambda_1, \dots, \lambda_N$  are the weights estimated based on variogram,  
 $N$  is the number of the stations used in the interpolation.

The variogram (as a measure of a spatial correlation) is estimated using a spherical function (with parameters *nugget*, *sill*, *range*). For details, see Horálek et al. (2007), Section 2.3.5 and Cressie (1993).

For PM<sub>2.5</sub> and NO<sub>x</sub>, both measurement data and the estimated data from the pseudo stations are used.

For the PM<sub>10</sub> and PM<sub>2.5</sub> indicators we apply, prior to linear regression and interpolation, a logarithmic transformation to measurement and EMEP model concentrations. In the case of PM<sub>2.5</sub> rural map layer creation, population density is also log-transformed. After interpolation, we apply a back-transformation. For details, see De Smet et al. (2011) and Denby et al. (2008). In the case of urban background PM<sub>2.5</sub> map, we do not use any supplementary data – we apply just lognormal kriging.

For the vegetation related indicators (AOT40 for vegetation and forests and NO<sub>x</sub>) we only construct rural maps based on rural background stations, based on the assumption that no vegetation is located in urban areas. For the health related indicators, we construct the rural and urban background map layers (and for NO<sub>2</sub> also urban traffic map layer) separately and then we merge them.

### **Merging of rural and urban background (and urban traffic) map layers**

Health related indicator map layers for PM<sub>10</sub>, PM<sub>2.5</sub> and ozone are constructed (using linear regression with kriging of its residuals) for the rural and urban background areas separately on a grid at 10x10 km resolution. The rural map is based on rural background stations and the urban background map on urban and suburban background stations. Subsequent to this, the rural and urban background maps are merged into one combined air quality indicator map using a European-wide population density grid at 1x1 km resolution. For the 1x1 km grid cells with a population density less than a defined value of  $\alpha_1$ , we select the rural map value and for grid cells with a population density greater than a defined value  $\alpha_2$ , we select the urban background map value. For areas with population density within the interval  $(\alpha_1, \alpha_2)$  a weighting function of  $\alpha_1$  and  $\alpha_2$  is applied (for details and the setting of the parameters  $\alpha_1$  and  $\alpha_2$ , see Horálek et al., 2005, 2007, 2010). This applies to the grid cells where the estimated rural value is lower (PM<sub>10</sub> and PM<sub>2.5</sub>) or higher (ozone), than the estimated urban background map value. In the exceptional cases when this criterion does not hold, we apply a joint urban/rural map layer (created using all background stations regardless their type), as far as its value lies in between the rural and urban background map value. For details, see De Smet et al. (2011).

Summarising, the separate rural, urban and joint urban/rural map layers are constructed at a resolution of 10x10 km; their merging however takes place on the basis of the 1x1 km resolution population density grid, resulting in a final combined pollutant indicator map on this 1x1 km resolution grid. This map is used both for the population exposure estimates and for presentational purposes.

In the case of NO<sub>2</sub>, separate map layers are created for rural, urban background and urban traffic areas on a grid at 1x1 km resolution. The rural background map layer is based on the rural background stations, the urban background map layer on the urban and the suburban background stations, and the urban traffic map layer on the urban and the suburban traffic stations. For different map layers (rural, urban background, urban traffic) different supplementary data are used, depending on their improvement to the fit of the regression. The three map layers are merged into one final map using a weighting procedure

$$\hat{Z}_F(s_0) = (1 - w_U(s_0)) \cdot \hat{Z}_R(s_0) + w_U(s_0)(1 - w_T(s_0)) \cdot \hat{Z}_{UB}(s_0) + w_U(s_0)w_T(s_0) \cdot \hat{Z}_T(s_0) \quad (\text{A1.5})$$

where  $\hat{Z}_F(s_0)$  is the resulting estimated concentration in a grid cell  $s_0$  for the final map,  
 $\hat{Z}_{UB}(s_0)$  is the estimated concentration in a grid cell  $s_0$  for the urban background map layer,  
 $\hat{Z}_R(s_0)$  is the estimated concentration in a grid cell  $s_0$  for the rural background map layer,  
 $\hat{Z}_T(s_0)$  is the estimated concentration in a grid cell  $s_0$  for the urban traffic map layer,  
 $w_U(s_0)$  is the weight representing the ratio of the urban character of the a grid cell  $s_0$ ,  
 $w_T(s_0)$  is the weight representing the ratio of areas exposed to traffic air quality in a grid cell  $s_0$ .

The weight  $w_U(s_0)$  is based on the population density grid, while  $w_T(s_0)$  is based on the buffers around the roads. For further details, see Horálek et al. (2017b and references therein).

In all calculations and map presentations the EEA standard projection ETRS89-LAEA5210 (also known as ETRS89 / LAEA Europe, see [www.epsg-registry.org](http://www.epsg-registry.org)) is used. The interpolation and mapping domain consists of the areas of all EEA member and cooperating countries, as far as they fall into the EEA map extent *Map\_2c* (EEA, 2018e). The mapping area covers the whole Europe apart from Belarus, Moldova, Ukraine and the European parts of Russia and Kazakhstan.

## A1.2 Calculation of population and vegetation exposure

Population and vegetation exposure estimates are based on the interpolated concentration maps, population density data and land cover data.

### Population exposure

Population exposure for individual countries and for Europe as a whole is calculated for PM<sub>10</sub>, PM<sub>2.5</sub> and ozone from the air quality maps and population density data, both at 1x1 km resolution. For each concentration class, the total population per country as well as the European-wide total is determined.

For NO<sub>2</sub>, the population exposure is calculated separately for the areas where the air quality is considered to be directly influenced by traffic and for the background (both rural and urban) areas. For

each concentration class ' $j$ ', the percentage population per country as well as the European-wide total is determined according to:

$$P_j = \frac{\sum_{i=1}^N I_{Bij}(1 - w_U(i)w_T(i))p_i + \sum_{i=1}^N I_{Tij}w_U(i)w_T(i)p_i}{\sum_{i=1}^N p_i} \cdot 100 \quad (\text{A1.6})$$

where  $P_j$  is the percentage population living in areas of the  $j$ -th concentration class in either the country or in Europe as a whole,  
 $p_i$  is the population in the  $i$ -th grid cell,  
 $I_{Bij}$  is the Boolean 0-1 indicator showing whether the background air quality concentration (estimated by the combined rural/urban background map layer) in the  $i$ -th grid cell is within the  $j$ -th concentration class ( $I_{Bij} = 1$ ), or not ( $I_{Bij} = 0$ ),  
 $I_{Tij}$  is the Boolean 0-1 indicator showing whether the traffic air quality concentration in the  $i$ -th grid cell is within the  $j$ -th concentration class ( $I_{Tij} = 1$ ), or not ( $I_{Tij} = 0$ ),  
 $N$  is the number of grid cells in the country or in Europe as a whole.

In addition, we express per-country and European-wide exposure as the population-weighted concentration, i.e. the average concentration weighted according to the population in a 1x1 km grid cell:

$$\hat{c} = \frac{\sum_{i=1}^N c_i p_i}{\sum_{i=1}^N p_i} \quad (\text{A1.7})$$

where  $\hat{c}$  is the population-weighted average concentration in the country or in the whole of Europe,  
 $p_i$  is the population in the  $i^{\text{th}}$  grid cell,  
 $c_i$  is the concentration in the  $i^{\text{th}}$  grid cell (based on the final merged map),  
 $N$  is the number of grid cells in the country or in Europe as a whole.

### Estimation of trends

For detecting and estimating the trends in time series of annual values of population exposure, the non-parametric Mann-Kendall's test for testing the presence of the monotonic increasing or decreasing trend is used. Next to that, the non-parametric Sen's method for estimating the slope of a linear trend is executed. For details, see Gilbert (1987). The significance of the Mann-Kendal test is shown by the usual way, i.e. + for 0.1, \* for 0.05, \*\* for 0.01, and \*\*\* for 0.001.

### Vegetation (and forest) exposure

Vegetation (and forest) exposure for individual countries and for Europe as a whole is calculated based on the air quality maps and land cover data, both in 2x2 km grid resolution. For each concentration class, the total vegetation (and forest) area per country as well as European-wide is determined.

Next to this, we express per-country and European-wide exposure as the vegetation (forest)-weighted concentration, i.e. the average concentration weighted according to the vegetation (and forest) in a 1x1 km grid cell, similarly like in Eq. A1.7.

### A1.3 Methods for uncertainty analysis

The uncertainty estimation of the European map is based on cross-validation. The cross-validation method computes the quality of the spatial interpolation for each measurement point from all available information except from the point in question, i.e. it withholds one data point and then makes a prediction at the spatial location of that point. This procedure is repeated for all measurement points in the available set. The predicted and measurement values at these points are plotted in the form of a scatter plot. With help of statistical indicators the quality of the predictions is demonstrated objectively. The advantage of the nature of this cross-validation technique is that it enables evaluation of the quality of the predicted values at locations without measurements, as long as they are within the area covered by the measurements.

In addition, we make a simple comparison between the point measurements and interpolated values of the 10x10 km grid for the separate rural and urban maps and the 1x1 km grid for the final combined maps, for the health-related indicators, resp. the 2x2 km grid in the case of AOT40 and NO<sub>x</sub>. Note that the grid cell value is the averaged result of the interpolation in this grid cell area. The interpolated value within a grid cell will only approximate the predicted value(s) at the station(s) lying within that cell.

Another method to estimate uncertainties is based on geostatistical theory: together with the prediction, the prediction standard error is computed at all the grid cells, which represents in fact the interpolation uncertainty map (see Cressie, 1993 for a detailed discussion). Based on the concentration and the uncertainty map, the exceedance probability map is created.

#### Cross-validation

The results of cross-validation are described by the statistical indicators and scatter plots. The main indicator used is root mean squared error (RMSE) and additional is bias (mean prediction error, MPE):

$$RMSE = \sqrt{\frac{1}{N} \sum_{i=1}^N (\hat{Z}(s_i) - Z(s_i))^2} \quad (A1.8)$$

$$bias(MPE) = \frac{1}{N} \sum_{i=1}^N (\hat{Z}(s_i) - Z(s_i)) \quad (A1.9)$$

where  $Z(s_i)$  is the air quality indicator value derived from the measured concentration at the  $i^{th}$  point,  $i = 1, \dots, N$ ,

$\hat{Z}(s_i)$  is the air quality estimated indicator value at the  $i^{th}$  point using other information, without the indicator value derived from the measured concentration at the  $i^{th}$  point,

$N$  is the number of the measuring points.

Next to the RMSE expressed in the absolute units, one could express this uncertainty in relative terms by relating the RMSE to the mean of the air pollution indicator value for all stations:

$$RRMSE = \frac{RMSE}{\bar{Z}} \cdot 100 \quad (A1.10)$$

where  $RRMSE$  is the relative RMSE, expressed in percent,

$\bar{Z}$  is the arithmetic average of the indicator values  $Z(s_1), \dots, Z(s_N)$ , as derived from measurement concentrations at the station points  $i = 1, \dots, N$ .

Other indicators are  $R^2$  and the regression equation parameters *slope* and *intercept*, following from the scatter plot between the predicted (using cross-validation) and the observed concentrations.

RMSE should be as small as possible, bias (MPE) should be as close to zero as possible,  $R^2$  should be as close to 1 as possible, slope  $a$  should be as close to 1 as possible, and intercept  $c$  should be as close to zero as possible (in the regression equation  $y = a.x + c$ ).

In the cross-validation of PM<sub>2.5</sub> and NO<sub>x</sub>, only stations with PM<sub>2.5</sub>, resp. NO<sub>x</sub>, measurement data are used (not the pseudo PM<sub>2.5</sub>, resp. NO<sub>x</sub>, stations).

### Comparison of the point measurement and interpolated grid values

The comparison of point measurement and predicted grid values is described by the linear regression equation and its parameters and statistical values. The comparison is executed separately for rural and urban background maps and for the final combined map. In the case of PM<sub>2.5</sub> and NO<sub>x</sub>, only the stations with actual PM<sub>2.5</sub> resp. NO<sub>x</sub> measurement data are used (not the pseudo PM<sub>2.5</sub> resp. NO<sub>x</sub> stations).

The point observation – point cross-validation prediction analysis (Annex 3) describes interpolation performance at point locations when there is no observation (as it follows the leave-one-out approach). In this case, the smoothing effect of the interpolation is most prevalent.

The point observation – grid prediction approach indicates performance of the value for the 10x10 km (resp. 2x2 km or 1x1 km) grid cell with respect to the observations that are located within that cell. As such, some variability is due to smoothing but it also includes smoothing due to spatial averaging into the 10x10 km (2x2 km, 1x1 km) grid cells. As such, the point-grid validation approach tells us how well our interpolated and aggregated grid values approximate the measurements at the actual station (point) locations. Whereas the point-point approach tells us how well our interpolated values estimate the indicator at a point where there is no actual measurement at that location, under the constrained that the point lies within the area covered by measurements.

### Exceedance probability mapping

The maps with the probability of exceedance (PoE) of a specific threshold value (e.g. limit or target value) are constructed using the concentration and uncertainty maps:

$$PoE(x) = 1 - \Phi\left(\frac{LV - C_c(x)}{\sigma_c(x)}\right) \quad (A1.11)$$

where  $PoE(x)$  is the probability of limit/target value (LV/TV) exceedance in the grid cell  $x$ ,  
 $\Phi()$  is the cumulative distribution function of the normal distribution,  
 $LV$  is the limit or target value of the relevant indicator,  
 $C_c(x)$  is the interpolated concentration in the grid cell  $x$ ,  
 $\sigma_c(x)$  is the standard error of the estimation in the grid cell  $x$ .

The standard error of the probability map of the combined (rural and urban background) map is calculated from the standard errors of the separate rural and urban background maps; see Horálek et al. (2008), Section 2.3 and De Smet et al. (2011), Chapter 2. The maps with the probability of threshold value exceedance (PoE) are constructed in 1 x 1 km grid resolution.

In the probability of exceedance maps in this paper, the areas with 33–50 % and 50–66 % probability of LV exceedance are marked in yellow and orange respectively. The yellow colour indicates the areas with the estimated concentrations below limit value, but for which there exists a *modest* probability of exceeding the limit. The orange coloured areas have estimated concentrations above the limit value, but with a *moderate* chance of non-exceedance caused by its accompanying uncertainty. On the contrary, the areas with 66–90 % and 90–100 % are marked with red colour in two shades, indicating

large or high probability of LV exceedance. Similarly, the areas with 0–10 % and 10–33 % are marked with green in two shades, indicating little or low probability of LV exceedance. Table A1.1 summarises the classes and terminology for probability (i.e. likelihood) that are distinguished in this paper.

*Table A1.1 Probability mapping classes and terminology use in this paper*

Map class colour	Percentage probability of threshold exceedance	Degree of probability (or likelihood) of exceedance	Likelihood of exceedance	
Green	0 – 10	Little	Very unlikely	More unlikely than likely
Light green	10 – 33	Low	Unlikely	
Yellow	33 – 50	Modest	About as likely as not	
Orange	50 – 66	Moderate	More likely than not	
Light red	66 – 90	Large		Likely
Dar red	90 – 100	High		Very likely

The probability classes are used based on the classification used in IPCC (2010). Its basic likelihood scale of “very likely”, “likely”, “about as likely as not”, “unlikely” and “very unlikely” is combined with an additional option of “more likely than not”.





## Annex 2 – Input data

The types of input data in this paper are not different from that of Horálek et al. (2017b). The air quality and meteorological data has been updated. No further changes in selecting and processing of the input data have been implemented. For readability of this paper, we reproduce here the list of the input data. The key data is the air quality measurements at the monitoring stations extracted from Air Quality e-Reporting database, including geographical coordinates (*latitude, longitude*). The supplementary data cover the whole mapping domain and are converted into the EEA reference projection ETRS89-LAEA5210 on a 10 x 10 km grid resolution (for health related indicators apart from NO<sub>2</sub>) resp. a 1x1 km grid resolution (for NO<sub>2</sub>). The data for the AOT40 maps of vegetation related indicators (particularly AOT40) were converted – like in the previous reports (Horálek et al., 2017b and references cited therein) – into a 2 x 2 km resolution to allow accurate land cover exposure estimates to be prepared for use in Core Set Indicator 005 of the EEA.

### A2.1 Air quality monitoring data

Air quality station monitoring data for the relevant year are extracted from the official EEA Air Quality e-Reporting database, made public on 25 April 2018, EEA (2018a). This data set is supplemented with several EMEP rural stations from the database EBAS (NILU, 2018) not reported to the Air Quality e-Reporting database. Specifically, 9 additional stations for PM<sub>10</sub>, 12 for PM<sub>2.5</sub>, 12 for NO<sub>2</sub> and 5 for NO<sub>x</sub> from the EBAS database are added. Only data from stations classified as *background* (for the three types of area, *rural, suburban* and *urban*) are used for most of the pollutants. *Industrial* and *traffic* station types are not considered; they represent local scale concentration levels not applicable at the mapping resolution employed. For NO<sub>2</sub>, next to the background stations, also the stations classified as *traffic* for the types of area *suburban* and *urban* are used.

The following pollutants and aggregations are considered:

- PM<sub>10</sub> – annual average [ $\mu\text{g}\cdot\text{m}^{-3}$ ], year 2016  
– 90.4 percentile of the daily average values [ $\mu\text{g}\cdot\text{m}^{-3}$ ], year 2016
- PM<sub>2.5</sub> – annual average [ $\mu\text{g}\cdot\text{m}^{-3}$ ], year 2016
- Ozone – 93.2 percentile of the maximum daily 8-hour average values [ $\mu\text{g}\cdot\text{m}^{-3}$ ], year 2016  
– SOMO35 [ $\mu\text{g}\cdot\text{m}^{-3}\cdot\text{day}$ ], year 2016  
– AOT40 for vegetation [ $\mu\text{g}\cdot\text{m}^{-3}\cdot\text{hour}$ ], year 2016  
– AOT40 for forests [ $\mu\text{g}\cdot\text{m}^{-3}\cdot\text{hour}$ ], year 2016
- NO<sub>2</sub> – annual average [ $\mu\text{g}\cdot\text{m}^{-3}$ ], year 2016
- NO<sub>x</sub> – annual average [ $\mu\text{g}\cdot\text{m}^{-3}$ ], year 2016
- NO – annual average [ $\mu\text{g}\cdot\text{m}^{-3}$ ], year 2016 (for the purposes of NO<sub>x</sub> mapping only)

The exact values of percentiles are actually 90.41 in the case of PM<sub>10</sub> daily means and 93.15 in the case of ozone maximum daily 8-hour means.

For a considerable number of stations NO<sub>x</sub> is measured, but it is not reported as such but separately as NO and NO<sub>2</sub>. For these stations reporting NO and NO<sub>2</sub> separately, the NO<sub>x</sub> concentrations were derived according to the equation

$$NO_x = NO_2 + \frac{46}{30} \cdot NO \quad (\text{A2.1})$$

In this equation, all components are expressed in  $\mu\text{g}\cdot\text{m}^{-3}$ , with a molecular mass for NO of  $30\text{ g}\cdot\text{mol}^{-1}$  and for NO<sub>2</sub> of  $46\text{ g}\cdot\text{mol}^{-1}$ .

SOMO35 is the annual sum of the differences between maximum daily 8-hour concentrations above  $70\text{ }\mu\text{g}\cdot\text{m}^{-3}$  (i.e. 35 ppb) and  $70\text{ }\mu\text{g}\cdot\text{m}^{-3}$ . AOT40 is the sum of the differences between hourly concentrations greater than  $80\text{ }\mu\text{g}\cdot\text{m}^{-3}$  (i.e. 40 ppb) and  $80\text{ }\mu\text{g}\cdot\text{m}^{-3}$ , using only observations between 08:00 and 20:00 CET, calculated over the three months from May to July for AOT40 for vegetation and over the six months from April to September for AOT40 for forests.

Only the stations with annual data coverage of at least 75 percent are used. In the case of SOMO35 and AOT40 indicators, a correction for the missing data is applied according to the equation

$$I_{corr} = I \cdot \frac{N_{max}}{N} \quad (\text{A2.2})$$

where  $I_{corr}$  is the corrected indicator (SOMO35, AOT40 for vegetation or AOT40 for forests),  
 $I$  is the value of the given indicator without any correction,  
 $N$  is the number of the available daily resp. hourly data in a year for the given station,  
 $N_{max}$  is the maximum possible number of the days or hours applicable for the given indicator.

For the  $x^{\text{th}}$  highest values (i.e. for the PM<sub>10</sub> indicator 36<sup>th</sup> highest daily mean and for the ozone indicator 26<sup>th</sup> highest maximum daily 8-hour running mean) used in earlier reports (Horálek et al., 2016b and references cited therein), no correction for missing data was applied. The most straightforward way to solve the missing data issue in these cases is to use percentiles instead of the  $x^{\text{th}}$  highest values. Since ETC/ACM Technical Paper 2016/6 with its 2014 maps, the 90.4 percentile of PM<sub>10</sub> daily means and the 93.2 percentile of ozone maximum daily 8-hour means is used.

For the indicators relevant to human health (i.e. for all PM<sub>10</sub> and PM<sub>2.5</sub> indicators, ozone indicators 93.2 percentile of maximum daily 8-hour means and SOMO35, and NO<sub>2</sub> annual average), data from *rural*, *urban* and *suburban background* stations are considered. (Throughout the paper, the urban and suburban stations are handled together). For NO<sub>2</sub>, also *urban* and *suburban traffic* stations are considered. For the indicators relevant to vegetation damage (i.e. for both ozone AOT40 parameters and NO<sub>x</sub> annual average), only *rural background* stations are considered. In case of existing data (with sufficient annual time coverage) from two or more different measurement devices in the same station location, the average of these data is used.

We excluded the stations from French overseas areas (departments), Svalbard, Azores, Madeira and Canary Islands. These areas outside the EEA map extent *Map\_2c* (EEA, 2018e) were excluded from the interpolation and mapping domain.

Table A2.1 shows the number of the measurement stations selected for the individual pollutants and their respective indicators.

Table A2.1 Number of stations selected for each pollutant indicator and area type, 2016

Station type	PM <sub>10</sub>		PM <sub>2.5</sub>	ozone				NO <sub>2</sub>	NO <sub>x</sub>
	Ann. avg.	90.4 perc. of d. means	Annual average	93.2 perc. of max. d. 8h	SOMO35	AOT40 for veg.	AOT40 for forests	Ann. avg.	Ann. avg.
Rural background	352	352	195	531	531	535	534	429	359
Urban/suburban backgr.	1313	1313	631	1145	1145			1300	
Urban/suburban traffic								790	

Compared to 2015, the number of rural background stations selected for 2016 is about the same for PM<sub>10</sub> and NO<sub>2</sub>, while it increased by approximately 17 % for PM<sub>2.5</sub>, by 8 – 12 % for ozone, and by about 13 % for NO<sub>x</sub>. The number of the urban/suburban background stations increased by approximately 19 % for PM<sub>10</sub>, by approximately 16 % for PM<sub>2.5</sub>, by about 13 % for ozone, and by about 10 % for NO<sub>2</sub>. The number of the NO<sub>2</sub> urban/suburban traffic stations increased by approximately 8 %. The increase of the station compared to 2015 is highly influenced by the addition of the Turkish stations.

For the PM<sub>2.5</sub> mapping, 186 additional rural background and 668 additional urban/suburban background PM<sub>10</sub> stations (at locations without PM<sub>2.5</sub> measurement) were also used for the purpose of calculating the pseudo PM<sub>2.5</sub> station data.

In the case of NO<sub>x</sub>, 321 stations NO<sub>x</sub> data is reported, while for 38 stations NO<sub>x</sub> values are calculated from reported NO<sub>2</sub> and NO data using Eq. A2.1. Next to this, for the NO<sub>x</sub> mapping 77 additional rural background NO<sub>2</sub> stations (at locations without NO<sub>x</sub> measurement) were also used for the purpose of calculating the pseudo NO<sub>x</sub> station data.

## A2.2 EMEP MSC-W model output

The chemical dispersion model used in this paper is the EMEP MSC-W (formerly called Unified EMEP) model (version rv4.17a), which is an Eulerian model. Simpson et al. (2012) and [https://wiki.met.no/emep/page1/emepmscw\\_opensource](https://wiki.met.no/emep/page1/emepmscw_opensource) (web site of Norwegian Meteorological Institute) describe the model in more detail. Emissions for the relevant year 2016 (Mareckova et al., 2018) are used and the model is driven by ECMWF meteorology for the relevant year 2016. EMEP (2018) provides details on the EMEP modelling for 2016. The resolution of the model is 0.1°x0.1°, i.e. circa 10x10 km. Information from this model was converted to the standard EEA 10x10 km grid resolution (for health related indicators apart from NO<sub>2</sub>), resp. into the 2x2 km grid resolution (for vegetation related indicators) or 1x1 km grid resolution (for NO<sub>2</sub>) for the interpolation process.

We downloaded the EMEP data from NMI (2018) in the form of annual means. Next to this, we received the EMEP data in the form of daily means for PM<sub>10</sub> and PM<sub>2.5</sub> and hourly means for ozone, and we aggregated these primary data to the same set of parameters as we have for the air quality observations:

- PM<sub>10</sub> – annual average [ $\mu\text{g}\cdot\text{m}^{-3}$ ], year 2016
  - 90.4 percentile of the daily average value [ $\mu\text{g}\cdot\text{m}^{-3}$ ], year 2016 (aggregated from daily means)
- PM<sub>2.5</sub> – annual average [ $\mu\text{g}\cdot\text{m}^{-3}$ ], year 2016
- Ozone – 93.2 percentile of the highest maximum daily 8-hour average value [ $\mu\text{g}\cdot\text{m}^{-3}$ ], year 2016 (aggregated from hourly means)
  - SOMO35 [ $\mu\text{g}\cdot\text{m}^{-3}\cdot\text{day}$ ], year 2016 (aggregated from hourly means)
  - AOT40 for vegetation [ $\mu\text{g}\cdot\text{m}^{-3}\cdot\text{hour}$ ], year 2016 (aggregated from hourly means)
  - AOT40 for forests [ $\mu\text{g}\cdot\text{m}^{-3}\cdot\text{hour}$ ], year 2016 (aggregated from hourly means)
- NO<sub>2</sub> – annual average [ $\mu\text{g}\cdot\text{m}^{-3}$ ], year 2016
- NO<sub>x</sub> – annual average [ $\mu\text{g}\cdot\text{m}^{-3}$ ], year 2016

Due to the complete temporal data coverage available at the modelled data, the PM<sub>10</sub> indicator 90.4 percentile of daily means is identical with the 36<sup>th</sup> highest daily mean and the ozone indicator 93.2 percentile of maximum daily 8-hour means is identical with the 26<sup>th</sup> highest maximum daily 8-hour mean.

In the original format of the model results, a point represents the centre of a grid cell (in 50x50 km resolution). The data was imported into ArcGIS as a point shapefile and converted into ETRS89-

LAEA5210 projection, subsequently converted into a 100x100 m resolution raster grid and spatially aggregated into the reference EEA 10x10 km grid (for PM and ozone health related indicators), 1x1 km grid (for NO<sub>2</sub>), resp. into the 2x2 km grid (for vegetation related indicators).

### A3.3 Other supplementary data

#### Altitude

We use the altitude data field (in meters) of *Global Multi-resolution Terrain Elevation Data 2010 (GMTED2010)*, with an original grid resolution of 15x15 arcseconds (some 463x463 m at 60N). Source: U.S. Geological Survey Earth Resources Observation and Science, see Danielson et al. (2011). We converted the field into the ETRS 1989 LAEA projection. (The resolution after projection was in 449.2x449.2 m). In the following step, we resampled the raster dataset to 100x100 m resolution and shifted it to the extent of EEA reference grid. As a final step, the dataset was spatially aggregated into 1x1 km, 2x2 km and 10x10 km resolutions.

#### Meteorological parameters

Actual meteorological surface layer parameters were extracted from the *Meteorological Archival and Retrieval System (MARS)* of the *ECMWF (European Centre for Medium-range Weather Forecasts)*. Currently we use the following ECMWF variables (details specified in Horálek et al. 2007, Section 4.5) on a 0.25x0.25 degrees (about 28x28 km at 60N) resolution as supplementary data in the regressions:

Wind speed	– annual average [m.s <sup>-1</sup> ], year 2016 (aggregated from 6-hour means)
Surface solar radiation	– annual average of daily sum [MWs.m <sup>-2</sup> ], year 2016 (aggregated from daily sums)

The 6-hour mean wind speed used in the aggregation is derived from the 10 meter height wind speed in U (10U) and V (10V) directions (where U and V are perpendicular vectors in horizontal directions) with magnitude  $\sqrt{(10U)^2 + (10V)^2}$ .

The data are imported into *ArcGIS* as a point shapefile. Each point represents the centre of a grid cell. The shapefile is converted into ETRS89-LAEA5210 projection, converted into a 100x100 m resolution raster grid and spatially aggregated into the reference EEA 1x1 km grid, 10x10 km grid, and 2x2 km grid.

#### Population density and population totals

Population density (in inhbs.km<sup>-2</sup>, census 2011) is based on *Geostat 2011* grid dataset, Eurostat (2014). The dataset is in 1x1 km resolution, in the EEA reference grid.

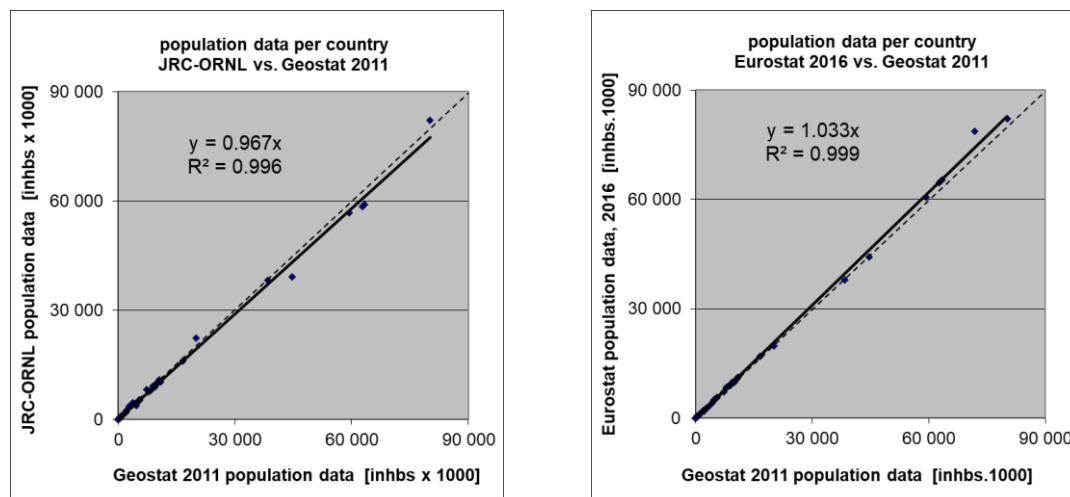
For regions not included in the Geostat 2011, alternative sources were used. Primarily, *JRC (Joint Research Centre)* population data in resolution 100x100 m were used (JRC, 2009). The JRC 100x100 m population density data is spatially aggregated into the reference 1x1 km EEA grid. For regions that are neither included in the Geostat 2011 nor in the JRC database, we used population density data from *ORNL LandScan Global Population Dataset* (ORNL, 2008). This dataset is in 30x30 arcsec resolution; its values are based on the annual mid-year national population estimates for 2008 from the Geographic Studies Branch, US Bureau of Census, <http://www.census.gov>. The ORNL data is re-projected and converted from its original WGS1984 30x30 arcsecs grids into EEA's reference projection ETRS89-LAEA5210 at 1x1 km resolution by EEA (eea\_r\_3035\_1\_m\_landscan-eurmed\_2008, EEA, 2008).

The areas lacking Geostat 2011 data, and supplemented with JRC or ORNL data were: Gibraltar (JRC); Faroe Islands, British crown dependencies (Jersey, Guernsey and Man) and northern Cyprus (ORNL). As such, the Geostat 2011 1x1 km data and these supplements cover the entire mapping area.

To verify the consistency of merging Geostat 2011 with JRC and ORNL data, we compared the Geostat 2011 data and the JRC supplemented with ORNL data on the basis of the national population totals of the individual countries (see Horálek et al., 2015 for details). Additionally, we verified the national population totals for the Geostat 2011 gridded data with the Eurostat national population data for 2016 (Eurostat, 2018). Figure A2.1 presents both comparisons. From these verifications, one can conclude a high correlation of the national population totals of each data source. Slight underestimation of the supplemented JRC and ORNL data in comparison with the Geostat 2011 data can be seen, which is caused by the fact that the Geostat 2011 data is more up-to-date than both the JRC and the ORNL data source. Geostat 2011 and Eurostat 2016 data correlate even better and leads to a similar conclusion. Based on this, we used in the further calculations on national population totals the actual Eurostat data for 2016 (Eurostat, 2018), as described further.

Population density data can be used to classify the spatial distribution of each type of area (rural, urban or mixed population density) in Europe. We use this information to select and weight the air quality values, grid cell by grid cell and merge them into a final combined map (Annex 1). Furthermore, we use it to estimate population health exposure and exceedance numbers per country and for Europe as a whole, including involved uncertainties. These activities take place on the 1x1 km resolution grid in accordance with the recommendations of Horálek et al. (2010). The supplemented Geostat data (as described above) are used in all the calculations.

*Figure A2.1 Correlation of national population totals for JRC supplemented with ORNL (left) and Eurostat 2016 (right) with Geostat 2011*



National population totals presented in the exposure tables of this paper are based on Eurostat national population data for 2016 (Eurostat, 2018). For France, Portugal and Spain, the population totals of areas outside the mapping area (i.e. Azores, Canarias, Madeira, French oversea departments) are subtracted. For northern part of Cyprus which do not have 2016 data in the Eurostat database, the population total is based on alternative data (namely <http://www.devplan.org/frame-eng.html>).

## Land cover

CORINE Land Cover 2012 – grid 100 x 100 m, Version 18.5 (09/2016) is used (EEA, 2016). The country missing in this database is Andorra, the area missing in this database is the Faroe Islands. Due to the

lack of land cover data for Andorra, we excluded this country from the process of exposure estimates related to the vegetation based AOT40 ozone indicators.

In agreement with Horálek et al. (2017b), the 44 CLC classes have been re-grouped into the 8 more general classes. In this paper we use four of these general classes, see Table A2.2.

*Table A0.2 General land cover classes, based on CLC2012 classes, used in mapping*

Label	General class description	CLC classes grid codes	CLC classes codes	CLC classes description
HDR	High density residential areas	1	111	Continuous urban fabric
LDR	Low density residential areas	2	112	Discontinuous urban fabric
AGR	Agricultural areas	12 – 22	211 – 244	Agricultural areas
NAT	Natural areas	23 – 34	311 – 335	Forest and semi natural areas

Two aggregations are used, i.e. into 1x1 km grid and into the circle with radius of 5 km. For each general CLC class we spatially aggregated the high land use resolution into the 1x1 km EEA standard grid resolution. The aggregated grid square value represents for each general class the total area of this class as percentage of the total 1x1 km square area. For details, see Horálek (2017b).

#### Road type vector data

GRIP (Meijer et al., 2016) vector road type data base provided by PBL is used. The road types are distributed into 5 classes, from highways to local roads and streets. In agreement with Horálek et al. (2017b), road classes No. 1 “Highways”, No. 2 “Primary roads” and No. 3 “Secondary roads” are used.

*Percentage of the area influenced by traffic* is represented by buffers around the roads: for the individual classes 1 – 3 and for classes 1 – 3 together, at all 1x1 grid cells; a buffer of 75 metres distance at each side from each road vector is taken for the roads of classes 1 and 2, while a buffer of 50 metres is taken for the roads of class 3. For motivation and calculation details, see Horálek et al. (2017b).

#### Satellite data

Annual average NO<sub>2</sub> dataset was constructed from data acquired by the *OMI* instrument onboard the Aura platform. The parameter used is

NO<sub>2</sub> – annual average tropospheric vertical column density (VCD) [number of NO<sub>2</sub> molecules per cm<sup>2</sup> of earth surface], year 2016 (aggregated from daily data).

The OMNO2d product generated by NASA was used as a basis, NASA (2018). The tropospheric column was used. All the orbits within a given day (typically observed between 13:00 and 14:00 local time) are mapped into a 0.25x0.25 degrees grid. For details, see Horálek et al. (2018b). The data were converted to ArcGIS and spatially transformed to the reference EEA 1x1 km grid, like in the case of modelled data.

## Annex 3 – Technical details and mapping uncertainties

This annex contains technical details on the linear regression models and the residual kriging, including the performance. Furthermore, uncertainty estimates for the maps of the indicators are given.

### A3.1 PM<sub>10</sub>

Technical details on the interpolation model and uncertainty estimates for both PM<sub>10</sub> indicators maps annual average (Map 2.1) and 90.4 percentile of daily means (Map 2.2) are presented in this section.

#### Technical details on the interpolation model

Table A3.1 presents the estimated parameters of the linear regression models ( $c$ ,  $a_1$ ,  $a_2$ , ...) and of the residual kriging (nugget, sill, range) and includes the statistical indicators of both the regression and the kriging, for both PM<sub>10</sub> indicators. The linear regression and ordinary kriging on its residuals is applied on the logarithmically transformed data of both measurement and modelled PM<sub>10</sub> values. In Table A3.1 the standard error and variogram parameters (nugget, sill and range) refer to these transformed data, whereas RMSE and bias refer to the interpolation after a back-transformation.

For both the annual average and the 90.4 percentile of daily means (indicated further as 'P90.4'), surface solar radiation was found to be statistically non-significant and thus it was not used in the 2016 mapping.

The adjusted  $R^2$  and standard error are indicators for the fit of the regression relationship, where the adjusted  $R^2$  should be as close to 1 as possible and the standard error should be as small as possible. The adjusted  $R^2$  for the rural areas was 0.62 at the annual average and 0.59 at the P90.4; for the urban areas 0.25 at the annual average and 0.24 at the P90.4.

RMSE (the smaller the better) and bias (the closer to zero the better), highlighted by orange, are the cross-validation indicators, showing the quality of the resulting map. The bias indicates to what extent the predictions are under- or overestimated on average. Further in this section, more detailed uncertainty analysis is presented. Annex 4 presents the comparison with results of the years 2005 – 2016.

*Table A3.1 Parameters and statistics of linear regression model and ordinary kriging of PM<sub>10</sub> indicators annual average and 90.4 percentile of daily means for 2016 in rural and urban areas for the final combined map*

		Annual average		90.4 percentile of daily means	
		Rural areas	Urban areas	Rural areas	Urban areas
<b>Linear regression model (LRM, Eq. A1.3)</b>	c (constant)	1.45	1.77	1.69	2.62
	a1 (log. EMEP model)	0.674	0.55	0.648	0.33
	a2 (altitude GMTED)	-0.00029		-0.00027	
	a3 (wind speed)	-0.064		-0.074	
	a4 (s. solar radiation)	<i>non signif.</i>		<i>non signif.</i>	
	<b>Adjusted R<sup>2</sup></b>	<b>0.62</b>	<b>0.25</b>	<b>0.59</b>	<b>0.24</b>
<b>Ordinary kriging (OK) of LRM residuals</b>	<b>Standard Error [µg.m<sup>-3</sup>]</b>	<b>0.26</b>	<b>0.37</b>	<b>0.26</b>	<b>0.39</b>
	nugget	0.038	0.033	0.043	0.025
	sill	0.066	0.079	0.067	0.095
	range [km]	1000	850	890	670
<b>LRM + OK of its residuals</b>	<b>RMSE [µg.m<sup>-3</sup>]</b>	<b>3.5</b>	<b>7.6</b>	<b>7.2</b>	<b>15.2</b>
	<b>Relative RMSE [%]</b>	<b>22.7</b>	<b>30.6</b>	<b>26.5</b>	<b>34.2</b>
	<b>Bias (MPE) [µg.m<sup>-3</sup>]</b>	<b>0.1</b>	<b>-0.1</b>	<b>0.2</b>	<b>-0.4</b>



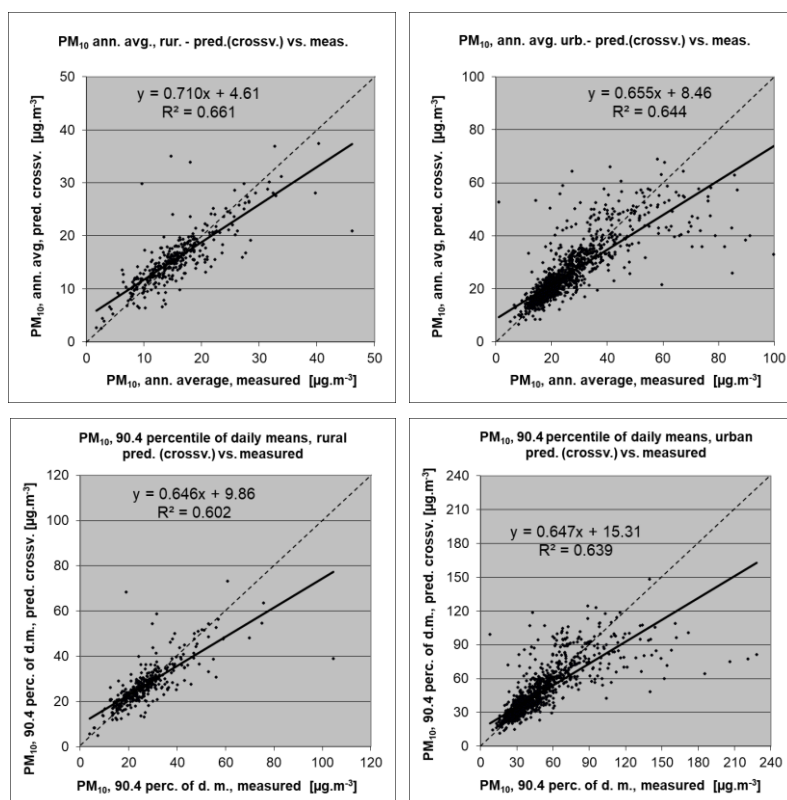
## Uncertainty estimated by cross-validation

Using RMSE as the most common indicator, the *absolute mean uncertainty* of the final combined map at areas 'in between' the station measurements can be expressed in  $\mu\text{g}\cdot\text{m}^{-3}$ . Table A3.1 shows that the absolute mean uncertainty of the final combined map of  $\text{PM}_{10}$  annual average resp. 90.4 percentile of daily means expressed by RMSE is  $3.5 \mu\text{g}\cdot\text{m}^{-3}$  resp.  $7.2 \mu\text{g}\cdot\text{m}^{-3}$  for the rural areas and  $7.6 \mu\text{g}\cdot\text{m}^{-3}$  resp.  $15.2 \mu\text{g}\cdot\text{m}^{-3}$  for the urban areas. Alternatively, one can express this uncertainty in relative terms by relating the absolute RMSE uncertainty to the mean air pollution indicator value for all stations. This *relative mean uncertainty* (Relative RMSE) of the final combined map of  $\text{PM}_{10}$  annual average resp. 90.4 percentile of daily means is 22.7 % resp. 26.5 % for rural areas and 30.6 % resp. 34.2 % for urban areas. These quite high numbers compared to previous years are caused by inclusion of Turkey in 2016 mapping. For the mapping results without Turkey, the relative mean uncertainty is 19.4 % resp. 22.3 % for rural areas and 20.0 % resp. 24.2 % for urban areas. Nevertheless, the relative uncertainty values including Turkey fulfil the data quality objectives for models as set in Annex I of the air quality Directive 2008/50/EC (EU, 2008).

See Annex 4 (and specifically Table A4.1) for a further discussion on uncertainties over the previous eleven modelling years.

Figure A3.1 shows the cross-validation scatter plots, obtained according to Annex 1, for both rural and urban areas, for both  $\text{PM}_{10}$  indicators. The  $R^2$  indicates that the variability is attributable to the interpolation for about 66 % resp. 60 % at the rural areas and for about 64 % at the urban areas.

*Figure A3.1 Correlation between cross-validated predicted (y-axis) and measurement values for  $\text{PM}_{10}$  indicators annual average (top) and 90.4 percentile of daily means (bottom) for 2016 for rural (left) and urban (right) areas*



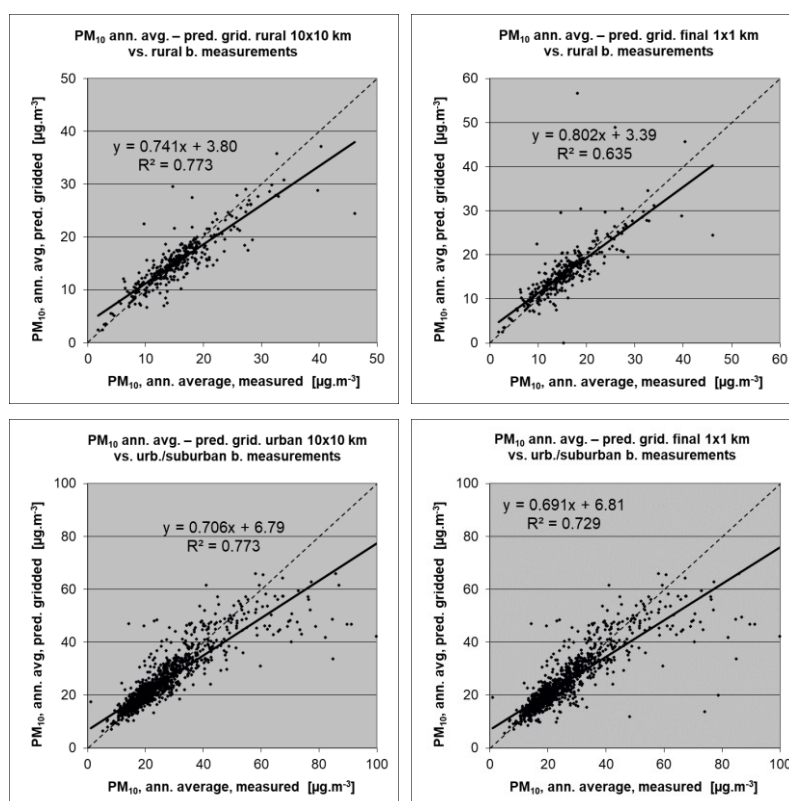
The trend line in the scatter-plots deviates at the lowest values somewhat above, and at the higher values under the symmetry axis, indicating that the interpolation methods tend to underestimate the high concentrations and overestimate the low concentrations. For example, in urban areas for annual

average an observed value of  $50 \mu\text{g}\cdot\text{m}^{-3}$  is estimated in the interpolations to be about  $41 \mu\text{g}\cdot\text{m}^{-3}$ , about 18 % lower. This underestimation at high values is common to all spatial interpolation methods. It could be reduced by either using a higher number of stations with an improved spatial distribution, or by introducing an improved regression that uses either other supplementary data or more advanced chemical transport model (resp. model in finer resolution).

### Comparison of point measurement values with the predicted grid value

In addition to the above *point observation – point prediction* cross-validation, a simple comparison has been made between the point observation values and interpolated prediction values spatially averaged at grid cells. This *point observation – grid averaged prediction* comparison indicates to what extent the predicted value of a grid cell represents the corresponding measurement values at stations located in that cell. The comparison has been made primarily for the separate rural and urban background map at 10x10 km resolution. (One can directly relate this comparison result to the cross-validation results of Figure A3.1). Next to this, the comparison has been done also for the final combined maps at 1x1 km resolution. Figure A3.2 shows the scatterplots for these comparisons, for PM<sub>10</sub> annual average only as an illustration.

**Figure A3.2** Correlation between predicted grid values from rural 10x10 km (upper left), urban 10x10 km (bottom left) and final combined 1x1 km (upper and bottom right) map (y-axis) versus measurements from rural (top), resp. urban/suburban (bottom) background stations (x-axis) for PM<sub>10</sub> annual average 2016



The results of the point observation – point prediction cross-validation of Figure A3.1 and those of the point observation – grid averaged prediction validation for separate rural and separate urban background maps, and for the final combined maps at both resolutions are summarised in Table A3.2 for both PM<sub>10</sub> indicators.

By comparing the scatterplots and the statistical indicators for the separate rural and separate urban background map with the final combined maps in both resolutions, one can evaluate the level of

representation of the rural resp. urban background areas in the final combined maps. Both the rural and the urban air quality are fairly well represented in the 1x1 km final combined map. This would not be the case in the urban areas for the aggregated final combined 10x10 km map (Horálek et al., 2016b). Therefore, we present the final combined maps just in the 1x1 km resolution, see Maps 2.1 and 2.2, contrary to the earlier reports up to Horálek et al. (2016b).

**Table A3.2** Statistical indicators from the scatter plots for the predicted point values based on cross-validation and the predicted grid values from separate (rural resp. urban) 10x10 km and final combined 1x1 km map versus the measurement point values for rural (left) and urban (right) background stations for PM<sub>10</sub> indicators annual average (top) and 90.4 percentile of daily means (bottom) for 2016

PM <sub>10</sub>	rural backgr. stations				urban/suburban backgr. stations			
	RMSE	bias	R <sup>2</sup>	lin. r. equation	RMSE	bias	R <sup>2</sup>	lin. r. equation
<b>Annual average</b>								
cross-valid. prediction, separate (r or ub) map	3.5	0.1	0.661	y = 0.710x + 4.61	7.6	-0.1	0.689	y = 0.691x + 7.34
grid prediction, 10x10 km separate (r or ub) map	2.9	-0.2	0.773	y = 0.741x + 3.80	3.7	-0.3	0.802	y = 0.733x + 6.05
grid prediction, 1x1 km final combined map	3.9	0.3	0.635	y = 0.802x + 3.39	4.0	-0.6	0.770	y = 0.726x + 5.84
<b>90.4 percentile of daily means</b>								
cross-valid. prediction, separate (r or ub) map	7.2	0.2	0.602	y = 0.646x + 9.86	15.2	-0.4	0.639	y = 0.647x + 15.31
grid prediction, 10x10 km separate (r or ub) map	6.1	-0.5	0.718	y = 0.678x + 8.33	10.8	-0.9	0.829	y = 0.737x + 10.80
grid prediction, 1x1 km final combined map	7.5	0.6	0.607	y = 0.750x + 7.37	12.1	-1.5	0.779	y = 0.715x + 11.11

The Table A3.2 shows a better relation (i.e. lower RMSE, higher R<sup>2</sup>, smaller intercept and slope closer to 1) between station measurements and the interpolated values of the corresponding grid cells at both rural and urban background map areas than it does at the point cross-validation predictions. That is because the simple comparison between point measurements and the gridded interpolated values shows the uncertainty at the actual station locations (points), while the point cross-validation prediction simulates the behaviour of the interpolation at point positions assuming no actual measurement would exist at that point. The uncertainty at measurement locations is introduced partly by the smoothing effect of the interpolation and partly by the spatial averaging of the values in the 10x10 km grid cells. The level of the smoothing effect leading to underestimation at areas with high values is there smaller than in situations where no measurement is represented in such areas. For example, in urban areas the predicted interpolation gridded annual average value in the separate urban background map will be about 43 µg·m<sup>-3</sup> at the corresponding station point with the measurement value of 50 µg·m<sup>-3</sup>. This means an underestimation of about 14 %. It is a slightly less than the prediction underestimation of 18 % at the same point location, when leaving out this one actual measurement point and the interpolation is done without this station (see the previous subsection).

### Probability of Limit Value exceedance

We constructed the map of probability of limit value exceedance (see Annex 1, Section A1.2). For this purpose, we used the final combined concentration map in the 1x1 km grid resolution. Based on this map, we derived, with support of the 1x1 km uncertainty map and the limit value (40 µg·m<sup>-3</sup>), the probability of exceedance (PoE) map at that same resolution.

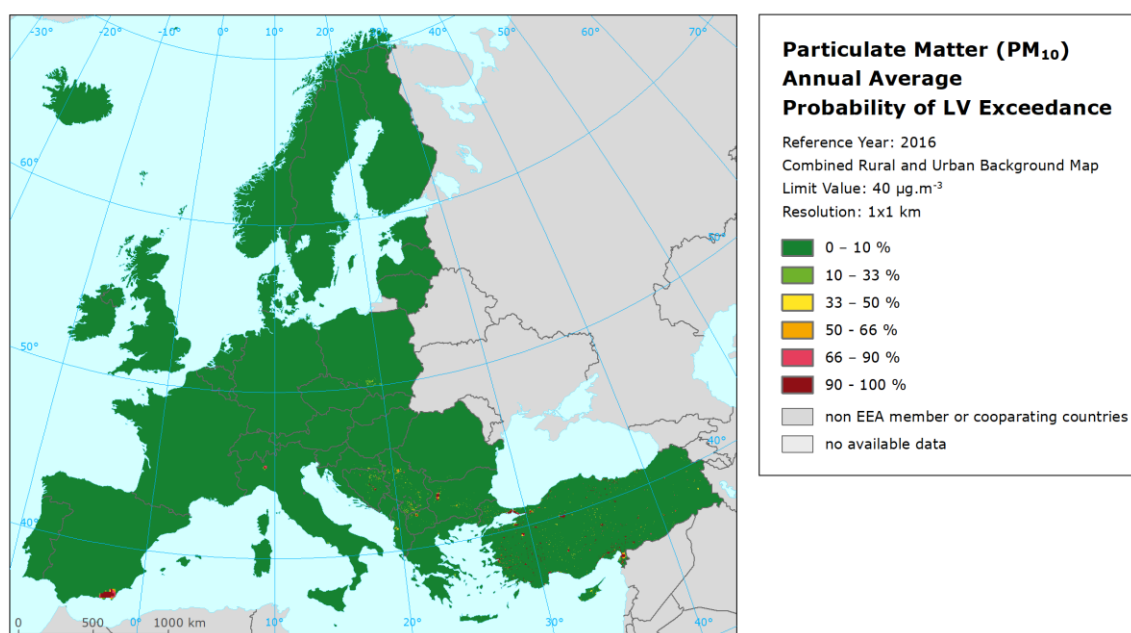
It is needed to keep in mind that the interpolated maps refer to the rural or urban/suburban *background* situations only, i.e. it cannot be excluded that exceedances of limit values may occur at *hotspot* and traffic locations throughout Europe, which are not resolved by this type of map.

The map shows areas with a probability of limit value exceedance (PoE) above 66 % marked in red (large or high PoE) and areas below 33 % in green (low or little PoE). Red in two shades indicate areas for which exceedance is *likely* or *very likely* (above 90 %) to occur due to either high concentrations close to or already above the LV accompanied with such uncertainty that exceedance is very likely, or areas with lower concentrations accompanied with high uncertainty levels so that exceedance is very

likely. Vice versa, in the green areas of two shades (below 33 %) it is *unlikely* to exceed the LV because we have predicted concentrations and accompanying uncertainties at levels that do not sum above the LV. The areas with 33–50 % and 50–66 % probability of LV exceedance are marked in yellow and orange respectively. Table A1.1 summarises the classes and terminology for probability (i.e. likelihood) that are used in this paper.

Maps A3.1 and A3.2 present the probability of the LV exceedance for PM<sub>10</sub> indicators annual average and 90.4 percentile of daily means. In case of the annual average (Map A3.1), only limited areas do show increased probability of LV exceedance, namely the surrounding of Almeria in southern Spain, around Sophia in Bulgaria, around Milan in the Po Valley, around Katowice in southern Poland, around Istanbul and in urbanised areas in the Balkans and Turkey.

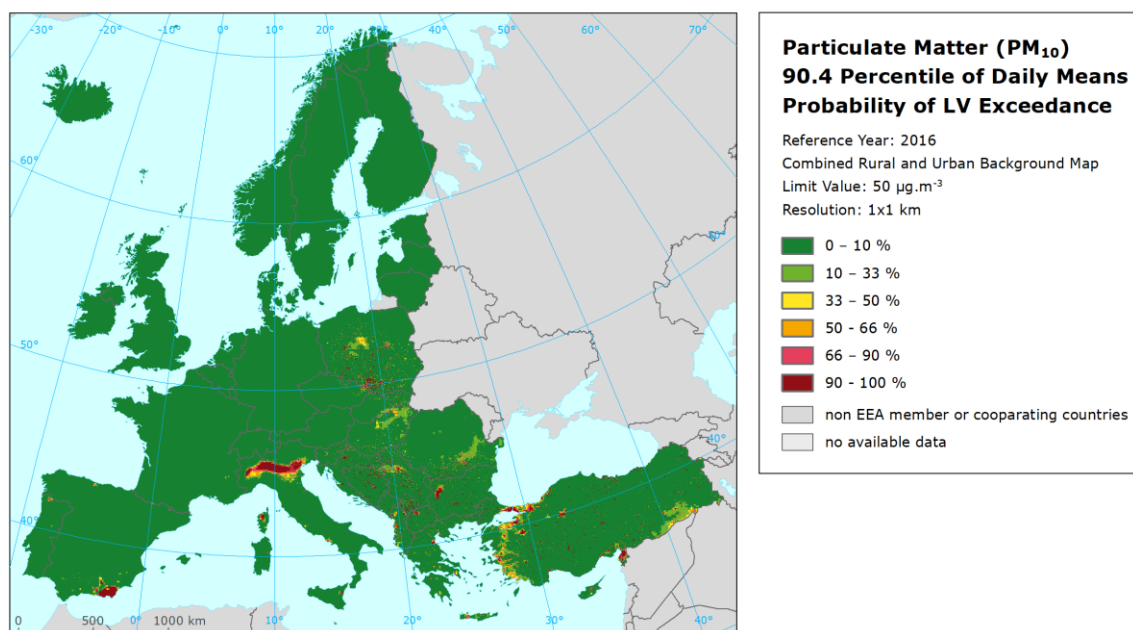
*Map A3.1 Map with the probability of the limit value exceedance, PM<sub>10</sub> annual average, 2016*



Note: Interpolation uncertainty is considered only, no other sources of uncertainty.

In case of the 90.4 percentile of daily means (Map A3.2), one observes considerably larger areas with relative quite high levels of PoE, namely the complete Po Valley in northern Italy, the region around Almeria in southern Spain, southern Poland and north-eastern Czech Republic (with industrial Ostrava–Katowice region), area around Sofia in Bulgaria, central part of Poland, urbanised areas in the whole Balkan region (in Croatia, Bosnia & Herzegovina, Serbia, Montenegro, North Macedonia, Greece, Bulgaria, southern and eastern Romania, the Albanian coastal zone) and also urbanised areas in Turkey.

Map A3.2 Map with the probability of the limit value exceedance, PM<sub>10</sub> indicator 90.4 percentile of daily means, 2016



Note: Interpolation uncertainty is considered only, no other sources of uncertainty.

### A3.2 PM<sub>2.5</sub>

Technical details and uncertainty estimates for Map 3.1 with the PM<sub>2.5</sub> annual average are presented in this section.

#### Technical details on the interpolation model

Table A3.3 presents the regression coefficients determined for pseudo PM<sub>2.5</sub> stations data estimation, based on the 563 stations that have both PM<sub>2.5</sub> and PM<sub>10</sub> measurements available (see Section 2.1.1).

Table A3.3 Parameters and statistics of linear regression model for generation of pseudo PM<sub>2.5</sub> data, regardless of rural or urban/suburban area, for PM<sub>2.5</sub> annual average 2016

		Both rural and urban areas
Linear regression model (LRM, Eq. A1.1)	c (constant)	19.7
	b (PM <sub>10</sub> measurement data)	0.736
	a1 (surface solar radiation)	-0.940
	a2 (latitude)	-0.244
	a3 (longitude)	0.080
	Adjusted R <sup>2</sup>	0.89
Standard Error [µg.m <sup>-3</sup> ]		2.0

The same supplementary data as in Denby (2011b) are used, apart from the population density, which was found not significant for several years (Horálek et al. 2018a) and is not further used.

Table A3.4 presents the estimated parameters of the linear regression models ( $c$ ,  $a_1$ ,  $a_2$ ,...) and of the residual kriging (*nugget*, *sill*, *range*) and includes the statistical indicators of both the regression and

the kriging of its residuals. Like in the case of PM<sub>10</sub>, the linear regression is applied on the logarithmically transformed data of both measurement and modelled PM<sub>2.5</sub> values. Thus, the standard error and variogram parameters refer to these transformed data, whereas RMSE and bias refer to the interpolation after the back-transformation.

For rural areas, no significant supplementary variable was found, apart from the EMEP model. Surface solar radiation was not found to be statistically significant in 2010 – 2016, and therefore it will not be further used.

*Table A3.4 Parameters and statistics of linear regression model and ordinary kriging of PM<sub>2.5</sub> annual average 2016 in rural and urban areas for final combined map*

PM <sub>2.5</sub>		Annual average	
		Rural areas	Urban areas
Linear regression model (LRM, Eq. A1.3)	c (constant)	0.69	1.56
	a1 (log. EMEP model)	0.779	0.49
	a2 (altitude GMTED)	<i>non signif.</i>	
	a3 (wind speed)	<i>non signif.</i>	
	a4 (s. solar radiation)	<i>non signif.</i>	
	a5 (log. population)	<i>non signif.</i>	
Adjusted R <sup>2</sup>		<b>0.55</b>	<b>0.25</b>
Standard Error [µg.m <sup>-3</sup> ]		<b>0.31</b>	<b>0.35</b>
Ordinary kriging (OK) of LRM residuals	nugget	0.064	0.019
	sill	0.094	0.077
	range [km]	1000	490
LRM + OK of its residuals	RMSE [µg.m <sup>-3</sup> ]	<b>2.5</b>	<b>2.7</b>
	Relative RMSE [%]	<b>24.3</b>	<b>18.3</b>
	Bias (MPE) [µg.m <sup>-3</sup> ]	<b>-0.2</b>	<b>0.2</b>

The adjusted R<sup>2</sup> (the closer to 1 the better) and standard error (the smaller the better) are indicators for the *quality of the fit of the regression relation*. The adjusted R<sup>2</sup> is 0.55 for the rural areas and 0.25 for urban areas. Somewhat weaker regression relation in the urban areas causes a higher impact of the interpolation part of the interpolation-regression-merging mapping methodology in these areas.

RMSE and bias – highlighted in orange – are the cross-validation indicators, showing the *quality of the resulting map*; the bias indicates to what extent the predictions are under- or overestimated on average. Only stations with PM<sub>2.5</sub> measurement data are used for calculating the RMSE and the bias (i.e. only non-pseudo PM<sub>2.5</sub> stations are used). These statistical indicators are calculated excluding the pseudo stations because they are estimated values only, not actual measurement values. According to Denby et al (2011b), the pseudo PM<sub>2.5</sub> data does not satisfy the quality objectives for fixed monitoring alone. The pseudo stations are used as they improve the mapping estimate. Whereas the actual measurements can be used for evaluating the *quality of the map*. For the future, we consider to quit the application of the PM<sub>2.5</sub> pseudo stations as the current number of the actual PM<sub>2.5</sub> measurement stations has increased over time such that the use of pseudo PM<sub>2.5</sub> stations may not contribute enough any longer to improve the mapping estimates.

Due to the lack of rural stations in Turkey for PM<sub>2.5</sub>, no proper interpolation results could be presented for this country in a rural map, so we do not present the estimated PM<sub>2.5</sub> values for Turkey in the final map. Thus, the stations located in Turkey have not been used in the uncertainty estimates (although used in the mapping process), as they lie outside the mapping area.

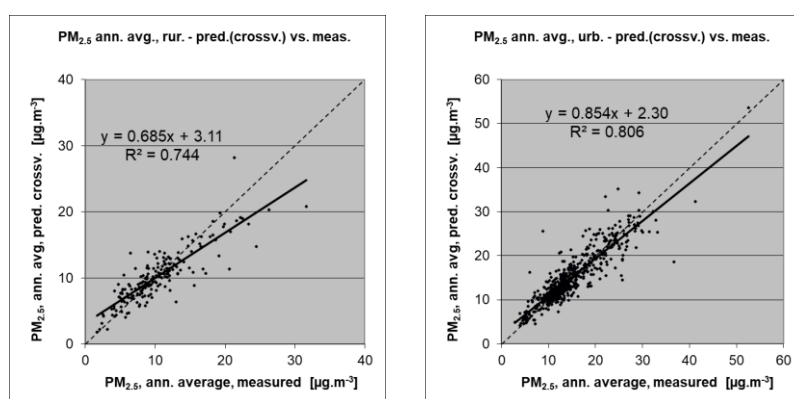


## Uncertainty estimated by cross-validation

Table A3.4 shows that the absolute mean uncertainty of the final combined map of PM<sub>2.5</sub> annual average expressed as RMSE is 2.5 µg·m<sup>-3</sup> for the rural areas and 2.7 µg·m<sup>-3</sup> for the urban areas. On the other hand, the *relative mean uncertainty* (Relative RMSE) of the final combined map of PM<sub>2.5</sub> annual average is 24.3 % for rural areas and 18.3 % for urban areas. These relative uncertainty values fulfil the data quality objectives for models as set in Annex I of the air quality Directive 2008/50/EC (EU, 2008). Annex 4 (and specifically Table A4.5) summarises both the absolute and relative uncertainties of different years.

Figure A3.3 shows the cross-validation scatter plots, obtained according to Section A1.3, for both the rural and urban areas. The R<sup>2</sup> indicates that about 74 % of the variability is attributable to the interpolation for the rural areas and 81 % for the urban areas.

*Figure A3.3 Correlation between cross-validated predicted and measurement values for PM<sub>2.5</sub> annual average 2016 for rural (left) and urban (right) areas*



The scatter plots indicate that in areas with high concentrations the interpolation methods tend to underestimate the levels. For example, in rural areas an observed value of 25 µg·m<sup>-3</sup> is estimated in the interpolations to be almost 20 µg·m<sup>-3</sup>, which is an underestimated prediction of about 20 %. This underestimation at high values is an inherent feature of all spatial interpolations. It could be reduced by either using a higher number of the stations at improved spatial distribution, or by introducing a closer regression that uses other supplementary data.

## Comparison of point measurement values with the predicted grid value

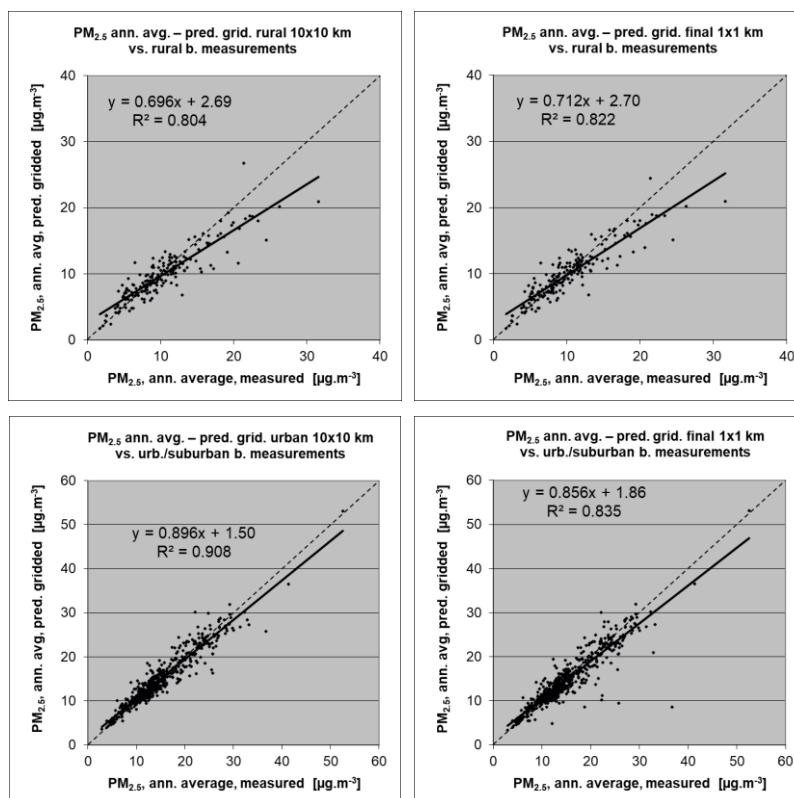
Next to the cross-validation comparison, a simple comparison has been made between the point observation values and interpolated prediction values spatially averaged in grid cells. This point-grid comparison indicates to what extent the predicted value of a grid cell represents the corresponding measurement values at stations located in that cell. The comparison has been made primarily for the separate rural and urban map at 10x10 km resolution. Next to this, the comparison has been done also for the final combined maps at 1x1 km resolution. Figure A3.4 shows the scatterplots for these comparisons.

The results of the point observation – point prediction cross-validation of Figure A3.3 and those of the point observation – grid averaged prediction validation of Figure A3.4 for separate rural and separate urban background maps, and for the final combined maps at both resolutions are summarised in Table A3.5.

By comparing the scatterplots and the statistical indicators for the separate rural and separate urban background map with the final combined maps, one can evaluate the level of representation of the rural resp. urban background areas in the final combined maps. Similar results as for PM<sub>10</sub> can be

observed: both the rural and urban air quality are fairly well represented in the 1x1 km final combined map.

**Figure A3.4** Correlation between predicted grid values from rural 10x10 km (upper left), urban 10x10 km (bottom left) and final combined 1x1 km (both right) map (y-axis) versus measurements from rural (top), resp. urban/suburban (bottom) background stations (x-axis) for PM<sub>2.5</sub> annual average 2016



Like in the case of PM<sub>10</sub>, Table A3.5 shows a better correlated relation with the station measurements (i.e. lower RMSE, higher R<sup>2</sup>, smaller intercept and slope closer to 1) for the simply interpolated gridded values than for the point cross-validation predictions, at both rural and urban background map areas. That is because the simple comparison shows the uncertainty at the actual station locations, while the cross-validation prediction simulates the behaviour of the interpolation (within the area covered by measurements) at point positions assuming no actual measurements would exist at these points.

**Table A3.5** Statistical indicators from the scatter plots for the predicted point values based on cross-validation and the predicted grid values from separate (rural resp. urban) 10x10 km and final combined 1x1 km versus the measurement point values for rural (left) and urban (right) background stations for PM<sub>2.5</sub> annual average 2016

PM <sub>2.5</sub>	rural backgr. stations				urban/suburban backgr. stations			
	RMSE	bias	R <sup>2</sup>	lin. r. equation	RMSE	bias	R <sup>2</sup>	lin r. equation
cross-valid. prediction, separate (r or ub) map	2.5	-0.2	0.744	y = 0.685x + 3.11	2.7	0.2	0.806	y = 0.854x + 2.30
grid prediction, 10x10 km separate (r or ub) map	2.3	-0.5	0.804	y = 0.696x + 2.69	1.8	0.0	0.908	y = 0.896x + 1.50
grid prediction, 1x1 km final combined map	2.2	-0.3	0.801	y = 0.712x + 2.70	2.5	-0.2	0.835	y = 0.856x + 1.86

The uncertainty at measurement locations is caused partly by the smoothing effect of the interpolation and partly by the spatial averaging of the values in the 10x10 km grid cells. For example, in urban areas the predicted interpolation gridded value in the final combined map will be about 28 µg·m<sup>-3</sup> at the

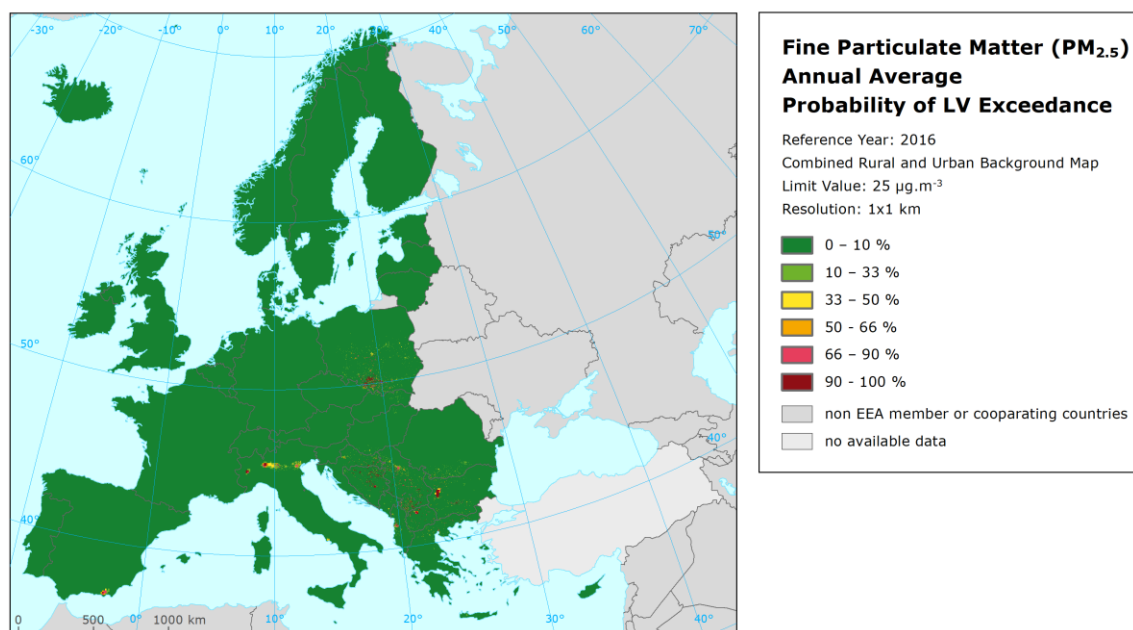


corresponding station point with the measurement value of  $30 \mu\text{g}\cdot\text{m}^{-3}$  (calculated based on the linear regression equation), which coincides with an underestimation of about 8 %.

### Probability of Limit Value exceedance

The probability of limit value exceedance map was created for the  $\text{PM}_{2.5}$  indicator in a similar way as the PoE maps for the  $\text{PM}_{10}$  indicators and presented at 1x1 km resolution with the Limit Value (LV) of  $25 \mu\text{g}\cdot\text{m}^{-3}$ .

*Map A3.3 Map with the probability of the limit value exceedance,  $\text{PM}_{2.5}$  annual average, 2016*



Note: Interpolation uncertainty is considered only, no other sources of uncertainty.

The areas with the highest probability of LV exceedance include most prominently the Po Valley in Italy, the area around Bulgaria's capital Sofia and locations around the Balkan cities, the region of southern Poland – north-eastern Czech Republic with the industrial zones of Krakow, Katowice and Ostrava, and the region around Almeria in southern Spain.

In the other parts of Europe, there is little to no likelihood of LV exceedance, at the level of 1x1 km grids.

One should bear in mind that the map is based on rural and urban/suburban *background* station data only. As such the map reflects rural and urban background situations only. Therefore, this type of map will not resolve the probability of exceedances of LV that may occur at the many *hotspot* and traffic locations throughout Europe.

### A3.3 Ozone

In this section, we present the technical details and the uncertainty estimates for the maps of ozone health-related indicators 93.2 percentile of maximum daily 8-hour means and SOMO35 (Maps 4.1 and

4.2), as well as for the maps of ozone vegetation-related indicators AOT40 for vegetation and AOT40 for forests (Maps 4.3 and 4.4).

### Technical details on the interpolation model

Table A3.6 presents the estimated parameters of the linear regression models and of the residual kriging, including the statistical indicators of both the regression and the kriging.

The adjusted  $R^2$  and standard error show the quality of the fit of the regression relation. For the rural areas, all indicators show the value of the adjusted  $R^2$  between 0.53 and 0.57. For the urban areas, the adjusted  $R^2$  is 0.50 for 93.2 percentile of daily 8-hour maximums and 0.48 for SOMO35. For the vegetation-related indicators the urban maps are not constructed.

*Table A3.6 Parameters and statistics of linear regression model and ordinary kriging for ozone indicators 93.2 percentile of maximum daily 8-hourly means and SOMO35 in rural and urban areas for the final combined map and for  $O_3$  indicators AOT40 for vegetation and for forests in rural areas for 2016*

		93.2 perc. of dmax 8h		SOMO35		AOT40v	AOT40f
		Rur. areas	Urb. areas	Rur. areas	Urb. areas	Rur. areas	Rur. areas
Linear regression model (LRM, Eq. A1.3)	c (constant)	-20.2	4.4	-2500	-1583	-12108	-18583
	a1 (EMEP model)	1.03	0.88	0.55	0.47	0.64	0.52
	a2 (altitude GMTED)	0.0032		0.98		non signif.	2.82
	a3 (wind speed)		-1.68		-80.01		
	a4 (s. solar radiation)	1.54	1.09	338.2	271.3	1464.8	2403.0
	Adjusted $R^2$	<b>0.53</b>	<b>0.50</b>	<b>0.57</b>	<b>0.48</b>	<b>0.55</b>	<b>0.57</b>
Ord. krig. (OK) of LRM	Stand. Err. [ $\mu\text{g}\cdot\text{m}^{-3}\cdot\text{x}$ ]*	<b>9.9</b>	<b>11.5</b>	<b>1680</b>	<b>1552</b>	<b>5326</b>	<b>9367</b>
	nugget	55	45	2.2E+06	8.2E+05	1.8E+07	5.3E+07
	sill	68	84	2.2E+06	1.7E+06	2.6E+07	7.8E+07
	range [km]	120	200	540	90	880	1000
	RMSE [ $\mu\text{g}\cdot\text{m}^{-3}\cdot\text{x}$ ]*	<b>9.4</b>	<b>9.0</b>	<b>1681</b>	<b>1182</b>	<b>4996</b>	<b>8982</b>
	Relative RMSE [%]	<b>8.4</b>	<b>8.3</b>	<b>33.3</b>	<b>32.5</b>	<b>36.9</b>	<b>36.9</b>
LRM + OK of its residuals	Bias (MPE) [ $\mu\text{g}\cdot\text{m}^{-3}\cdot\text{x}$ ]*	<b>0.0</b>	<b>0.1</b>	<b>7</b>	<b>30</b>	<b>-3</b>	<b>10</b>

\*) Units – 93.2 percentile of daily 8-h maximums: [ $\mu\text{g}\cdot\text{m}^{-3}$ ], SOMO35: [ $\mu\text{g}\cdot\text{m}^{-3}\cdot\text{d}$ ], AOT40v and AOT40f: [ $\mu\text{g}\cdot\text{m}^{-3}\cdot\text{h}$ ].

RMSE and bias – highlighted by orange – are the cross-validation indicators, showing the quality of the resulting map.

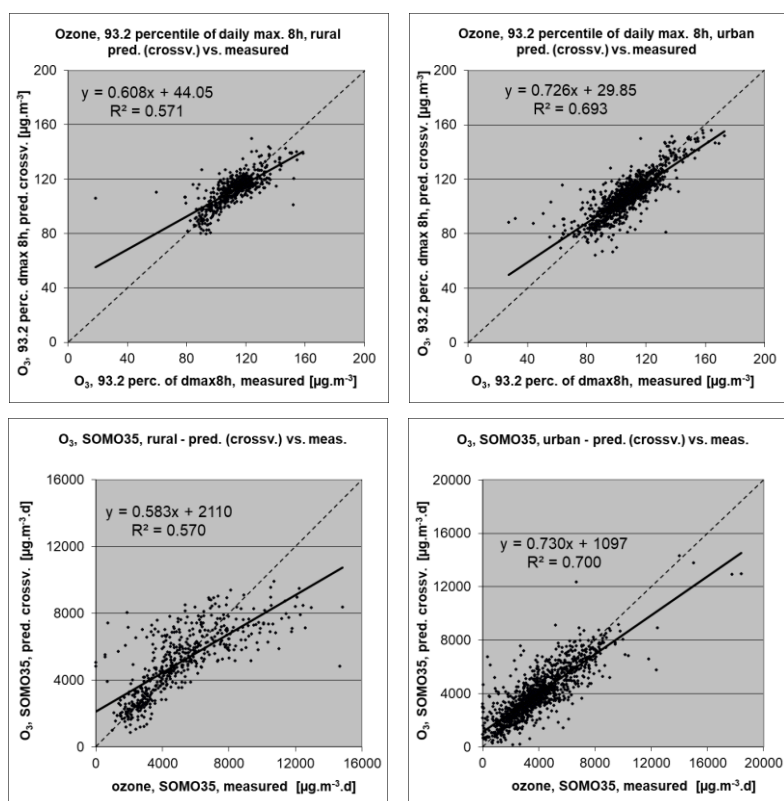
### Uncertainty estimated by cross-validation

The basic uncertainty analysis is provided by cross-validation. Table A3.6 shows both absolute and relative mean uncertainty, expressed by RMSE and Relative RMSE. The relative mean uncertainty of the 2016 ozone map is at the 93.2 percentile of daily 8-h maximums about 8 % for both rural and urban areas, around 33 % for both rural and urban areas at the SOMO35, and about 37 % at AOT40 for both vegetation and forests. The small level of the relative uncertainty for the 93.2 percentile of maximum daily 8-h means is highly influenced by the relation between the mean concentration level and the spatial variance of this indicator (i.e. high numerical values of the concentration level compared to small values of the spatial variance). The uncertainty results are influenced by the inclusion of Turkey in mapping: without Turkey, the relative mean uncertainty is about 7 % for both rural and urban areas at the 93.2 percentile of daily 8-h maximums, around 31 % for rural and 28 % for urban areas for the SOMO35, and about 35 % resp. 34 % for AOT40 for vegetation resp. forests.

Annex 4 (and specifically Table A4.9) summarises both the absolute and relative uncertainties of different years.

Figure A3.5 shows the cross-validation scatter plots for both the rural and urban areas of the 2016 map for the two health-related ozone indicators.

Figure A3.5 Correlation between cross-validated predicted (y-axis) and measurement values for ozone indicators 93.2 percentile of max. daily 8-hourly means (top) and SOMO35 (bottom) for 2016 for rural (left) and urban (right) areas



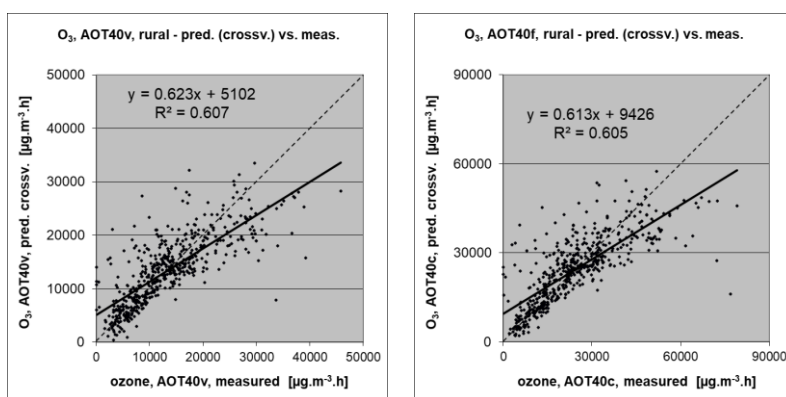
The  $R^2$ , an indicator for the interpolation correlation with the observations, shows that for the health related ozone indicators, about 57 % is attributable to the interpolation in the rural areas, while in the urban areas it is about 70 %.

The scatter plots indicate that the higher values are underestimated and the lower values somewhat overestimated by the interpolation method; a typical smoothing effect inherent to the interpolation method with the linear regression and its residuals kriging. For example, in the case of the 93.2 percentile of daily 8-h maximums, in urban areas (Figure A.3.5, upper right panel) an observed value of  $160 \mu\text{g}\cdot\text{m}^{-3}$  is estimated in the interpolation as  $146 \mu\text{g}\cdot\text{m}^{-3}$ , which is 9 % lower. Or, in the case of SOMO35, in rural areas (Figure A.3.5, bottom left panel) an observed value of  $9\,000 \mu\text{g}\cdot\text{m}^{-3}\cdot\text{d}$  is estimated in the interpolation as about  $7\,400 \mu\text{g}\cdot\text{m}^{-3}\cdot\text{d}$ , which is 18 % lower.

Figure A3.6 shows the cross-validation scatter plots of the AOT40 for both vegetation and forests.  $R^2$  indicates that about 61 % of the variability is attributable to the interpolation, for both AOT40 indicators.

The cross-validation scatter plots show again that in areas with higher accumulated ozone concentrations the interpolation methods tend to deliver underestimated predicted values. For example, in agricultural areas (Figure A3.6, left panel) an observed value of  $30\,000 \mu\text{g}\cdot\text{m}^{-3}\cdot\text{h}$  is estimated in the interpolation as about  $24\,000 \mu\text{g}\cdot\text{m}^{-3}\cdot\text{h}$ , i.e. an underestimation of about 20 %. In addition, an overestimation at the lower end of predicted values occurred. One could reduce this under- and overestimation by extending the number of measurement stations and by optimising the spatial distribution of those stations, specifically in areas with elevated values over years.

Figure A3.6 Correlation between cross-validated predicted (y-axis) and measurement values for ozone indicators AOT40 for vegetation (left) and AOT40 for forests (right) for 2016 for rural areas



### Comparison of point measurement values with the predicted grid value

In addition to the above point observation – point prediction cross-validation, a simple comparison was made between the point observation values and interpolated predicted grid values.

For health related indicators, the comparison has been made primarily for the separate rural and separate urban background maps at 10x10 km resolution. (One can directly relate this comparison result to the cross-validation of the previous section.) Next to this, the comparison has been done also for the final combined maps at 1x1 km resolution.

Figure A3.7 shows the scatterplots for these comparisons, for ozone indicator 93.2 percentile of maximum daily 8-hour means only, as an illustration.

The results of the point observation – point prediction cross-validation of Figure A3.6 and those of the point observation – grid averaged prediction validation for the separate rural and the separate urban background map, and for the final combined maps at both resolutions are summarised in Table A3.7.

By comparing the scatterplots and the statistical indicators for the separate rural and separate urban background map with the final combined maps, one can evaluate the level of representation of the rural resp. urban background areas in the final combined maps. Both the rural and the urban air quality are fairly well represented in the 1x1 km final combined map.

The uncertainty of the rural and urban background maps at measurement locations is caused partly by the smoothing effect of interpolation and partly by the spatial averaging of the values in the 10x10 km grid cells. The level of smoothing, which leads to underestimation in areas with high values, is weaker in areas where measurements exist than in areas where a measurement point is not available. For example, in the case of the SOMO35, in rural areas an observed value of 9 000 µg.m<sup>-3</sup>.d is estimated in the interpolation as about 8 100 µg.m<sup>-3</sup>.d, which is about 10 % lower. It is less than the cross-validation underestimation of 18 % at the same point location, when leaving out this one actual measurement point and the interpolation without this station is done (see the previous subsection).

Figure A3.7 Correlation between predicted grid values from rural 10x10 km (upper left), urban 10x10 km (bottom left) and final combined 1x1 km (both right) map (y-axis) versus measurements from rural (top), resp. urban/suburban (bottom) background stations (x-axis) for ozone indicator 93.2 percentile of daily max. 8-hourly means for 2016

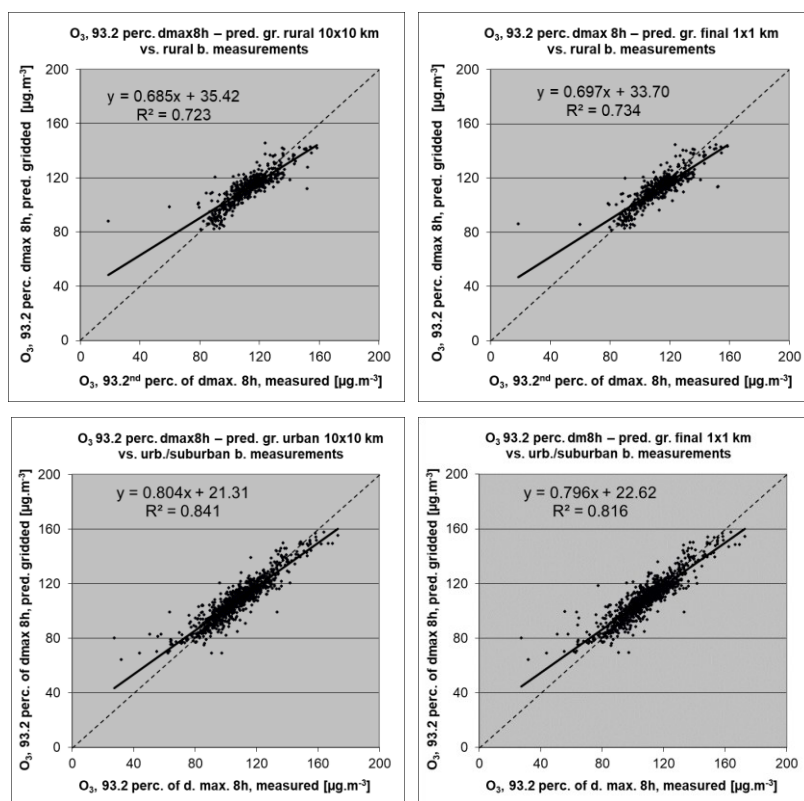


Table A3.7 Statistical indicators from the scatter plots for the predicted point values based on cross-validation and the predicted grid values from separate (rural resp. urban) 10x10 km and final combined 1x1 km map versus the measurement point values for rural (left) and urban (right) background stations for ozone indicators 93.2 percentile of daily max 8h means (top) and SOMO35 (bottom) for 2016

	rural backgr. stations				urban/suburban backgr. stations			
	RMSE	bias	R <sup>2</sup>	lin. r. equation	RMSE	bias	R <sup>2</sup>	lin r. equation
<b>93.2 percentile of daily max. 8-hour means</b>								
cross-valid. prediction, separate (r or ub) map	9.0	0.1	0.571	$y = 0.608x + 44.1$	8.6	0.2	0.693	$y = 0.726x + 29.9$
grid prediction, 10x10 km separate (r or ub) map	6.2	0.0	0.723	$y = 0.685x + 35.4$	5.5	0.0	0.841	$y = 0.804x + 21.3$
grid prediction, 1x1 km final merged map	6.4	0.2	0.734	$y = 0.697x + 33.7$	6.3	0.1	0.813	$y = 0.796x + 22.6$
<b>SOMO35</b>								
cross-valid. prediction, separate (r or ub) map	1578	21	0.570	$y = 0.583x + 2110$	1221	43	0.700	$y = 0.730x + 1097$
grid prediction, 10x10 km separate (r or ub) map	1348	13	0.613	$y = 0.604x + 2003$	830	17	0.885	$y = 0.827x + 692$
grid prediction, 1x1 km final merged map	1300	-58	0.632	$y = 0.611x + 1870$	992	38	0.829	$y = 0.805x + 849$

Table A3.8 presents the results of the point observation – point prediction cross-validation of Figure A3.6 and those of the point-grid validation for the rural map, for vegetation related indicators AOT40 for vegetation and AOT40 for forests. Again, one can see for both indicators a better correlation between the station measurements and the averaged interpolated predicted values of the corresponding grid cells, than at the point cross-validation predictions, of Figure A3.6.

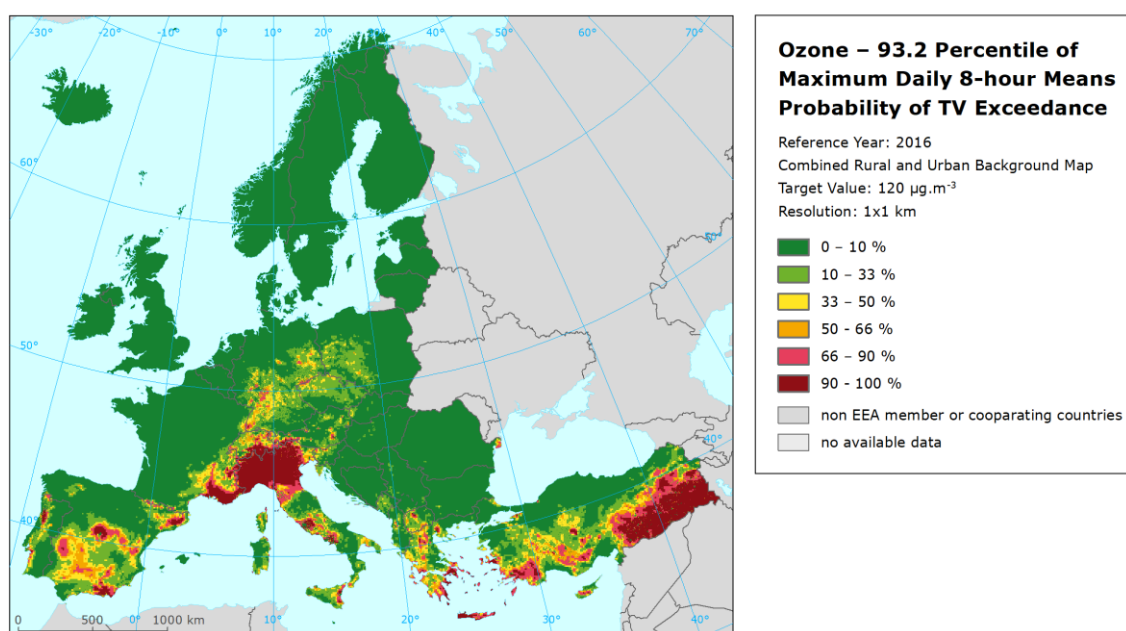
Table A3.8 Statistical indicators from the scatter plots for predicted point values based on cross-validation and predicted grid values from rural 2x2 km map versus measurement point values for rural background stations for  $O_3$  indicators AOT40 for vegetation (top) and for forests (bottom) for 2016

	rural backgr. stations			
	RMSE	bias	R <sup>2</sup>	linear regression equation
<b>AOT40 for vegetation</b>				
cross-valid. prediction, rural map	4996	-3	0.607	$y = 0.623x + 5102$
grid prediction, 2x2 km rural map	4366	1	0.701	$y = 0.671x + 4452$
<b>AOT40 for forests</b>				
cross-valid. prediction, rural map	8982	10	0.605	$y = 0.613x + 9426$
grid prediction, 2x2 km rural map	7852	20	0.700	$y = 0.663x + 8213$

### Probability of Target Value exceedance

Map A3.4 presents the gridded map of 1x1 km resolution showing the probability of target value exceedance for the 93.2 percentile of maximum daily 8-hour means. It was constructed on the basis of the 1x1 km gridded concentration map (Map 4.1), the 1x1 km gridded uncertainty map and the target value (TV) of  $120 \mu\text{g}\cdot\text{m}^{-3}$ . Table A1.1 explains the significance of the colour classes in the map.

Map A3.4 Map with the probability of the target value exceedance, ozone indicator 93.2 percentile of maximum daily 8-hour means, 2016



Note: Interpolation uncertainty is considered only, no other sources of uncertainty.

The PoE map for 2016 demonstrates the extended red and dark red areas (high or large PoE) in the Alpine region, northern, central and southern Italy, southern France, central and southern Spain, Portugal, south-western Germany, North Macedonia, Greece, Cyprus, and Turkey.

No Limit Value or Target Value is set for the WHO recommended ozone health indicator SOMO35, therefore no probability of exceedance map has been prepared.



### A3.4 NO<sub>2</sub> and NO<sub>x</sub>

In this section, the technical details and the uncertainty estimates for the maps of NO<sub>2</sub> annual average and NO<sub>x</sub> annual average, for Maps 5.1 and 5.2, are presented.

#### Technical details on the interpolation model

In agreement with Horálek et al. (2007) and Annex 1, the NO<sub>x</sub> measurements are supplemented by the so-called *pseudo* NO<sub>x</sub> stations. The pseudo NO<sub>x</sub> data are calculated based on the NO<sub>2</sub> data, using quadratic regression Eq. A1.2. The regression coefficients were estimated based on the rural background stations with both NO<sub>x</sub> and NO<sub>2</sub> measurements (see Section 2.1.1). The number of such type of stations is 318. The estimated coefficients of Eq. A1.2 are:  $a = 0.0401$ ,  $b = 0.725$ ,  $c = 1.75$ . Adjusted R<sup>2</sup> is 0.95, the standard error is 2.0 µg·m<sup>-3</sup>.

Table A3.9 presents the estimated parameters of the linear regression models and of the residual kriging and includes the statistical indicators of both the regression and the kriging.

Only stations with actual measurement data of the relevant pollutant (i.e. not the pseudo stations) are used for calculating of the cross-validation parameters RMSE and bias.

Table A3.9 Parameters and statistics of linear regression model and ordinary kriging of NO<sub>2</sub> annual average for 2016 in rural and urban areas for the final combined map (left) and NO<sub>x</sub> annual average for 2016 in rural areas (right)

		NO <sub>2</sub> Annual average			NO <sub>x</sub> Annual average
		Rural areas	Urb. b. areas	Urb. tr. areas	Rural areas
Linear regression model (LRM, Eq. A1.3)	c (constant)	7.6	18.1	17.18	17.5
	a1 (EMEP model)	0.409	0.132	0.182	0.867
	a2 (altitude)	-0.0089	-0.0069	<i>non signif.</i>	-0.0065
	a3 (altitude_5km_radius)	0.0083	0.0095	0.0096	
	a4 (wind speed)	-0.92	-2.02	<i>non signif.</i>	-2.59
	a5 (satellite OMI)	1.00	1.29	1.58	
	a6 (population*1000)	0.00231	0.00028		
	a7 (NAT_1km)		-0.0836		
	a8 (AGR_1km)		-0.0221		
	a9 (LDR_5km_radius)	0.0684	0.0505	0.2269	
	a10 (HDR_5km_radius)		0.2168	0.3639	
	a11 (NAT_5km_radius)	-0.0414			
	a12 (TRAF_5km_radius)		0.2265		
Adjusted R <sup>2</sup>		0.80	0.35	0.36	0.59
Standard Error [µg·m <sup>-3</sup> ]		2.5	7.9	10.7	6.4
Ordinary kriging (OK) of LRM residuals	nugget	5	15	57	24
	sill	6	27	101	32
	range [km]	210	210	380	320
LRM + OK of its residuals	RMSE [µg·m <sup>-3</sup> ]	2.5	6.7	8.9	6.0
	Relative RMSE [%]	27.8	32.2	25.7	50.4
	Bias (MPE) [µg·m <sup>-3</sup> ]	0.0	0.1	0.0	0.2

#### Uncertainty estimated by cross-validation

Table A3.9 shows both absolute and relative mean uncertainty, expressed by RMSE and Relative RMSE. The absolute mean uncertainty of the final combined map of NO<sub>2</sub> annual average expressed as RMSE is 2.5 µg·m<sup>-3</sup> for the rural areas, 6.7 µg·m<sup>-3</sup> for the urban background areas and 8.9 µg·m<sup>-3</sup> for the urban traffic areas. For the NO<sub>x</sub> rural map it is 6.0 µg·m<sup>-3</sup>.

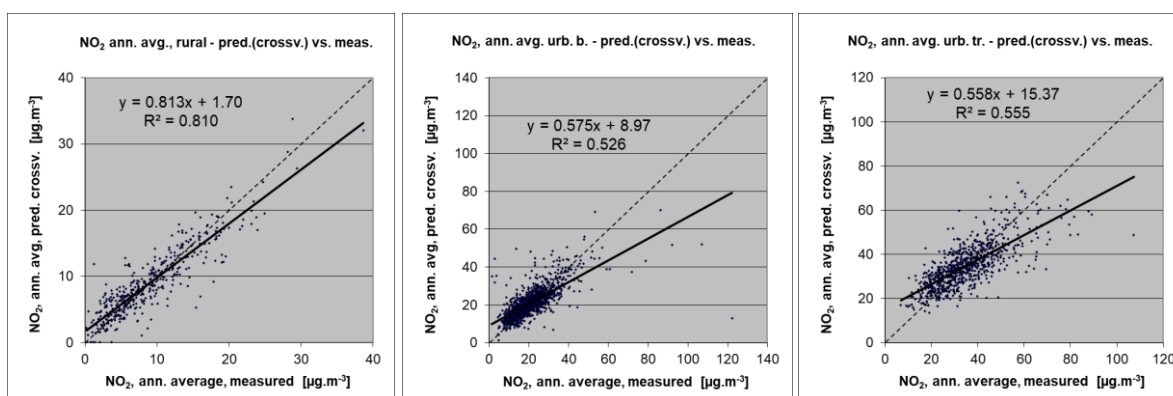
The relative mean uncertainty of the NO<sub>2</sub> annual average map is 28 % for rural, 32 % for urban background areas and 26 % for the urban traffic areas. The results are influenced by the inclusion of a

large number of Turkish stations, mainly in the urban background areas: the relative mean uncertainty of the map outside Turkey is 27 % for rural, 24 % for urban background areas and 25 % for the urban traffic areas.

The NO<sub>x</sub> annual average rural map has a relative mean uncertainty of 50 %. The relative mean uncertainty for the area outside Turkey is 39 %.

Figure A3.8 shows the point observation – point prediction cross-validation scatter plots for NO<sub>2</sub> annual average. The R<sup>2</sup> indicates that about 81 % of the variability is attributable to the interpolation for the rural areas, while for the urban background areas it is 53 % and for the urban traffic 56 %.

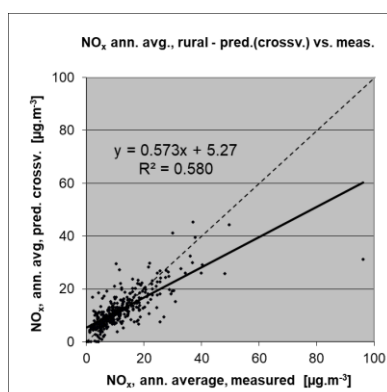
*Figure A3.8 Correlation between cross-validated predicted and measurement values for NO<sub>2</sub> annual average 2016 for rural (left), urban background (middle) and urban traffic (right) areas*



Like in the case of other pollutants, the cross-validation scatter plots show the underestimation of predictions at high concentrations at locations with no measurements. For example, in urban areas an observed value of 40 µg·m<sup>-3</sup> is estimated in the interpolations to be about 32 µg·m<sup>-3</sup>, which is an underestimated prediction of about 20 %.

Figure A3.9 shows the cross-validation scatter plot for NO<sub>x</sub> annual average rural map. The R<sup>2</sup> indicates that about 58 % of the variability is attributable to the interpolation.

*Figure A3.9 Correlation between cross-validated predicted and measurement values for NO<sub>x</sub> annual average 2016 for rural areas*



### Comparison of point measurement values with the predicted grid value

Next to the above presented cross-validation, a simple comparison was made between the point observation values and interpolated predicted 1x1 km resp. 2x2 grid values.

For NO<sub>2</sub> annual average, the comparison has been made primarily for the separate rural, separate urban background and separate urban traffic map layers at 1x1 km resolution. Besides, the comparison



has been done also for the final combined map. Table A3.10 presents the results of this comparison, together with the results of cross-validation prediction of Figure A3.8. One can conclude that the final combined map in 1x1 km resolution is representative for rural and urban background areas, but not for urban traffic areas.

*Table A3.10 Statistical indicators from the scatter plots for the predicted grid values from separate (rural, urban background or urban traffic) map layers and final combined map versus the measurement point values for rural (upper left), urban background (upper right) and urban traffic (bottom left) stations for NO<sub>2</sub> annual average 2016*

	rural backgr. stations				urban/suburban backgr. stations			
	RMSE	bias	R <sup>2</sup>	lin. r. equation	RMSE	bias	R <sup>2</sup>	lin r. equation
cross-valid. prediction, separate (r or ub) map	2.5	0.0	0.810	$y = 0.813x + 1.70$	6.7	0.1	0.526	$y = 0.575x + 8.97$
grid prediction, 1x1 km separate (r or ub) map	2.5	-0.4	0.814	$y = 0.764x + 1.71$	5.1	0.0	0.728	$y = 0.685x + 6.62$
grid prediction, 1x1 km final merged map	2.7	0.3	0.785	$y = 0.875x + 1.37$	5.6	0.6	0.670	$y = 0.696x + 6.94$

	urban/suburban traffic stations			
	RMSE	bias	R <sup>2</sup>	lin. r. equation
cross-valid. prediction, urban traffic map	8.9	0.0	0.555	$y = 0.558x + 15.37$
grid prediction, 1x1 km urban traffic map	7.1	0.0	0.727	$y = 0.652x + 12.06$
grid prediction, 1x1 km final merged map	14.7	-11.1	0.484	$y = 0.430x + 8.73$

Table A3.11 presents the cross-validation results of Figure A3.9 and those of the point observation – grid averaged prediction validation for the rural map of NO<sub>x</sub> annual average.

*Table A3.11 Statistical indicators from the scatter plots for predicted point values based on cross-validation and predicted grid values from rural 2x2 km map versus measurement point values for rural background stations for NO<sub>x</sub> annual average 2016*

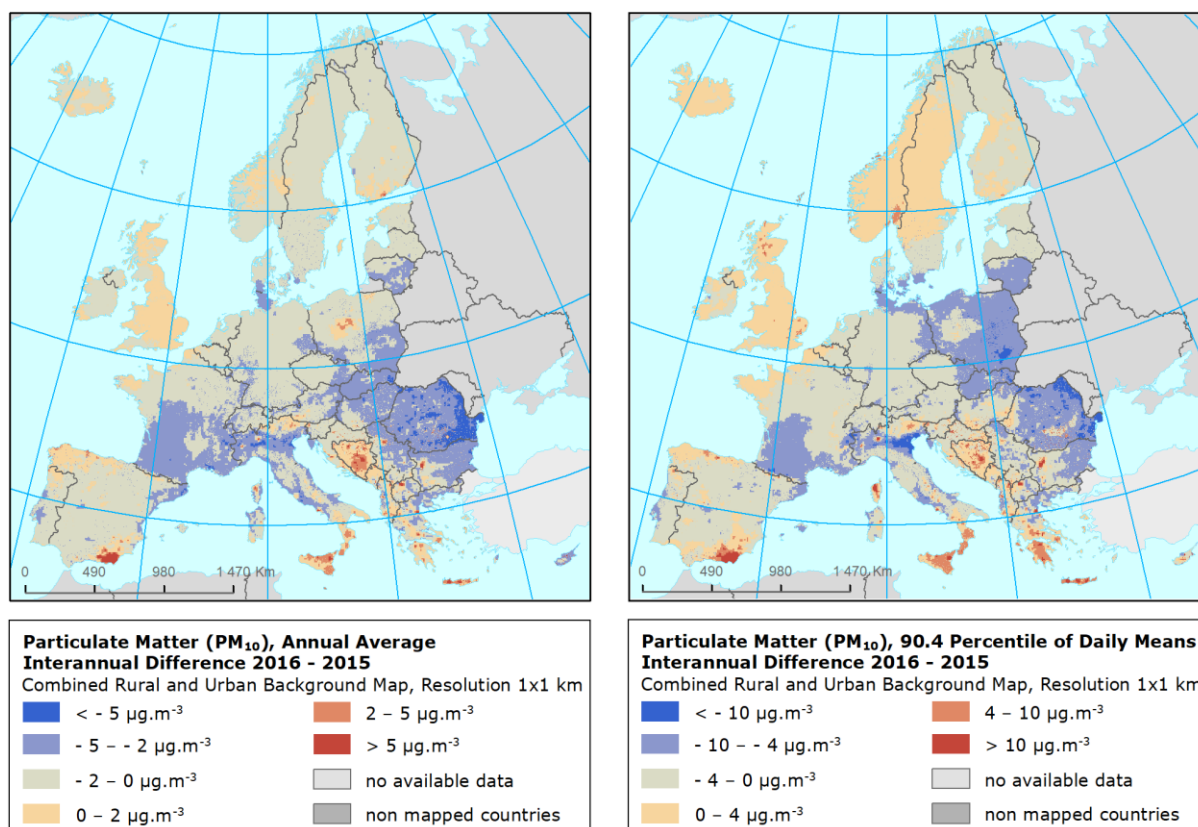
	rural background stations			
	RMSE	bias	R <sup>2</sup>	linear regression equation
cross-valid. prediction, rural map	6.0	0.2	0.580	$y = 0.573x + 5.27$
grid prediction, 2x2 km rural map	4.9	0.1	0.712	$y = 0.647x + 4.26$

## Annex 4 – Inter-annual changes

### A4.1 PM<sub>10</sub>

Map A4.1 presents the inter-annual difference between 2015 and 2016 for annual average and the 90.4 percentile of daily means for PM<sub>10</sub>. Red areas show an increase of PM<sub>10</sub> concentration in 2016, while blue areas show a decrease.

*Map A4.1 Difference concentrations between 2015 and 2016 for PM<sub>10</sub> indicators annual average (left) and 90.4 percentile (right)*



At the annual average PM<sub>10</sub> difference map the highest increases are observed in southern Spain near Almeria, south Italy, isle of Crete, Bosnia & Herzegovina and some large urban areas in Albania, Greece, North Macedonia, Bulgaria, and Serbia. Other increases are at central Poland and near Helsinki. Contrary to that, decreases occur at the most of Romania, eastern Bulgaria, northern Italy and southern France. In some areas (specifically northern Italy and southern France), the pattern of the 2016-2015 difference map seems to be for large part rather the opposite of that of the 2015-2014 difference in Horálek et al (2018a). The fluctuations over years seem to be mostly related to the annual meteorological variability. Besides the actual changes in the concentrations, the variability of the linear regression model and variogram parameters may cause minor differences in the concentration levels estimated.

At the 90.4 percentile of daily means for PM<sub>10</sub> the highest increases are observed again in southern Spain near Almeria, south Italy, Bosnia & Herzegovina, large urban areas in west Balkan and Bulgaria, and also in southern Greece. Decreases are observed in the Po valley in northern Italy, in the eastern Romania, southern France and south western Poland.

## Population exposure

The Tables A4.1 and A4.2 provide the inter-annual variation for PM<sub>10</sub> annual average and the 90.4 percentile of daily PM<sub>10</sub> means over the twelve year period 2005 – 2016 and the inter-annual difference between the last two years (2015 and 2016) for individual countries and for Europe as a whole (without Turkey). The reason for not inclusion of Turkey is the comparability with the previous years.

In 2016, the overall average population-weighted annual mean PM<sub>10</sub> concentration for the whole of Europe was 20.2  $\mu\text{g}\cdot\text{m}^{-3}$ , i.e. its value decreased by of about 1  $\mu\text{g}\cdot\text{m}^{-3}$  compared to the previous year. This is the lowest level of the twelve years period 2005 – 2016. One may observe a steady reduction of the population-weighted concentration over the period of time 2005 – 2011, with perhaps some flattening effect in 2011 – 2013 and further reduction in 2014 and again in 2016. The steepest decreases of population-weighted concentration per country compared to 2016 took place in San Marino, Slovakia, Liechtenstein, Switzerland, and Sweden. The highest increases were detected in Bosnia and Herzegovina, Cyprus and North Macedonia.

Table A4.2 shows the evolution of the annual population exposure in the period 2005-2016 and the inter-annual difference between 2016 and 2015 in relation to the DLV. For the period 2005 – 2011, the results of the 36<sup>th</sup> highest daily mean are presented, while the results of the 90.4 percentile of daily means are given for the period 2012 – 2016. Both statistics are related with the PM<sub>10</sub> daily limit value according to the AQ Directive (EU, 2008), however the 36<sup>th</sup> highest daily mean results are somewhat underestimated due to the incompleteness in time series of the measurement data. The level of the underestimation of the population exposure for the whole Europe is almost 1  $\mu\text{g}\cdot\text{m}^{-3}$  (see Table 6.1), and can explain the most of the increase in 2012 with respect to 2011.

In Table A4.2 the European-wide population-weighted 90.4 percentile of the daily mean PM<sub>10</sub> concentrations is estimated for 2016 at 35.7  $\mu\text{g}\cdot\text{m}^{-3}$ , the lowest in the period of 2005 – 2016 (even if until 2011 the underestimated 36<sup>th</sup> highest daily mean was used instead of the more realistic percentile approach that accounts for measurement incompleteness in time series).

The steepest decreases of population-weighted concentration per country compared to 2016 took place in Poland, Denmark, San Marino and Slovakia. The highest increases were detected in Bosnia and Herzegovina, North Macedonia and Cyprus, i.e. in the same countries like for the annual mean.

Table A4.1 Evolution in 2005–2016 and difference between 2015 and 2016 for population-weighted concentration, PM<sub>10</sub> annual average.

Country		Population-weighted conc. [µg·m <sup>-3</sup> ]												Differ. '16 - '15
		2005	2006	2007	2008	2009	2010	2011	2012	2013	2014	2015	2016	
Albania	AL	36.3	31.8	31.6	33.3	35.3	45.5	26.5	32.0	32.5	25.7	30.2	31.6	1.4
Andorra	AD	19.5	22.5	20.5	18.7	17.7	17.9	18.0	33.2	25.0	21.3	24.7	23.8	-0.9
Austria	AT	25.4	26.0	22.1	21.3	21.6	22.7	20.8	20.0	20.2	17.8	18.7	16.7	-2.0
Belgium	BE	29.2	31.3	24.8	23.9	26.5	25.7	24.8	23.2	23.6	20.2	20.4	19.7	-0.6
Bosnia-Herzegovina	BA	34.3	33.1	32.4	29.3	37.2	30.8	22.3	27.2	23.1	22.1	26.8	35.1	8.3
Bulgaria	BG	42.6	41.6	40.2	44.2	39.8	38.0	27.3	36.6	36.7	36.2	33.1	33.2	0.2
Croatia	HR	33.6	31.5	30.0	28.1	29.0	27.3	25.0	24.7	23.5	21.7	25.1	26.3	1.2
Cyprus	CY	38.9	35.4	33.9	76.1	41.0	50.2	31.1	42.9	35.8	32.1	31.4	36.6	5.2
Czechia	CZ	32.9	33.5	25.6	24.2	25.3	28.3	23.7	25.4	25.6	25.5	23.3	21.9	-1.4
Denmark	DK	21.3	23.5	20.8	18.8	16.3	15.7	18.4	16.3	16.3	18.5	17.1	15.1	-1.9
Estonia	EE	17.7	19.7	15.7	12.9	13.4	14.1	9.8	12.1	13.5	14.8	12.1	11.2	-0.9
Finland	FI	14.2	17.0	13.7	12.5	11.7	12.2	9.5	10.2	10.5	12.0	9.1	9.4	0.3
France	FR	19.3	20.4	24.6	22.6	24.0	23.0	21.8	21.4	20.7	16.7	18.2	16.8	-1.4
Germany	DE	23.0	24.2	20.7	19.6	20.7	21.2	19.6	18.4	19.0	18.7	17.8	16.5	-1.3
Greece	GR	38.0	33.6	33.5	39.7	35.3	37.3	24.6	30.3	34.6	27.4	28.7	29.3	0.5
Hungary	HU	34.8	32.9	28.7	26.8	27.6	28.1	29.1	26.1	25.3	25.4	26.3	24.7	-1.6
Iceland	IS	13.8	17.4	12.2	15.2	9.0	10.7	9.3	9.6	11.8	12.7	9.7	9.1	-0.6
Ireland	IE	12.7	14.9	14.7	15.4	12.8	13.7	12.8	12.4	15.1	13.7	11.9	11.7	-0.2
Italy	IT	34.9	33.9	33.2	30.1	28.7	26.4	27.7	27.0	27.0	24.0	26.6	25.2	-1.4
Latvia	LV	19.8	21.9	17.8	19.1	18.8	21.5	14.6	18.0	19.5	20.3	16.5	15.8	-0.7
Liechtenstein	LI	23.4	24.9	20.7	20.6	18.3	17.3	11.3	14.3	15.5	13.1	16.3	13.7	-2.6
Lithuania	LT	20.7	22.5	18.5	17.3	19.0	22.0	14.8	18.1	20.4	21.7	18.5	17.6	-0.9
Luxembourg	LU	18.7	20.8	19.5	18.2	21.0	19.4	16.4	17.2	18.8	17.4	18.5	16.9	-1.6
Malta	MT	37.1	29.4	27.0	27.5	27.2	32.5	27.8	25.4	35.7	28.9	26.4	29.5	3.1
Monaco	MC		36.7	34.5	29.5	26.8	24.0	22.8	28.0	22.7	22.3	23.2	21.9	-1.3
Montenegro	ME	35.1	33.1	33.1	33.6	35.0	32.8	21.5	28.3	27.0	24.6	26.7	27.0	0.4
Netherlands	NL	29.2	29.1	25.8	24.0	24.3	24.3	25.1	21.1	20.7	20.2	18.7	17.9	-0.8
North Macedonia	MK	46.2	39.3	38.5	41.6	45.4	43.9	23.0	42.3	44.5	39.3	37.3	42.4	5.0
Norway	NO	18.1	19.6	15.6	15.7	14.1	14.7	9.3	12.2	13.8	12.6	11.1	10.5	-0.6
Poland	PL	32.7	37.0	28.8	28.3	30.8	35.2	27.2	32.4	30.4	31.5	29.5	27.6	-1.9
Portugal	PT	30.9	28.4	27.0	21.8	22.9	21.7	20.8	19.9	20.3	16.9	18.7	17.5	-1.2
Romania	RO	42.7	39.1	35.0	30.8	28.9	25.2	27.2	28.9	26.0	25.9	25.7	24.7	-1.0
San Marino	SM	31.7	33.9	31.2	29.6	26.0	25.0	20.9	25.8	22.1	21.2	24.6	21.0	-3.6
Serbia (incl. Kosovo*)	RS	44.2	41.8	39.4	40.1	39.5	33.1	30.1	34.9	31.8	32.1	32.7	33.8	1.1
Slovakia	SK	34.3	33.8	29.1	26.7	26.9	30.2	27.4	27.9	26.8	27.2	26.3	23.4	-2.9
Slovenia	SI	30.8	29.0	27.2	25.0	25.2	26.0	25.4	24.3	22.7	20.3	23.3	22.3	-1.0
Spain	ES	29.6	31.4	29.6	25.2	23.7	21.4	18.8	20.9	19.1	19.7	21.6	20.2	-1.5
Sweden	SE	16.9	19.0	15.7	16.3	13.8	12.8	12.3	12.4	13.2	13.8	13.3	11.1	-2.3
Switzerland	CH	21.3	23.2	21.4	20.5	21.0	19.8	17.7	17.6	18.3	16.5	17.4	15.0	-2.4
United Kingdom	UK	21.4	23.2	21.6	19.5	18.4	18.2	17.5	16.5	17.0	16.6	15.1	15.5	0.4
Total		28.0	28.5	26.2	24.8	24.6	24.3	22.1	22.7	22.2	21.1	21.2	20.2	-0.9
EU-28		27.6	28.3	26.0	24.4	24.2	24.0	22.1	22.4	22.1	20.9	20.9	19.9	-1.0

\*) under the UN Security Council Resolution 1244/99

Next to the population-weighted concentration, another trend indicator is the evolution of the percentage of population living in areas with concentrations above the limit value. However, the percentage of population living above the limit value is not a very robust statistical parameter: just small changes in the level of concentrations closely around the threshold and over extended areas might result in large changes in exposed population. The evolution of this statistics for European area as a whole is presented in Table 6.1.

Table A4.2 Evolution in 2005–2016 and difference between 2015 and 2016 for population-weighted concentration, PM<sub>10</sub> indicator 36<sup>th</sup> highest daily mean / 90.4 percentile of daily means.

Country		Population-weighted conc. [µg·m <sup>-3</sup> ]												
		36 <sup>th</sup> highest daily mean							90.4 perc. of daily means					
		2005	2006	2007	2008	2009	2010	2011	2012	2013	2014	2015	2016	diff. '16 - '15
Albania	AL	59.8	54.0	53.3	55.7	51.3	69.5	42.8	57.2	61.4	47.4	56.6	62.2	5.5
Andorra	AD	31.1	35.7	32.1	29.3	29.4	28.5	29.2	78.4	47.6	41.9	45.7	47.2	1.5
Austria	AT	45.7	47.1	39.9	36.9	36.7	42.8	38.7	36.1	37.0	32.4	32.4	30.1	-2.3
Belgium	BE	46.9	51.3	43.5	38.4	45.8	42.7	45.1	43.9	41.2	35.0	34.6	34.4	-0.2
Bosnia-Herzegovina	BA	57.3	57.4	52.7	50.6	57.8	53.7	40.8	52.8	44.2	44.2	54.5	81.2	26.8
Bulgaria	BG	73.3	74.2	67.5	78.2	70.3	69.2	46.6	66.9	67.9	68.4	62.2	63.4	1.2
Croatia	HR	57.6	53.7	49.6	48.6	46.9	50.5	46.6	45.5	44.6	42.1	46.8	54.3	7.5
Cyprus	CY	63.7	58.2	54.4	130.7	68.6	74.5	46.2	62.0	56.9	47.4	45.2	54.0	8.8
Czechia	CZ	60.2	57.5	46.2	42.5	43.6	53.7	46.2	47.6	46.9	47.3	41.6	38.9	-2.6
Denmark	DK	34.5	37.0	32.5	29.0	26.0	25.5	31.6	26.3	26.7	32.6	29.3	24.7	-4.6
Estonia	EE	31.7	34.1	28.0	22.4	22.4	25.8	17.6	21.6	22.6	26.4	20.7	19.7	-1.0
Finland	FI	24.2	29.5	23.9	21.9	19.4	22.7	16.9	18.3	18.0	22.4	15.0	16.1	1.2
France	FR	29.8	32.9	41.0	36.3	39.2	37.1	36.6	38.1	36.9	28.2	30.2	28.9	-1.4
Germany	DE	38.6	41.3	35.7	31.7	34.4	37.2	35.7	32.8	32.9	33.0	30.6	27.9	-2.6
Greece	GR	59.9	54.3	53.0	64.9	54.7	64.8	37.6	47.8	61.2	46.4	48.2	51.7	3.5
Hungary	HU	61.6	58.5	48.5	47.5	46.4	52.3	55.4	47.2	44.6	45.3	46.2	46.0	-0.3
Iceland	IS	19.0	27.2	21.4	25.4	15.8	16.8	15.8	17.6	20.1	22.3	14.5	16.8	2.3
Ireland	IE	17.8	24.1	24.8	25.8	21.7	23.2	23.2	21.8	26.3	23.6	21.3	21.4	0.0
Italy	IT	60.2	58.6	57.4	51.7	48.6	45.2	48.6	48.0	49.7	42.1	47.4	44.4	-3.0
Latvia	LV	35.9	40.0	31.9	32.7	33.4	37.8	26.7	33.7	33.0	36.1	29.0	27.2	-1.8
Liechtenstein	LI	40.2	47.5	39.3	38.5	31.5	33.6	21.3	27.7	32.4	23.6	28.9	25.8	-3.1
Lithuania	LT	37.7	39.7	33.2	29.5	32.7	39.5	26.6	33.9	34.1	38.8	34.0	30.1	-3.9
Luxembourg	LU	31.2	35.9	32.5	29.1	34.3	31.9	29.4	30.6	31.5	29.6	31.1	28.1	-3.0
Malta	MT	62.7	44.8	42.6	40.3	38.7	49.4	39.7	37.8	62.2	42.4	41.7	44.7	3.0
Monaco	MC		59.7	46.2	46.0	41.5	36.1	37.0	46.0	39.0	34.8	35.0	36.3	1.3
Montenegro	ME	58.7	57.9	53.6	56.7	51.8	54.0	36.2	55.9	53.6	49.2	52.9	54.9	2.0
Netherlands	NL	47.5	46.1	41.9	37.7	39.0	40.2	44.0	35.8	34.2	34.5	30.2	29.7	-0.5
North Macedonia	MK	77.5	69.9	57.8	71.5	75.6	80.1	37.9	80.4	93.1	80.9	78.1	93.0	14.9
Norway	NO	29.3	31.9	26.3	26.1	24.0	25.7	16.3	21.9	23.7	22.4	19.3	19.3	0.0
Poland	PL	58.6	64.0	50.8	48.6	55.4	65.7	51.4	62.7	55.4	58.0	55.7	49.5	-6.2
Portugal	PT	52.0	48.3	45.0	35.5	38.5	35.6	35.4	35.8	34.5	29.9	31.8	28.6	-3.3
Romania	RO	73.4	65.4	57.7	53.1	49.0	45.2	48.1	50.0	45.4	45.4	43.8	43.9	0.0
San Marino	SM	51.7	57.4	54.1	48.9	40.6	44.0	35.9	44.3	40.2	38.5	43.7	39.2	-4.5
Serbia (incl. Kosovo*)	RS	73.1	73.1	61.8	68.6	67.6	60.1	54.6	65.9	61.3	63.3	65.7	66.3	0.6
Slovakia	SK	60.9	58.5	50.5	47.5	46.2	56.0	51.5	51.6	47.5	48.7	47.4	43.3	-4.1
Slovenia	SI	53.7	49.2	46.1	42.7	41.9	47.2	48.1	44.0	42.2	37.3	42.6	43.4	0.9
Spain	ES	46.7	49.3	46.9	40.1	38.0	33.4	30.5	34.2	30.7	32.0	34.9	32.8	-2.2
Sweden	SE	27.7	32.0	25.8	26.4	23.3	22.1	21.1	21.2	22.5	24.3	22.4	19.6	-2.7
Switzerland	CH	36.0	43.9	39.9	36.5	37.1	36.3	33.0	32.8	36.5	28.3	30.1	27.4	-2.7
United Kingdom	UK	32.5	35.5	34.7	32.1	30.1	28.8	30.3	29.6	29.0	28.7	25.3	27.1	1.8
Total		46.8	47.8	44.1	41.3	41.2	41.9	39.0	40.6	39.4	37.1	36.9	35.7	-1.2
EU-28		46.1	47.2	43.8	40.5	40.5	41.3	39.0	40.0	38.8	36.6	36.2	34.7	-1.6

\*) under the UN Security Council Resolution 1244/99

## Uncertainties

Table A4.3 summarises the twelve-year evolution of the absolute and relative mean interpolation uncertainties, and also R<sup>2</sup> from cross-validation scatterplots, for the rural and urban background maps, for both PM<sub>10</sub> indicators.

In the year 2016, both the absolute and the relative uncertainty results show slightly worse levels for rural areas and quite worse levels for urban areas, compared to 2015. The results for  $R^2$  from cross-validation scatterplots show slightly worse compared to 2015, for most of the cases. The poorer results in 2016 compared to previous years are mainly caused by the inclusion of Turkey in the mapping.

*Table A4.3 Absolute and relative mean uncertainty and  $R^2$  from cross-validation scatterplot for the total European rural and urban areas,  $PM_{10}$  indicators annual average and 90.4 percentile of daily means, years 2005 – 2016*

PM10			2005	2006	2007	2008	2009	2010	2011	2012	2013	2014	2015	2016
Annual average														
rural areas	abs. mean uncertainty	RMSE [ $\mu\text{g.m}^{-3}$ ]	5.5	5.8	4.6	5.0	4.6	4.5	4.1	3.8	3.4	3.5	3.2	3.5
	rel. mean uncertainty	RRMSE [%]	25.9	26.6	23.5	27.2	23.9	22.7	21.1	21.4	19.6	20.7	19.4	22.7
	coeff. of determination	$R^2$	0.52	0.52	0.59	0.48	0.54	0.62	0.68	0.67	0.70	0.68	0.71	0.66
urban areas	abs. mean uncertainty	RMSE [ $\mu\text{g.m}^{-3}$ ]	5.5	6.1	5.0	6.3	6.7	6.6	6.1	6.1	4.3	4.2	4.5	7.6
	rel. mean uncertainty	RRMSE [%]	20.0	20.9	18.4	22.4	23.0	22.5	20.7	22.1	17.3	17.7	19.2	30.6
	coeff. of determination	$R^2$	0.71	0.69	0.66	0.82	0.73	0.75	0.77	0.76	0.74	0.76	0.69	0.64
36 <sup>th</sup> max. daily mean (2005 - 2011) / 90.4 percentile of daily means (2012 - 2016)														
rural areas	abs. mean uncertainty	RMSE [ $\mu\text{g.m}^{-3}$ ]	9.7	9.9	8.0	8.8	8.0	8.6	8.4	7.8	6.5	6.5	6.2	7.2
	rel. mean uncertainty	RRMSE [%]	26.3	26.6	23.5	28.2	24.1	24.4	23.5	24.3	21.0	21.5	21.1	26.5
	coeff. of determination	$R^2$	0.55	0.56	0.60	0.52	0.56	0.64	0.66	0.64	0.69	0.69	0.70	0.60
urban areas	abs. mean uncertainty	RMSE [ $\mu\text{g.m}^{-3}$ ]	9.9	11.7	9.1	12.7	13.2	12.2	13.0	12.1	8.6	8.6	10.8	15.2
	rel. mean uncertainty	RRMSE [%]	21.4	23.5	19.6	24.4	26.7	23.7	24.3	25.0	19.5	20.4	25.6	34.2
	coeff. of determination	$R^2$	0.75	0.65	0.65	0.79	0.72	0.77	0.75	0.75	0.75	0.76	0.64	0.64

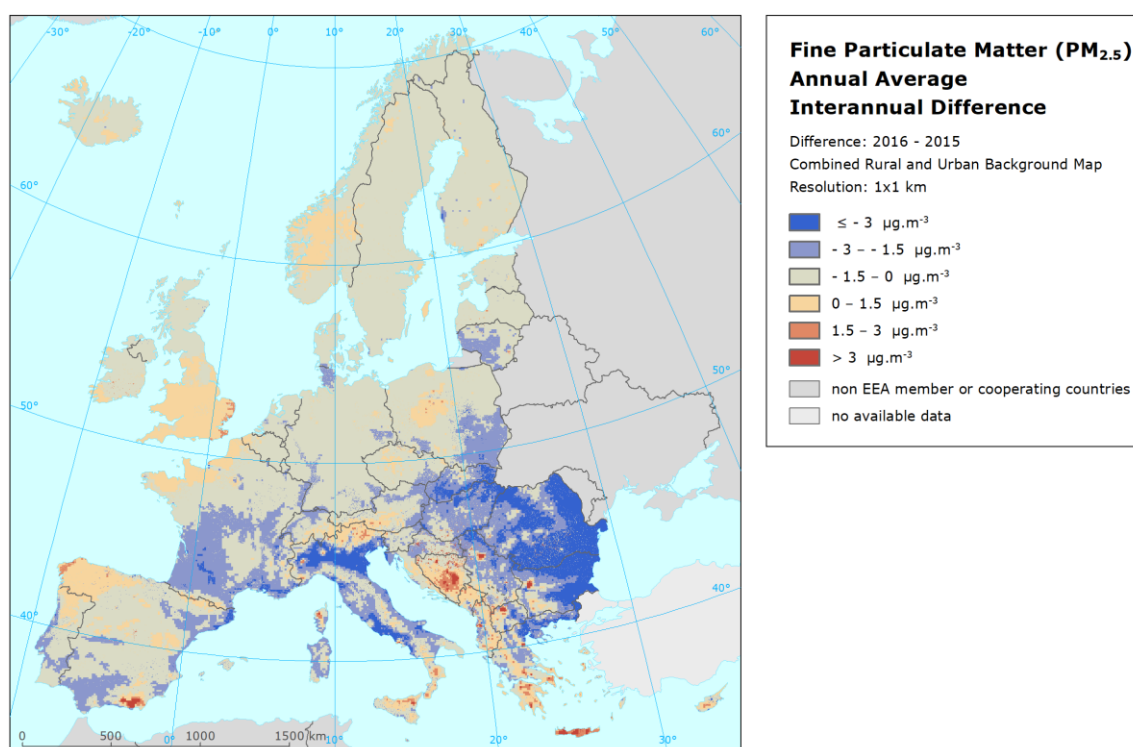
## A4.2 $PM_{2.5}$

### Air concentrations

Map A4.2 presents the inter-annual difference between 2016 and 2015 for annual average  $PM_{2.5}$ .

The highest increases are seen in the Almeria region in southern Spain, isle of Crete, southern Greece, Bosnia & Herzegovina and urban areas in west Balkan and western Bulgaria. The steepest decrease from 2015 to 2016 is observed in Po Valley and large rural areas of Romania and eastern Bulgaria.

Map A4.2 Difference  $PM_{2.5}$  annual average concentrations between 2015 and 2016



## Population exposure

Table A4.4 shows the evolution of the population exposure for the years 2007 – 2016, with missing calculations for 2009, based on the results presented in Chapter 3.1 and in Horálek et al. (2017b) resp. references cited therein. Next to this, the inter-annual difference between 2015 and 2016 is presented in this table.

One may observe similar levels in the population-weighted concentration across Europe as a whole in 2007 – 2008, an increase in 2010, slightly continuous reduction for the period 2010 – 2014, stagnation in 2015, and further reduction in 2016. For the whole period 2007 – 2016, a downward trend is detected (Section 6.2.1). The steepest decreases of population-weighted concentration per country in 2016 compared to 2015 took place in Cyprus, San Marino, Italy, Bulgaria, Malta, and Switzerland. The highest increases were detected in Bosnia and Herzegovina, North Macedonia and Croatia.

The evolution of the percentage population living in areas with concentrations above the  $PM_{2.5}$  limit value in Europe as a whole is presented in Table 6.2. In 2016, the percentage is slightly below the average of the limited time series. Throughout the years, fluctuations do occur. However, as stated earlier, the percentage population living in areas with concentrations above the limit value is not statistically a very robust parameter.



Table A4.4 Evolution and trend in 2007–2016 and difference between 2015 and 2016 for population-weighted concentration, PM<sub>2.5</sub> annual average.

Country		Population-weighted conc. [µg·m <sup>-3</sup> ]										Differ. '15
		2007	2008	2009	2010	2011	2012	2013	2014	2015	2016	
Albania	AL	20.8	19.6	not mapped	25.1	17.2	21.1	20.3	16.5	20.5	22.3	1.8
Andorra	AD	11.5	11.3		12.4	13.7	15.9	11.9	10.0	13.3	12.1	-1.1
Austria	AT	16.3	16.4		17.7	16.3	14.8	15.7	12.9	13.3	12.0	-1.4
Belgium	BE	16.6	17.1		18.8	17.3	15.8	16.6	13.7	13.0	12.7	-0.3
Bosnia-Herzegovina	BA	21.7	20.3		22.2	17.2	18.5	16.0	15.3	18.9	28.7	9.8
Bulgaria	BG	28.8	28.4		24.5	18.3	24.9	24.1	24.0	24.1	22.3	-1.8
Croatia	HR	19.5	18.5		20.0	19.6	16.8	16.8	15.6	17.4	19.4	2.0
Cyprus	CY	25.0	25.3		21.8	21.0	25.0	17.0	17.0	16.9	13.7	-3.3
Czech Republic	CZ	17.5	17.7		21.5	18.8	18.8	19.6	18.7	17.0	16.6	-0.4
Denmark	DK	11.5	11.1		11.4	12.5	10.0	9.6	11.6	9.7	9.2	-0.5
Estonia	EE	8.8	8.9		8.9	8.0	7.9	7.8	8.7	6.7	5.9	-0.8
Finland	FI	7.7	7.4		7.8	7.4	7.1	5.9	7.4	5.3	5.1	-0.2
France	FR	14.9	14.7		16.2	15.3	14.7	14.5	11.0	11.9	10.9	-1.0
Germany	DE	14.0	14.1		16.3	14.8	13.3	14.2	13.4	12.3	11.6	-0.7
Greece	GR	22.0	21.7		20.0	16.8	19.2	19.7	17.0	19.1	19.6	0.5
Hungary	HU	19.3	19.4		20.3	23.1	18.9	18.2	17.3	18.9	17.5	-1.4
Iceland	IS	7.1	7.1		6.9	4.6	4.7	6.5	6.6	5.5	4.8	-0.6
Ireland	IE	8.5	9.6		10.3	7.9	8.1	9.2	9.0	6.5	6.8	0.3
Italy	IT	19.0	19.1		17.5	19.8	18.9	18.2	15.8	18.5	16.6	-1.8
Latvia	LV	15.3	16.4		14.7	11.1	12.4	12.8	14.1	10.6	10.9	0.2
Liechtenstein	LI	15.5	15.5		15.3	8.5	10.2	11.4	9.0	11.0	10.3	-0.6
Lithuania	LT	13.8	15.5		15.6	12.7	12.9	13.9	15.5	11.7	11.8	0.0
Luxembourg	LU	13.9	14.5		15.8	13.3	12.6	14.3	11.9	12.0	11.4	-0.7
Malta	MT	14.9	14.9		13.8	15.6	12.4	12.5	12.0	12.8	11.1	-1.7
Monaco	MC	16.5	16.5		14.9	16.4	18.2	13.8	12.9	14.4	14.3	-0.2
Montenegro	ME	21.4	19.9		24.6	15.1	18.7	17.1	15.6	18.5	20.3	1.8
Netherlands	NL	16.9	17.0		17.6	17.1	13.7	14.3	13.8	12.3	11.3	-1.0
North Macedonia	MK	24.4	23.6		27.5	15.8	29.2	30.4	27.4	28.7	34.6	5.9
Norway	NO	8.6	8.2		8.8	6.3	7.2	7.1	7.2	5.9	5.9	0.0
Poland	PL	20.8	21.1		26.4	21.8	23.9	22.8	22.9	21.6	20.6	-1.0
Portugal	PT	11.5	10.9		10.5	10.5	9.9	10.0	8.7	9.8	8.3	-1.5
Romania	RO	22.4	21.8		17.0	20.5	20.8	18.5	17.5	18.1	16.8	-1.3
San Marino	SM	18.2	18.2		16.3	14.7	16.7	15.1	13.5	16.2	14.3	-1.9
Serbia (incl. Kosovo*)	RS	26.6	25.4		22.7	21.2	24.3	22.5	22.4	23.9	25.1	1.2
Slovakia	SK	20.2	20.6		21.3	21.8	20.5	20.1	19.2	19.1	17.6	-1.5
Slovenia	SI	18.5	18.0		19.0	19.4	17.7	17.4	15.1	17.4	16.0	-1.4
Spain	ES	14.1	13.6		11.8	11.1	11.9	11.0	10.7	12.7	11.1	-1.5
Sweden	SE	9.2	8.8		8.1	8.1	7.2	6.0	7.6	5.9	5.7	-0.3
Switzerland	CH	14.9	14.8		15.5	12.6	12.6	13.9	11.6	11.8	10.1	-1.7
United Kingdom	UK	12.2	12.5		13.0	12.4	11.9	11.8	11.6	9.4	9.5	0.1
Total		16.3	16.3		16.8	15.9	15.6	15.3	14.1	14.2	13.4	-0.7
EU-28		16.1	16.1		16.7	15.9	15.5	15.1	14.0	14.0	13.1	-0.9

\*) under the UN Security Council Resolution 1244/99

## Uncertainties

Table A4.5 presents the uncertainty results for PM<sub>2.5</sub> maps for the years 2007 – 2016 (excluding the ‘not-mapped’ year 2009). The results for 2016 lie within the range of previous five years, both for absolute and relative uncertainties.



Table A4.5 Absolute and relative mean uncertainty and  $R^2$  from cross-validation scatterplot for the total European rural and urban areas,  $PM_{2.5}$  annual average, years 2007 – 2016

PM <sub>2.5</sub>			2007	2008	2009	2010	2011	2012	2013	2014	2015	2016
Annual average												
rural areas	abs. mean uncertainty	RMSE [ $\mu\text{g.m}^{-3}$ ]	3.3	3.5	not mapped	3.4	2.8	3.0	2.7	2.5	2.5	2.5
	rel. mean uncertainty	RRMSE [%]	27.4	29.8		25.0	16.8	24.9	22.1	22.4	21.9	24.3
	coeff. of determination	$R^2$				0.74	0.82	0.78	0.78	0.78	0.78	0.74
urban areas	abs. mean uncertainty	RMSE [ $\mu\text{g.m}^{-3}$ ]	4.1	3.6	not mapped	3.1	3.2	3.3	2.9	2.6	2.6	2.7
	rel. mean uncertainty	RRMSE [%]	23.7	20.0		16.8	16.7	18.7	17.5	16.4	16.6	18.3
	coeff. of determination	$R^2$				0.81	0.80	0.78	0.78	0.81	0.82	0.81

### A4.3 Ozone

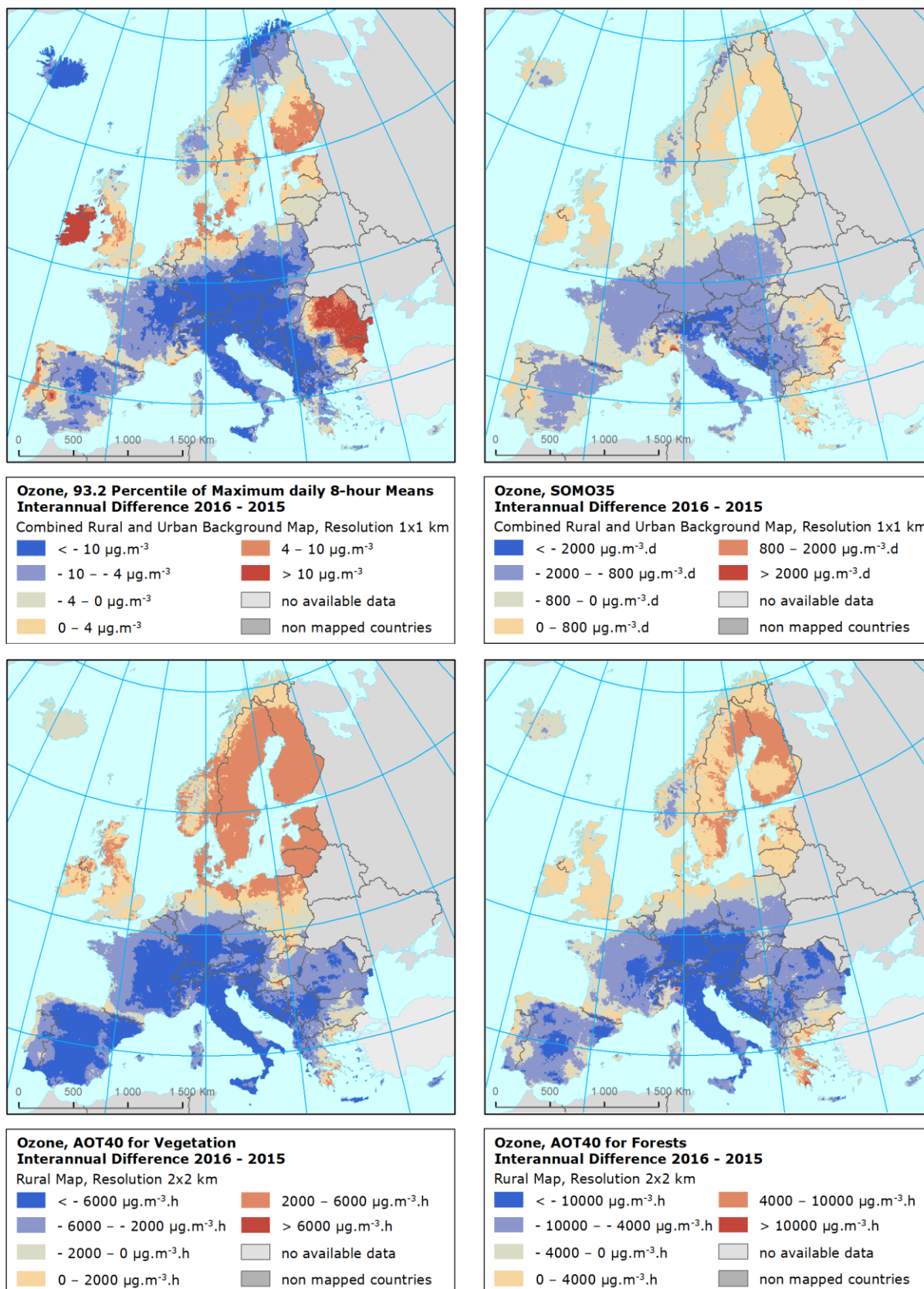
Map A4.3 presents the inter-annual difference between 2015 and 2016 for health related ozone indicators, i.e. for 93.2 percentile of maximum daily 8-hour means and SOMO35; and for vegetation related ozone indicators, i.e. for AOT40 for vegetation and AOT40 for forests. In all the maps, red areas show an increase of ozone concentrations, while blue areas show a decrease.

Most of the European continent and Iceland show a quite steep decrease for 93.2 percentile of maximum daily 8-hour means from 2015 to 2016, i.e. the opposite of that of the 2015-2014 difference in Horálek et al (2018a). This development is caused by the extraordinary 2015 year with high ozone concentrations. The steepest increase can be seen in the Romanian-Bulgarian region, Sweden, southern Finland, and Ireland, i.e. again in the opposite direction compared to 2015-2014 difference.

The difference pattern for SOMO35 is quite similar to that of the percentile indicator, however, the extremes are less elevated or prominent, except for central Italy, some areas around the Alps and the Balkan region, where elevated decreases are observed. Increases are only observed in the Romanian-Bulgarian region, and a few location in north-western Italy. Mostly the opposite development compared to the 2015-2014 difference is observed.

In the case of AOT40 for vegetation, decreases are observed in the large extend of south-western, south, central and south-eastern of Europe. Contrary to that, increases are observed in the most of Scandinavia, Denmark, northern Poland and Baltic countries. In the case of AOT40 for forests, the whole continental area except Scandinavia, Denmark, Baltic countries and Greece shows decreases. The main increase is visible in eastern Sweden, Finland and Greece.

Map A4.3 Difference concentrations between 2015 and 2016 for ozone indicators 93.2 percentile of daily 8-hour maximums (top left), SOMO35 (top right), AOT40v (bottom left) and AOT40f (bottom right)



## Population exposure

Table A4.6 provides the evolution of the annual population exposure in the period 2005–2016 and the inter-annual difference between 2015 and 2016. For the period 2005 – 2011, the results of the 26<sup>th</sup> highest maximum daily 8-hour mean are presented, while the results of the 93.2 percentile of maximum daily 8-hour means are given for the period 2012 – 2016. Both statistics are related to the ozone target value threshold for the protection of health according to the AQ Directive (EU, 2008), however the 26<sup>th</sup> highest maximum daily 8-hour mean results are somewhat underestimated due to the incomplete time series of the measurement data. The level of the underestimation of the population exposure for the whole Europe is about  $0.6 \mu\text{g}\cdot\text{m}^{-3}$  (see Table 6.3).

In 2016 the overall population-weighted concentration for ozone indicator 93.2 percentile of maximum daily 8-hour means for whole of Europe (without Turkey) was  $104.8 \mu\text{g}\cdot\text{m}^{-3}$ . This is the second lowest value of the whole twelve years period (the lowest values is detected for 2014). Examining the time series 2005 – 2016, one could conclude that 2006 was an exceptional year with highly elevated ozone, which was followed by the decrease of concentration levels in 2007 – 2010 and some increase and flattening in 2011 – 2013, further reduction in 2014, increase in 2015 and reduction in 2016.

The steepest decreases of population-weighted concentration per country compared to 2015 were detected in North Macedonia, Serbia, Albania, Austria, Hungary, and Czechia. The highest increases are seen in Ireland, Iceland and Denmark.

Table A4.7 provides the evolution of the annual population exposure in the period 2005–2016 and the inter-annual difference between 2015 and 2016 for SOMO35, based on the results presented in Chapter 4.2 and in Horálek et al. (2018a). In 2016 the overall population-weighted value of ozone indicator SOMO35 for whole of Europe (without Turkey) was  $3619 \mu\text{g}\cdot\text{m}^{-3}\cdot\text{d}$ . This is the second lowest value of the whole twelve years period, when the lowest value was detected in 2014.

The steepest decreases of population-weighted concentration per country compared to 2015 were detected in North Macedonia, Albania, Serbia, Austria and Slovenia. The steepest increases took place in Ireland, Iceland, and Latvia.

Next to the population-weighted concentration evolution, the evolution of the percentage European population living in areas with concentrations above the ozone target value for the 93.2 percentile of maximum daily 8-hour means resp. above a level of  $6\,000 \mu\text{g}\cdot\text{m}^{-3}\cdot\text{d}$  for SOMO35 is presented in Table 6.3. However, as stated earlier, the percentage population living in areas with concentrations above the target value threshold is not statistically a very robust indicator.

Table A4.6 Evolution in 2005–2016 and difference between 2015 and 2016 for population-weighted concentration, ozone indicator 26<sup>th</sup> highest maximum daily 8-hour mean / 93.2 percentile of maximum daily 8-hour means.

Country		Population-weighted conc. [ $\mu\text{g}\cdot\text{m}^{-3}$ ]												
		26 <sup>th</sup> highest daily maximum 8-hour mean							93.2 perc. of d. max. 8-h m.					
		2005	2006	2007	2008	2009	2010	2011	2012	2013	2014	2015	2016	Differ. '15
Albania	AL	122.7	117.9	126.9	115.3	114.7	109.5	121.1	134.4	117.8	107.4	127.3	107.7	-19.6
Andorra	AD	127.2	119.1	118.6	122.0	115.6	122.4	120.6	122.5	122.4	117.4	114.3	109.2	-5.0
Austria	AT	120.6	124.9	122.8	114.8	116.4	118.4	118.6	118.7	121.4	112.0	131.1	111.8	-19.3
Belgium	BE	104.0	126.0	98.9	103.6	101.5	97.7	104.4	94.7	102.5	99.0	104.3	100.2	-4.1
Bosnia-Herzegovina	BA	119.9	118.1	122.5	113.7	114.5	107.4	109.9	126.3	116.2	105.6	118.2	105.2	-12.9
Bulgaria	BG	109.9	105.0	115.7	114.4	112.0	103.8	105.1	116.5	103.5	94.6	106.5	98.7	-7.8
Croatia	HR	122.8	124.8	124.7	115.5	115.6	114.3	118.3	125.7	119.4	109.5	121.4	109.5	-11.9
Cyprus	CY	114.5	102.1	116.9	115.2	120.8	109.8	112.0	116.2	110.9	104.6	110.3	105.0	-5.2
Czechia	CZ	121.6	126.5	121.0	114.6	113.5	114.1	114.8	116.7	113.9	109.6	129.2	114.7	-14.6
Denmark	DK	95.0	104.9	95.2	102.6	95.5	91.4	96.9	95.7	96.7	96.6	89.1	95.3	6.2
Estonia	EE	94.2	105.1	94.1	96.3	90.8	97.2	94.8	93.3	97.6	92.8	89.3	92.6	3.3
Finland	FI	92.9	100.7	89.0	94.3	90.6	92.2	93.0	88.8	92.6	89.1	85.3	88.8	3.5
France	FR	113.8	122.0	109.0	107.3	107.3	111.6	112.8	104.7	113.2	105.6	110.0	104.8	-5.2
Germany	DE	113.8	125.8	113.3	113.5	108.8	112.8	111.5	107.1	110.2	107.9	118.5	110.7	-7.8
Greece	GR	125.4	115.8	126.5	131.1	122.8	119.4	126.5	133.1	123.5	112.2	121.4	115.8	-5.6
Hungary	HU	119.7	121.7	125.0	117.5	124.2	110.9	117.1	122.3	113.9	103.2	123.9	106.2	-17.8
Iceland	IS	85.2	93.3	81.1	90.8	81.4	78.3	83.6	81.1	87.8	69.0	70.1	78.3	8.2
Ireland	IE	86.5	90.2	84.2	92.1	84.9	85.6	84.4	87.1	91.6	58.1	56.1	84.4	28.3
Italy	IT	131.1	135.1	129.5	123.2	125.8	124.3	127.7	130.5	126.1	116.2	130.9	122.1	-8.8
Latvia	LV	91.3	104.5	95.8	94.9	91.9	93.2	96.3	99.0	98.0	91.8	98.5	99.0	0.5
Liechtenstein	LI	106.9	127.3	119.9	119.4	118.9	123.3	116.4	118.0	124.8	113.4	128.2	117.3	-10.9
Lithuania	LT	103.0	110.1	98.1	102.0	95.8	96.9	101.4	101.4	98.8	96.5	100.5	98.1	-2.4
Luxembourg	LU	119.9	130.0	111.7	112.1	108.6	111.4	110.4	99.0	109.5	105.5	114.1	99.6	-14.5
Malta	MT	105.9	115.6	109.1	108.4	107.7	109.4	112.6	116.7	112.0	115.8	107.1	106.5	-0.6
Monaco	MC		142.4	127.3	123.1	127.2	124.0	126.6	118.9	122.5	116.3	122.9	120.2	-2.7
Montenegro	ME	120.8	114.3	122.3	118.1	111.7	108.6	115.1	127.1	113.2	105.6	120.6	106.3	-14.4
Netherlands	NL	93.7	116.1	94.1	98.4	94.7	90.7	98.6	94.1	99.5	97.5	101.4	100.9	-0.5
North Macedonia	MK	117.5	110.3	121.1	121.0	111.3	109.0	117.4	136.3	118.1	102.0	119.6	95.2	-24.5
Norway	NO	98.1	101.7	91.3	99.0	94.0	88.8	93.7	90.9	94.5	88.7	83.8	84.0	0.1
Poland	PL	113.6	120.4	112.9	109.7	107.8	106.6	109.5	112.0	109.4	107.2	117.9	109.2	-8.7
Portugal	PT	119.0	119.4	111.0	102.7	112.4	112.0	108.4	106.0	113.5	101.0	103.4	107.0	3.6
Romania	RO	112.1	105.7	116.9	110.1	108.8	94.0	91.1	103.1	86.5	83.3	89.8	90.4	0.7
San Marino	SM	130.8	120.8	130.4	119.0	118.1	116.1	117.9	121.2	110.7	118.4	129.3	118.0	-11.3
Serbia (incl.	RS	115.6	108.5	122.5	117.3	115.8	102.5	112.0	124.1	110.5	95.6	117.0	96.9	-20.0
Slovakia	SK	121.3	122.2	122.2	116.4	122.7	112.8	118.5	121.2	117.4	110.2	120.3	109.0	-11.4
Slovenia	SI	122.6	132.6	126.6	116.9	119.7	122.1	125.5	125.8	125.5	115.0	126.3	111.9	-14.4
Spain	ES	117.7	116.2	115.4	110.7	113.1	115.4	112.1	112.7	114.9	112.2	114.1	109.7	-4.5
Sweden	SE	97.6	104.5	93.5	97.6	94.2	91.2	96.1	94.0	94.8	95.4	89.7	90.7	0.9
Switzerland	CH	122.6	132.6	120.1	116.8	117.3	124.7	120.8	117.3	124.2	113.8	131.1	117.3	-13.8
United Kingdom	UK	87.2	98.0	83.3	93.1	86.8	81.6	87.8	84.0	89.7	84.1	83.2	84.1	0.9
Total		112.1	118.2	110.7	109.8	108.1	106.8	108.9	108.5	108.9	102.9	110.4	104.8	-5.6
EU-28		111.8	118.3	110.2	109.5	107.8	106.8	108.7	107.7	108.6	103.0	110.0	105.0	-5.1

\*) under the UN Security Council Resolution 1244/99

Table A4.7 Evolution in 2005–2016 and difference between 2015 and 2016 for population-weighted concentration, ozone indicator SOM035.

Country		Population-weighted conc. [ $\mu\text{g}\cdot\text{m}^{-3}\cdot\text{d}$ ]												Differ. '16 - '15
		2005	2006	2007	2008	2009	2010	2011	2012	2013	2014	2015	2016	
Albania	AL	7 911	7 193	7 817	7 668	6 754	5 617	7 769	8 760	7 179	4 376	7 215	5 475	-1 740
Andorra	AD	7 520	6 587	7 121	6 319	7 186	7 282	7 891	8 058	7 303	6 692	6 050	4 423	-1 627
Austria	AT	5 946	6 237	5 874	5 099	5 050	4 969	5 452	5 419	5 389	4 423	6 169	4 522	-1 647
Belgium	BE	2 775	4 017	2 235	2 520	2 599	2 401	2 714	2 050	2 520	2 297	2 792	2 203	-589
Bosnia-Herzegovina	BA	6 714	6 571	6 938	5 972	5 536	4 879	5 702	7 322	5 670	3 852	6 053	4 409	-1 644
Bulgaria	BG	5 311	4 896	6 064	5 797	5 686	4 377	5 215	5 960	4 082	2 519	4 182	3 347	-835
Croatia	HR	6 324	6 928	6 756	5 899	5 491	5 419	6 470	7 143	5 989	4 503	6 239	4 996	-1 243
Cyprus	CY	7 155	5 759	7 739	8 027	8 788	7 374	8 773	8 369	7 909	5 426	6 390	5 612	-778
Czechia	CZ	5 845	6 097	5 123	4 576	4 487	4 160	4 743	4 806	4 266	3 822	5 556	4 353	-1 203
Denmark	DK	2 519	3 578	2 440	3 080	2 440	2 245	2 752	2 662	2 749	2 611	2 200	2 293	93
Estonia	EE	2 437	3 594	2 061	2 363	1 762	2 646	2 516	2 310	2 545	1 991	1 775	1 949	174
Finland	FI	2 275	3 141	1 332	1 938	1 623	1 925	2 052	1 650	2 011	1 615	1 358	1 510	153
France	FR	4 591	4 972	3 686	3 563	4 025	4 139	4 439	3 635	4 098	3 786	4 245	3 420	-826
Germany	DE	3 940	4 860	3 648	3 822	3 507	3 652	3 668	3 357	3 506	3 287	4 300	3 368	-933
Greece	GR	8 321	6 657	8 330	8 969	8 330	7 483	9 182	9 378	8 532	5 926	6 908	6 871	-36
Hungary	HU	5 751	5 738	6 547	5 751	6 631	4 408	5 828	6 342	4 604	3 620	5 553	3 952	-1 601
Iceland	IS	1 329	2 265	1 168	2 224	833	775	1 094	1 242	1 473	218	258	499	241
Ireland	IE	1 701	2 453	1 412	2 096	1 487	1 419	1 353	1 479	2 043	868	856	1 323	467
Italy	IT	7 634	8 205	7 506	6 386	6 986	6 302	7 532	7 328	6 576	5 569	6 856	6 058	-799
Latvia	LV	2 391	3 734	2 262	2 347	1 837	2 304	2 708	3 103	2 614	2 213	2 562	2 773	211
Liechtenstein	LI	5 233	6 258	4 826	4 930	5 271	5 244	5 128	5 132	5 221	4 360	5 802	4 945	-857
Lithuania	LT	3 671	4 535	2 744	3 059	2 291	2 608	3 131	3 358	2 703	2 457	2 804	2 456	-348
Luxembourg	LU	4 769	5 090	3 424	3 557	3 500	3 505	3 527	2 561	3 167	2 872	3 461	2 211	-1 250
Malta	MT	6 971	7 797	7 209	6 582	6 634	6 722	7 127	8 022	7 403	6 946	5 791	5 985	194
Monaco	MC		8 903	8 381	7 246	8 325	8 028	8 354	6 979	7 795	7 112	8 015	7 186	-829
Montenegro	ME	7 608	6 554	7 379	7 120	6 237	5 653	6 970	8 584	6 674	4 012	6 793	5 269	-1 524
Netherlands	NL	1 901	3 245	1 816	2 104	1 922	1 916	2 283	1 949	2 410	2 244	2 678	2 428	-250
North Macedonia	MK	7 069	6 297	6 690	7 133	6 229	5 081	7 110	8 472	6 326	3 215	6 197	4 434	-1 763
Norway	NO	2 580	3 496	1 705	2 514	2 000	1 803	2 395	2 128	2 443	2 113	1 764	1 502	-262
Poland	PL	4 784	5 416	4 179	3 951	3 747	3 278	4 065	4 045	3 792	3 425	4 528	3 699	-828
Portugal	PT	5 510	5 257	4 863	3 851	5 003	5 133	4 552	4 240	5 091	3 519	3 989	4 074	85
Romania	RO	5 238	4 798	5 882	5 039	5 044	3 033	3 276	3 967	2 221	1 842	2 952	2 485	-468
San Marino	SM	7 540	6 321	7 296	5 863	5 860	5 331	6 220	6 048	5 067	5 949	7 176	5 667	-1 509
Serbia (incl.	RS	5 947	5 239	6 768	6 378	6 118	4 001	5 793	6 844	4 738	2 762	5 449	3 755	-1 694
Slovakia	SK	6 141	6 261	6 098	5 455	6 348	4 748	6 051	6 103	5 116	4 344	5 456	4 232	-1 223
Slovenia	SI	6 242	7 480	6 671	5 761	5 775	5 998	7 062	7 092	6 540	5 086	6 649	5 007	-1 642
Spain	ES	6 139	5 813	5 992	5 110	5 983	6 088	5 858	5 850	5 895	5 436	5 820	5 212	-608
Sweden	SE	2 682	3 635	1 795	2 387	2 100	2 025	2 628	2 233	2 317	2 318	2 084	1 819	-265
Switzerland	CH	5 740	6 321	5 114	4 619	5 139	5 127	5 435	4 990	4 919	4 417	6 174	4 842	-1 332
United Kingdom	UK	1 551	2 676	1 174	2 044	1 433	1 072	1 471	1 183	1 606	1 337	1 287	1 168	-119
Total		4 706	5 167	4 411	4 275	4 275	3 917	4 414	4 279	4 089	3 500	4 312	3 619	-693
EU28		4 613	5 128	4 319	4 178	4 208	3 888	4 339	4 154	4 040	3 506	4 249	3 598	-651

\*) under the UN Security Council Resolution 1244/99

## Vegetation exposure

Table A4.8 provides the evolution of the annual vegetation exposure for AOT40 for vegetation in the period 2005–2016 and the inter-annual difference between 2015 and 2016. In 2016 the overall agricultural-weighted concentration for whole Europe (without Turkey) was 10 942  $\mu\text{g}\cdot\text{m}^{-3}\cdot\text{h}$ , which is the lowest value of the whole twelve years period.

*Table A4.8 Evolution in 2005–2016 and difference between 2016 and 2015 for agricultural-weighted concentration, ozone indicator AOT40 for vegetation.*

Country		Agricultural-weighted conc. [ $\mu\text{g}\cdot\text{m}^{-3}\cdot\text{h}$ ]												Differ. '16 - '15
		2005	2006	2007	2008	2009	2010	2011	2012	2013	2014	2015	2016	
Albania	AL	28 831	39 959	40 051	20 388	41 766	16 335	22 561	28 949	36 337	18 063	25 781	19 923	-5 858
Austria	AT	21 123	27 496	21 558	18 494	14 296	18 477	17 201	18 631	16 949	17 251	21 542	15 086	-6 456
Belgium	BE	12 764	24 201	6 538	11 609	7 404	12 324	8 158	8 005	9 110	9 144	10 122	6 728	-3 394
Bosnia-Herzegovina	BA	21 866	19 086	28 503	19 769	24 333	17 931	17 968	22 534	17 068	15 738	17 842	11 732	-6 110
Bulgaria	BG	21 523	18 607	22 707	15 221	20 752	11 471	14 728	17 335	11 731	12 552	13 450	11 006	-2 444
Croatia	HR	20 016	24 168	26 847	19 415	20 809	18 987	19 391	23 193	17 520	15 445	19 052	13 737	-5 315
Cyprus	CY	31 742	22 820	28 080	12 000	29 579	21 092	22 690	23 482	26 761	21 667	26 572	21 704	-4 867
Czechia	CZ	19 006	27 909	19 825	19 571	11 341	16 047	15 508	16 979	13 173	15 857	18 462	14 158	-4 304
Denmark	DK	7 411	16 411	6 887	13 615	6 393	7 579	7 146	7 355	6 043	8 357	3 169	6 252	3 083
Estonia	EE	5 198	12 873	4 631	7 117	3 317	4 312	6 068	5 275	5 226	3 959	1 771	5 236	3 465
Finland	FI	4 267	11 373	3 447	6 399	2 993	4 138	5 151	3 275	4 039	3 486	680	4 585	3 906
France	FR	16 973	22 759	7 614	12 202	9 448	13 855	12 510	9 112	11 712	10 630	12 715	7 386	-5 329
Germany	DE	14 946	25 938	12 510	18 715	8 888	15 831	12 898	11 182	10 878	13 745	13 817	10 650	-3 167
Greece	GR	27 613	25 433	29 271	19 689	27 723	17 700	19 869	26 543	23 529	19 991	24 499	22 763	-1 735
Hungary	HU	19 070	22 325	25 664	19 652	20 434	14 493	16 245	20 710	15 192	14 890	14 962	11 927	-3 036
Iceland	IS	367	4 748	177	5 310	3 332	237	125	160	30	9	1	32	31
Ireland	IE	2 619	5 454	1 978	5 212	2 222	1 843	1 109	2 211	2 015	718	927	2 331	1 404
Italy	IT	31 334	35 407	25 987	22 407	27 302	22 171	22 928	27 365	24 241	22 028	30 626	21 620	-9 007
Latvia	LV	6 304	13 023	5 434	6 446	3 924	4 691	6 765	7 259	5 310	4 958	2 498	6 047	3 549
Liechtenstein	LI	16 781	27 422	12 479	17 409	12 394	17 226	17 126	15 241	14 632	13 324	20 189	15 168	-5 021
Lithuania	LT	7 297	12 390	6 800	7 582	4 950	5 626	7 680	8 681	5 205	6 340	3 594	7 019	3 425
Luxembourg	LU	18 878	28 422	9 749	15 471	11 244	17 259	12 858	9 079	12 423	13 993	13 414	7 679	-5 735
Malta	MT	24 698	24 162	20 604	24 373	24 935	18 815	26 442	27 327	30 088	28 986	28 982	21 344	-7 638
Monaco	MC		35 762	20 979	17 071	26 212	32 986	27 282	21 969	26 572	21 361	23 960	24 531	570
Montenegro	ME	27 800	30 608	35 559	21 588	33 770	16 514	19 684	24 728	27 676	17 933	22 231	15 161	-7 070
Netherlands	NL	7 966	18 087	5 201	8 781	3 826	8 350	6 764	6 363	6 108	8 572	7 512	6 472	-1 040
North Macedonia	MK	26 298	38 217	37 041	20 139	41 337	14 858	18 713	27 086	34 364	17 385	21 857	18 701	-3 156
Norway	NO	4 084	12 296	3 553	7 841	2 586	2 913	4 186	3 596	2 595	4 103	824	3 645	2 820
Poland	PL	13 558	24 487	14 751	15 869	9 341	10 298	13 374	13 283	10 269	11 921	11 400	12 180	780
Portugal	PT	22 127	20 634	8 585	13 191	11 083	16 715	13 007	10 919	15 847	9 400	13 921	10 141	-3 780
Romania	RO	17 654	14 435	23 657	15 372	15 373	9 472	12 085	15 782	7 595	10 419	11 224	6 847	-4 377
San Marino	SM	32 857	39 916	29 665	21 844	26 414	23 088	24 630	29 244	21 972	25 774	32 517	18 841	####
Serbia (incl.	RS	22 588	22 768	30 064	18 958	28 406	14 677	17 081	22 737	17 931	13 591	17 687	12 542	-5 145
Slovakia	SK	19 408	24 674	23 750	19 471	18 344	14 609	15 615	19 746	15 970	15 576	14 374	13 276	-1 099
Slovenia	SI	20 368	32 119	26 452	19 608	20 176	23 787	22 145	25 103	22 809	18 445	24 054	16 251	-7 803
Spain	ES	27 207	25 913	14 800	18 045	16 172	19 040	17 204	19 213	20 399	17 882	23 126	15 845	-7 281
Sweden	SE	6 356	15 201	5 951	9 398	3 992	6 197	7 021	5 515	5 626	5 640	2 213	5 761	3 548
Switzerland	CH	23 807	33 834	15 170	19 476	15 354	22 349	17 432	15 522	18 032	16 109	23 953	14 255	-9 698
United Kingdom	UK	4 437	12 629	1 929	7 808	4 535	3 869	3 066	3 570	3 304	3 385	2 485	3 435	950
Total		17 481	22 344	14 597	15 214	13 157	13 310	13 255	14 041	12 838	12 427	14 223	10 942	-3 281
EU28		17 313	22 245	13 981	15 081	12 512	13 259	13 116	13 719	12 536	12 378	14 084	10 872	-3 213

\*) under the UN Security Council Resolution 1244/99



The highest increase of agricultural-weighted concentration per country in 2016 compared to 2015 is seen in Finland, Latvia and Sweden. The steepest decrease was detected in San Marino, Switzerland, and Italy.

Table A4.9 provides the similar data as presented in Table A4.8, but for the forest-weighted concentrations of the AOT40 for forests. Considering Europe as a whole (without Turkey), Table A4.9 shows that the overall forest-weighted ozone concentration for AOT40 for forests in 2016 was 17 573  $\mu\text{g}\cdot\text{m}^{-3}\cdot\text{h}$ . This is the second lowest value of the whole twelve years period, while the lowest values is detected for 2014.

*Table A4.9 Evolution in 2005–2016 and difference between 2016 and 2015 for forest-weighted concentration, ozone indicator AOT40 for forests.*

Country		Forest-weighted conc. [ $\mu\text{g}\cdot\text{m}^{-3}\cdot\text{h}$ ]												Differ. '16 - '15
		2005	2006	2007	2008	2009	2010	2011	2012	2013	2014	2015	2016	
Albania	AL	60 607	61 982	65 662	43 220	87 193	33 340	49 630	55 361	85 847	29 463	47 249	38 763	-8 486
Austria	AT	35 595	41 055	38 212	30 098	31 444	31 533	32 660	33 264	34 596	25 863	42 247	28 224	-14 023
Belgium	BE	21 612	31 473	16 478	16 062	17 678	18 564	19 011	14 020	17 632	13 912	20 597	15 301	-5 296
Bosnia-Herzegovina	BA	42 195	36 956	50 356	36 609	51 704	32 849	37 877	45 680	40 787	24 565	36 818	25 520	-11 299
Bulgaria	BG	43 105	40 043	48 421	32 861	47 861	29 283	34 407	39 810	32 232	23 880	32 992	29 709	-3 283
Croatia	HR	35 742	42 453	46 583	34 999	41 730	32 875	39 051	44 435	39 110	23 758	38 425	26 764	-11 661
Cyprus	CY	63 155	43 595	59 808	31 069	65 009	44 352	51 896	55 212	59 206	39 387	49 998	43 831	-6 168
Czechia	CZ	32 597	39 537	33 821	29 839	26 662	25 399	27 988	29 594	26 850	23 293	38 374	26 610	-11 765
Denmark	DK	13 463	22 648	12 207	17 567	13 125	10 888	12 510	12 148	12 862	13 942	7 837	9 799	1 962
Estonia	EE	10 502	20 025	6 905	11 790	7 610	7 424	9 721	9 417	10 663	9 166	3 680	7 076	3 397
Finland	FI	8 173	16 269	3 669	8 501	5 802	4 119	5 828	4 315	6 541	5 869	1 037	4 888	3 851
France	FR	33 155	36 827	24 669	22 423	25 406	28 948	28 480	23 250	24 851	19 582	28 443	21 858	-6 586
Germany	DE	27 043	34 988	24 881	26 204	22 792	23 842	24 645	21 298	21 595	20 573	30 044	22 086	-7 958
Greece	GR	53 769	47 853	52 992	40 147	56 584	35 623	43 629	46 622	48 333	32 627	43 974	43 901	-73
Hungary	HU	30 852	36 583	43 380	33 923	41 478	26 384	31 155	39 635	33 702	23 031	32 198	24 543	-7 655
Iceland	IS	1 250	7 384	585	9 832	5 932	839	1 426	1 162	1 001	415	2	4	2
Ireland	IE	5 064	9 940	4 002	8 279	4 304	5 084	4 367	4 820	5 226	2 367	3 227	3 561	334
Italy	IT	53 285	57 440	51 128	40 702	45 537	41 607	47 253	47 981	43 513	34 575	52 978	39 860	-13 118
Latvia	LV	12 820	19 956	7 491	11 195	8 888	9 267	11 226	14 436	10 190	10 859	5 520	8 410	2 890
Liechtenstein	LI	31 218	43 271	34 987	31 307	30 688	32 476	34 267	32 540	32 446	24 101	42 159	31 769	-10 391
Lithuania	LT	16 029	20 167	10 807	13 171	11 161	11 995	13 367	16 938	8 727	13 128	9 138	10 661	1 524
Luxembourg	LU	25 981	33 147	20 525	18 920	23 187	22 183	22 834	15 562	20 543	17 723	23 110	15 960	-7 150
Malta	MT	66 996	46 492	47 217	42 969	53 717	42 815	54 429	51 481	51 800	47 687	50 585	42 542	-8 043
Monaco	MC		47 644	36 743	29 096	42 620	47 582	44 467	33 083	41 118	28 905	34 712	38 471	3 759
Montenegro	ME	56 716	51 440	55 227	43 867	72 376	33 764	42 272	51 198	64 979	28 071	44 266	31 868	-12 398
Netherlands	NL	11 607	22 894	9 580	10 649	9 261	10 928	13 333	10 975	12 036	10 942	13 966	12 647	-1 319
North Macedonia	MK	58 866	63 450	70 095	42 569	86 656	33 254	43 696	52 315	85 248	29 275	44 629	39 663	-4 966
Norway	NO	8 666	19 301	7 897	11 541	7 391	5 731	7 758	6 145	8 027	8 719	3 880	5 235	1 356
Poland	PL	25 243	34 212	24 306	24 709	22 048	18 833	23 343	23 275	20 748	18 931	24 684	20 242	-4 442
Portugal	PT	40 217	37 193	24 072	23 473	27 949	34 640	26 004	21 550	30 994	15 245	24 378	21 598	-2 780
Romania	RO	33 840	30 684	43 702	30 270	36 887	23 858	26 452	28 586	14 966	19 749	26 336	17 098	-9 238
San Marino	SM	49 031	54 866	49 275	37 902	43 800	37 732	51 272	46 136	37 606	34 782	50 773	31 897	-18 876
Serbia (incl.	RS	46 891	43 047	52 348	35 582	64 808	28 951	36 589	46 627	50 338	22 935	39 388	29 436	-9 952
Slovakia	SK	33 953	40 634	41 135	34 174	38 330	26 906	32 984	36 307	34 092	23 784	31 278	24 212	-7 066
Slovenia	SI	33 853	47 136	46 330	34 709	40 996	38 197	44 032	48 996	47 292	27 386	43 600	30 110	-13 490
Spain	ES	45 027	43 398	32 909	31 045	33 479	34 380	33 390	34 679	34 785	27 458	34 409	28 396	-6 013
Sweden	SE	9 918	18 646	6 799	10 833	7 608	5 860	8 124	5 762	9 270	8 592	2 833	6 300	3 468
Switzerland	CH	42 076	48 933	40 157	30 734	34 665	36 640	34 872	31 854	35 076	26 016	40 890	29 953	-10 937
United Kingdom	UK	6 533	14 595	3 961	11 214	6 985	5 513	6 538	5 958	6 244	4 489	3 804	4 784	980
Total		25 900	31 154	23 744	21 951	23 532	19 625	21 892	21 580	21 753	17 124	21 150	17 573	-3 577
EU28		25 849	31 110	23 130	21 806	22 407	19 902	21 915	21 252	20 855	17 255	21 272	17 714	-3 558

\*) under the UN Security Council Resolution 1244/99

The highest increase of forest-weighted concentration per country compared to 2015 can be seen in Finland, Sweden, and Estonia. The steepest decrease was detected in San Marino, Austria, Slovenia, and Italy.

The evolution of the agricultural land (*crops*) exposed to accumulated ozone concentrations (AOT40 for vegetation) exceeding the target value (TV) threshold and the long-term objective (LTO) for Europe as a whole in the twelve years period 2005 – 2016 is presented in Table 6.5. The same table also shows the evolution of the *forest* land exposed to accumulated ozone concentrations (AOT40 for forests) exceeding the level of 20 000  $\mu\text{g}\cdot\text{m}^{-3}\cdot\text{h}$  (earlier used Reporting Value, RV) and Critical Level (CL) for Europe as a whole. The results are discussed in Chapter 6.

## Uncertainties

Table A4.10 shows the evolution of the absolute and relative mean interpolation uncertainties and also  $R^2$  from cross-validation scatterplots for the maps of all four ozone indicators, in the period 2005 – 2016.

*Table A4.10 Absolute and relative mean uncertainty and  $R^2$  from cross-validation scatterplot for the total European areas, ozone indicators 93.2 percentile of maximum daily 8-hour means, SOM035, AOT40 for vegetation and AOT40 for forests, years 2005 – 2016*

Ozone			2005	2006	2007	2008	2009	2010	2011	2012	2013	2014	2015	2016
<b>26<sup>th</sup> highest daily max. 8-hr mean (2005 - 2011) / 93.2 percentile of daily max. 8-hr means (2012 - 2016)</b>														
rural areas	abs. mean uncertainty	RMSE [ $\mu\text{g}\cdot\text{m}^{-3}$ ]	12.3	11.2	8.8	8.7	8.2	8.9	8.4	8.5	8.5	7.4	9.0	9.4
	rel. mean uncertainty	RRMSE [%]	10.3	8.9	7.5	7.6	7.2	7.7	7.2	7.4	7.3	6.7	7.5	8.4
	coeff. of determination	$R^2$	0.51	0.49	0.71	0.56	0.69	0.68	0.67	0.71	0.72	0.65	0.73	0.57
urban areas	abs. mean uncertainty	RMSE [ $\mu\text{g}\cdot\text{m}^{-3}$ ]	10.0	10.2	8.9	8.8	9.3	9.2	9.1	9.1	9.1	7.9	8.6	9.0
	rel. mean uncertainty	RRMSE [%]	8.9	8.4	7.9	7.9	8.4	8.2	8.1	8.3	8.1	7.4	7.4	8.3
	coeff. of determination	$R^2$	0.50	0.53	0.66	0.61	0.64	0.71	0.66	0.68	0.70	0.64	0.82	0.69
<b>SOM035</b>														
rural areas	abs. mean uncertainty	RMSE [ $\mu\text{g}\cdot\text{m}^{-3}\cdot\text{d}$ ]	2 173	2 077	1 801	1 609	1 635	1 608	1 747	1 633	1 596	1 414	1 578	1 681
	rel. mean uncertainty	RRMSE [%]	35.5	31.6	33.3	30.7	29.7	29.6	29.6	29.2	29.2	29.2	27.1	33.3
	coeff. of determination	$R^2$	0.55	0.47	0.63	0.63	0.63	0.62	0.63	0.68	0.61	0.61	0.68	0.57
urban areas	abs. mean uncertainty	RMSE [ $\mu\text{g}\cdot\text{m}^{-3}\cdot\text{d}$ ]	1 459	1 472	1 260	1 293	1 475	1 278	1 374	1 362	1 194	1 133	1 221	1 182
	rel. mean uncertainty	RRMSE [%]	32.0	29.2	29.5	31.3	33.1	29.6	29.7	31.7	28.1	29.3	25.6	32.5
	coeff. of determination	$R^2$	0.58	0.49	0.67	0.54	0.62	0.65	0.66	0.67	0.66	0.62	0.72	0.70
<b>AOT40 for vegetation</b>														
rural areas	abs. mean uncertainty	RMSE [ $\mu\text{g}\cdot\text{m}^{-3}\cdot\text{h}$ ]	7 677	7 674	5 876	5 283	5 138	5 198	5 263	5 062	5 179	4 518	5 256	4 996
	rel. mean uncertainty	RRMSE [%]	40.7	29.6	39.6	31.3	37.7	30.8	34.9	32.9	34.6	30.5	28.7	36.9
	coeff. of determination	$R^2$	0.58	0.53	0.63	0.53	0.69	0.67	0.62	0.70	0.68	0.67	0.78	0.61
<b>AOT40 for forests</b>														
rural areas	abs. mean uncertainty	RMSE [ $\mu\text{g}\cdot\text{m}^{-3}\cdot\text{h}$ ]	12 474	11 990	10 190	8 750	9 304	8 384	9 341	8 847	9 257	7 354	9 141	8 982
	rel. mean uncertainty	RRMSE [%]	41.5	33.6	37.1	34.0	33.9	31.4	32.7	32.8	34.7	33.8	29.1	36.9
	coeff. of determination	$R^2$	0.55	0.49	0.67	0.56	0.68	0.69	0.67	0.70	0.68	0.62	0.75	0.61



The absolute mean interpolation uncertainty results of 2016 fit within the fluctuation of the previous years. The relative uncertainties for 2016 show poorer results compared to several previous years,  $R^2$  from cross-validation scatterplots of 2016 show poorer results compared to 2015. These results are highly influenced by the inclusion of Turkey in the mapping.

#### A4.4 NO<sub>2</sub> and NO<sub>x</sub>

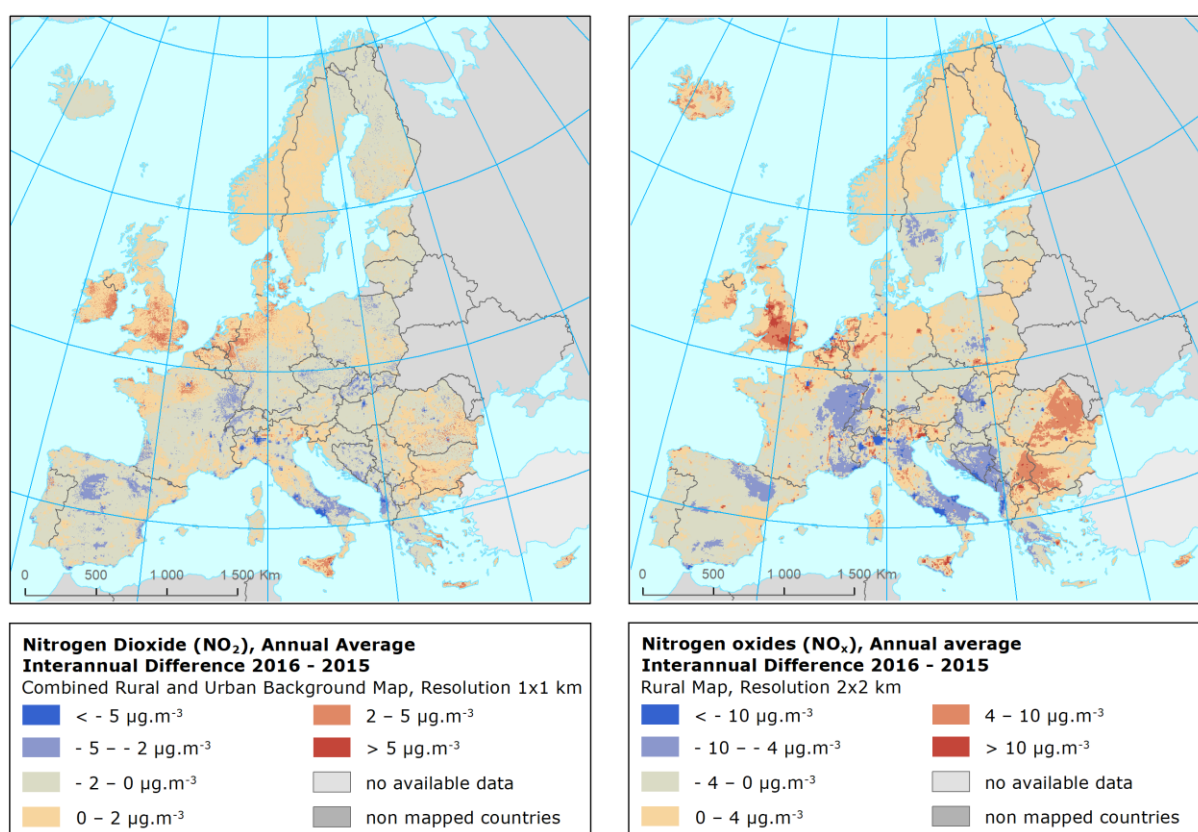
##### Air concentrations

Map A4.4 presents the inter-annual difference between 2016 and 2015 for NO<sub>2</sub> and NO<sub>x</sub> annual averages. Red areas show an increase of concentration in 2016, while blue areas show a decrease.

The highest increases for NO<sub>2</sub> are seen in southern England, in Benelux, Ireland and in the broader metropolitan area surrounding Paris. The steepest decreases are shown in some parts of Italy and west Balkan.

In the case of NO<sub>x</sub>, highest increases are observed in England, in Benelux, Romania and Bulgaria, and near large cities. The steepest decreases are seen in some parts of Italy and in west Balkan.

Map A4.4 Difference concentrations between 2014 and 2015 for NO<sub>2</sub> annual average (left) and NO<sub>x</sub> annual average (right)



## Population exposure

Table A4.11 provides the evolution of the annual population exposure for NO<sub>2</sub> annual average in the period 2013–2016 and the inter-annual difference between 2015 and 2016. In 2016 the overall population-weighted concentration for NO<sub>2</sub> annual average for whole of Europe (without Turkey) was 18.6 µg·m<sup>-3</sup>, i.e. same like in 2014 and slightly less than in 2013 and 2015.

*Table A4.11 Evolution in 2013–2016 and difference between 2015 and 2016 for population-weighted concentration, NO<sub>2</sub> annual average.*

Country		Population-weighted conc. [µg·m <sup>-3</sup> ]						Country		Population-weighted conc. [µg·m <sup>-3</sup> ]				
		2013	2014	2015	2016	diff. '16 - '15				2013	2015	2015	2016	diff. '16 - '15
Albania	AL	17.5	14.8	18.1	13.7	-4.4		Lithuania	LT	12.4	12.5	12.2	11.7	-0.5
Andorra	AD	14.0	15.0	20.5	18.2	-2.4		Luxembourg	LU	23.0	19.9	19.9	20.7	0.7
Austria	AT	20.2	19.2	19.8	18.9	-0.9		Malta	MT	15.2	16.0	16.5	14.9	-1.6
Belgium	BE	24.0	21.9	20.9	21.7	0.8		Monaco	MC	30	24	29.7	26.8	-2.8
Bosnia-Herzegovina	BA	14.4	15.1	16.2	13.2	-2.9		Montenegro	ME	16.4	13.9	16.4	11.9	-4.5
Bulgaria	BG	17.0	16.5	16.1	18.8	2.7		Netherlands	NL	22.0	21.9	20.5	20.5	-0.1
Croatia	HR	15.8	15.7	17.3	15.2	-2.0		North Macedonia	MK	20.3	16.0	18.1	17.4	-0.8
Cyprus	CY	10.5	12.8	14.1	24.0	10.0		Norway	NO	14.4	12.4	12.3	12.4	0.1
Czechia	CZ	17.2	16.8	16.6	15.2	-1.4		Poland	PL	16.0	15.1	15.6	15.2	-0.4
Denmark	DK	12.6	11.0	10.5	10.4	-0.1		Portugal	PT	15.7	13.7	15.7	15.3	-0.4
Estonia	EE	10.0	9.0	8.2	7.8	-0.3		Romania	RO	18.6	16.5	14.9	17.6	2.7
Finland	FI	9.3	8.3	8.8	8.0	-0.8		San Marino	SM	12.0	14.7	16.2	16.3	0.1
France	FR	19.0	17.7	17.9	17.3	-0.6		Serbia (incl. Kosovo*)	RS	18.8	18.5	17.9	18.4	0.5
Germany	DE	20.7	20.2	20.0	20.2	0.2		Slovakia	SK	16.4	15.2	16.9	13.5	-3.4
Greece	GR	16.0	14.9	18.1	19.6	1.6		Slovenia	SI	16.8	14.9	16.7	15.4	-1.3
Hungary	HU	17.0	17.1	18.0	16.6	-1.3		Spain	ES	19.1	19.9	21.2	20.0	-1.1
Iceland	IS	13.4	10.9	11.9	10.1	-1.9		Sweden	SE	10.9	9.9	10.8	10.7	-0.1
Ireland	IE	11.8	6.1	7.6	11.0	3.5		Switzerland	CH	21.6	20.9	21.4	19.7	-1.7
Italy	IT	23.8	22.5	24.9	22.1	-2.8		United Kingdom	UK	22.5	22.2	19.7	21.8	2.1
Latvia	LV	13.8	12.3	12.1	12.0	-0.2								
Liechtenstein	LI	20.6	18.5	20.5	17.8	-2.7								
								<b>Total</b>		<b>19.4</b>	<b>18.6</b>	<b>18.8</b>	<b>18.6</b>	<b>-0.2</b>
								<b>EU-28</b>		<b>19.5</b>	<b>18.7</b>	<b>18.9</b>	<b>18.7</b>	<b>-0.1</b>

\*) under the UN Security Council Resolution 1244/99

## Uncertainties

Table A4.12 presents the uncertainty results for NO<sub>2</sub> maps for the years 2013 – 2016 and for and NO<sub>x</sub> maps for 2014 – 2016. For NO<sub>2</sub>, all indicators show for 2016 better results in rural areas, worse results in urban background areas and similar results in urban traffic areas compared to previous years. Poorer results in the urban background areas compared to previous years are caused by inclusion of a large number of Turkish stations in 2016.

For NO<sub>x</sub>, all indicators show for 2016 somewhat poorer results compared to 2014 and 2015. The main reason again is the inclusion of Turkish stations.

Table A4.12 Absolute and relative mean uncertainty and  $R^2$  from cross-validation scatterplot for the total European rural and urban areas,  $\text{NO}_2$  and  $\text{NO}_x$  annual average, years 2010 and 2013 – 2016

NO <sub>2</sub> / NO <sub>x</sub>			2010	2013	2014	2015	2016
NO <sub>2</sub> Annual average							
rural areas	abs. mean uncertainty	RMSE [ $\mu\text{g.m}^{-3}$ ]	3.1	2.8	3.3	2.9	2.5
	rel. mean uncertainty	RRMSE [%]	26.8	29.2	36.6	31.9	27.8
	coeff. of determination	$R^2$	0.75	0.78	0.68	0.74	0.81
urban background areas	abs. mean uncertainty	RMSE [ $\mu\text{g.m}^{-3}$ ]	5.2	4.6	4.8	4.6	6.7
	rel. mean uncertainty	RRMSE [%]	21.4	21.3	23.6	22.2	32.2
	coeff. of determination	$R^2$	0.61	0.65	0.61	0.67	0.53
urban traffic areas	abs. mean uncertainty	RMSE [ $\mu\text{g.m}^{-3}$ ]	10.6	9.2	8.9	9.2	8.9
	rel. mean uncertainty	RRMSE [%]	26.4	24.3	25.5	25.3	25.7
	coeff. of determination	$R^2$	0.47	0.51	0.53	0.54	0.56
NO <sub>x</sub> Annual average							
rural areas	abs. mean uncertainty	RMSE [ $\mu\text{g.m}^{-3}$ ]	not mapped		5.7	4.9	6.0
	rel. mean uncertainty	RRMSE [%]			47.0	42.5	50.4
	coeff. of determination	$R^2$			0.52	0.65	0.58

## Annex 5 – Concentration maps including station points

Throughout the report, the concentration maps presented do not include station points, contrary to the previous reports up to Horálek et al. (2016b). The reason is to better visualise the health related indicators with their distinct concentration levels at the more fragmented and smaller urban areas in predominant rural areas. The allocation of these smaller ‘patches’ is better discriminated now that the map is presented in a 1x1 km grid resolution, as the smoothing effect of the formerly used 10x10 km grid resolution does not play a role any longer.

As presented in Annex 3, the kriging interpolation methodology somewhat smooths the concentration field. Therefore, it is valuable to present in this Annex 5 the indicator maps *including* the concentration values resulting from the measurement data at the station points. These points provide important additional visual information on the smoothing effect caused by the interpolation. For instance, maps A5.1 and A5.2 present PM<sub>10</sub> indicators annual average and 90.4 percentile of daily means and include the stations points used in the interpolation. They correspond to Maps 2.1 and 2.2 of the main report, which do not have station points. Table A5.1 provides an overview on the maps of the main report and the corresponding maps including stations point values as presented in this annex.

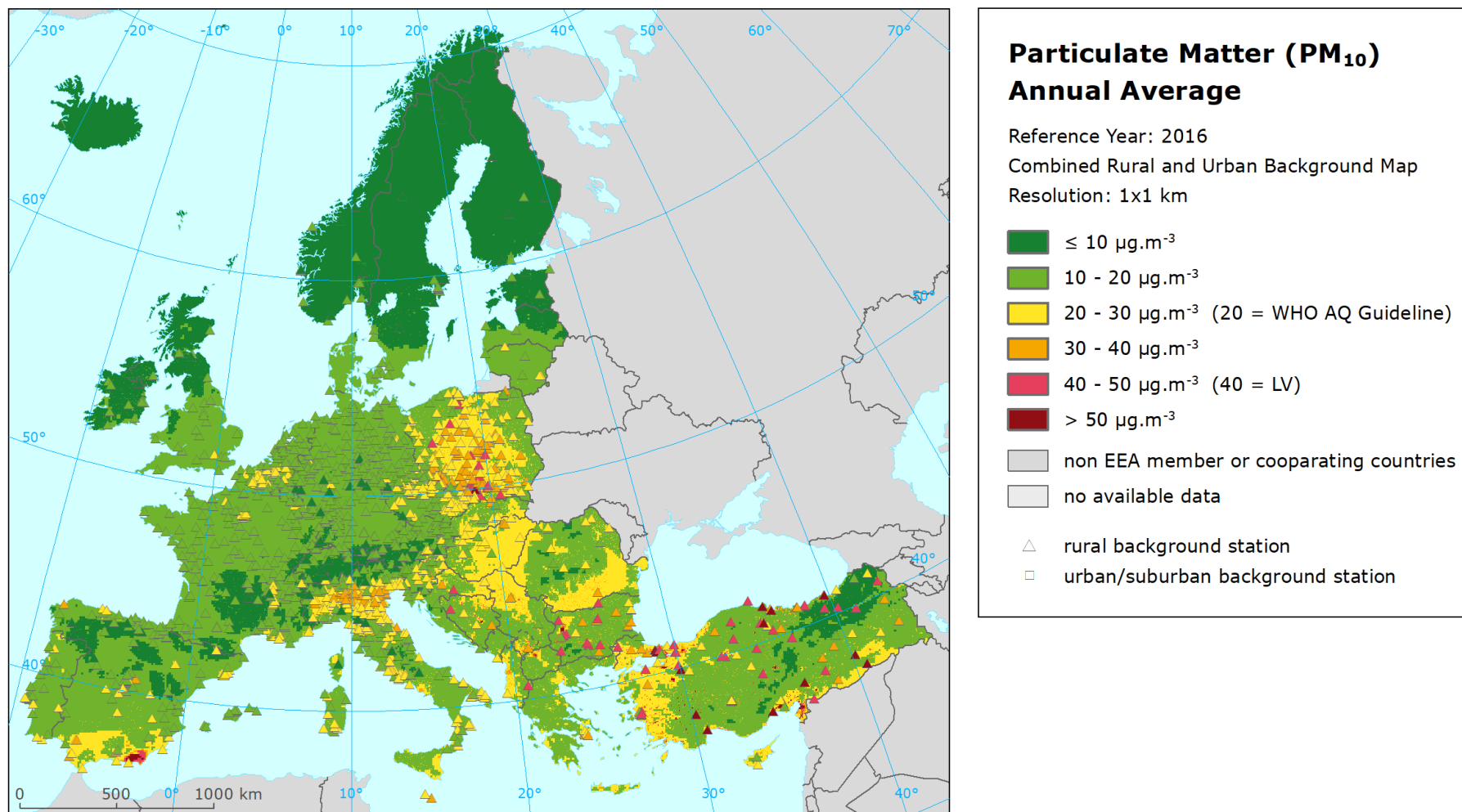
Both the rural and the urban/suburban background stations are included in the maps of the health related indicators, while the rural stations only are shown in the maps of vegetation related indicators. For PM<sub>2.5</sub> and NO<sub>x</sub>, only the stations with relevant measured data (i.e. not the pseudo stations) are presented.

*Table A5.1 Overview of maps presented in this Annex 5 and their relation with the maps presented in the main report*

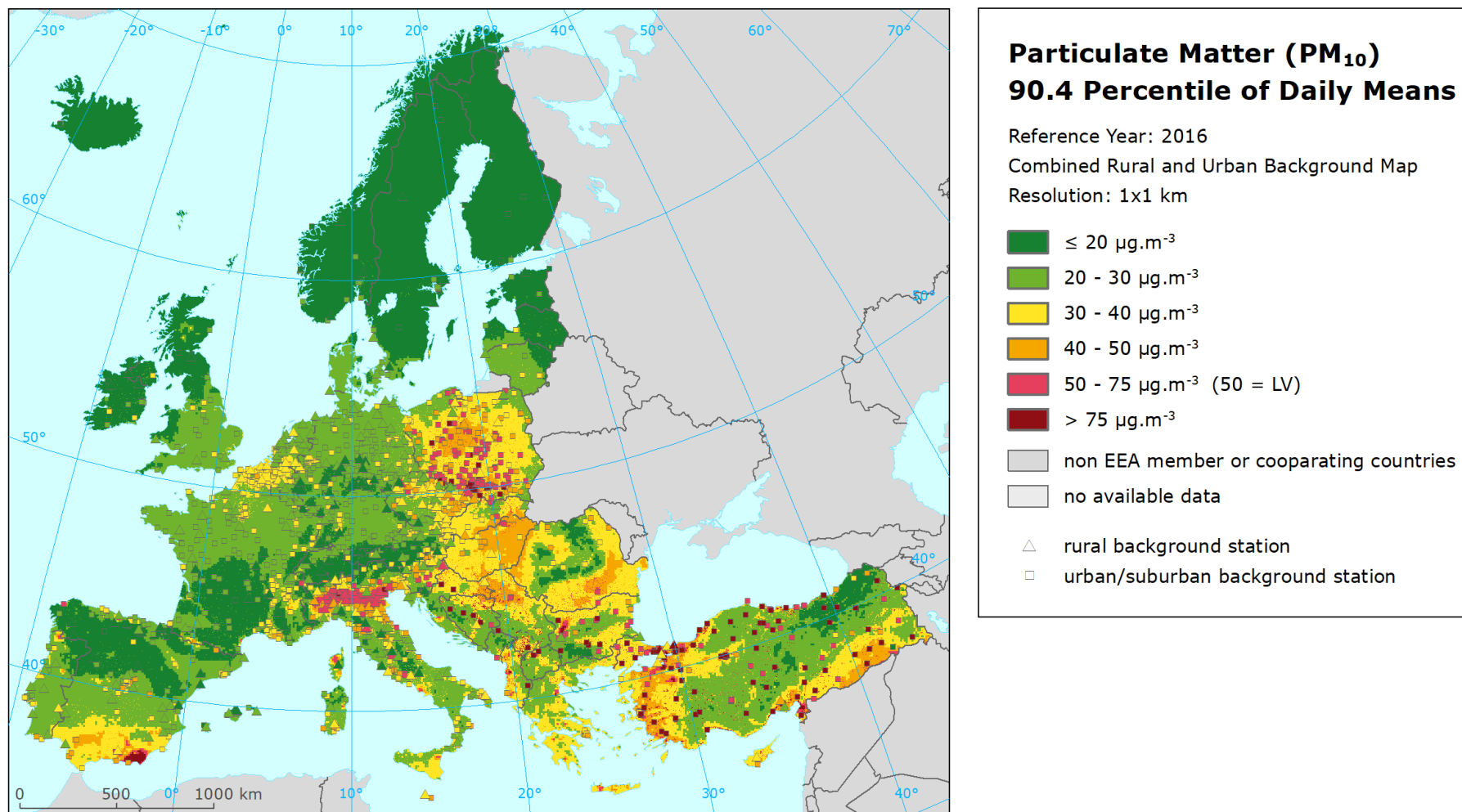
Air pollutant	Indicator	Map including station points	Map without station points
PM <sub>10</sub>	Annual average	A5.1	2.1
	90.4 percentile of daily means	A5.2	2.2
PM <sub>2.5</sub>	Annual average	A5.3	3.1
Ozone	93.2 percentile of maximum daily 8-hour means	A5.4	4.1
	SOMO35	A5.5	4.2
	AOT40 for vegetation <sup>(a)</sup>	A5.6	4.3
	AOT40 for forests <sup>(a)</sup>	A5.7	4.4
NO <sub>2</sub>	Annual average	A5.8	5.1
NO <sub>x</sub>	Annual average <sup>(a)</sup>	A5.9	5.2

<sup>(a)</sup> Rural map, applicable for rural areas only.

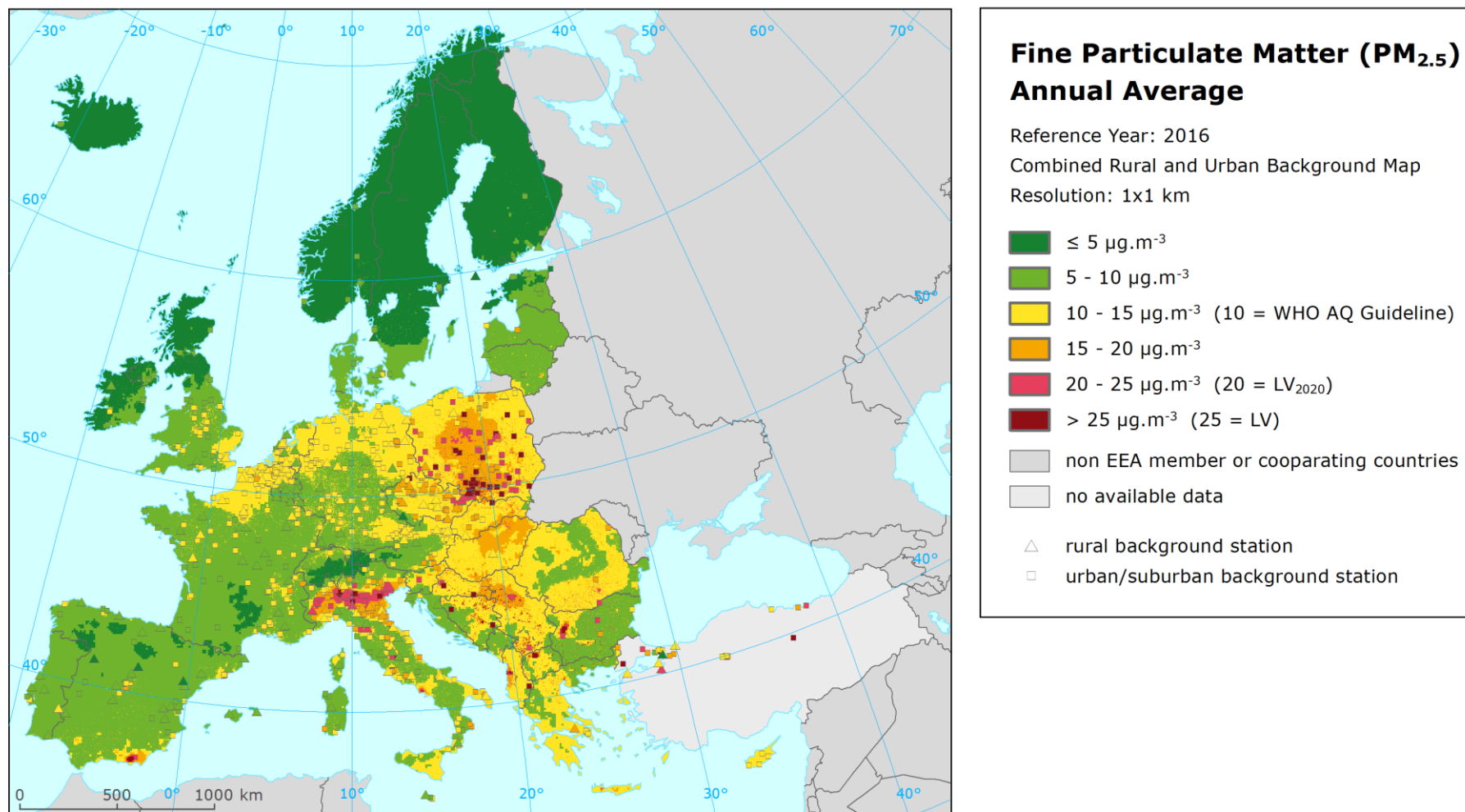
Map A5.1 Concentration map of PM<sub>10</sub> annual average including station points, 2016



Map A5.2 Concentration map of PM<sub>10</sub> indicator 90.4 percentile of daily means including station points, 2016

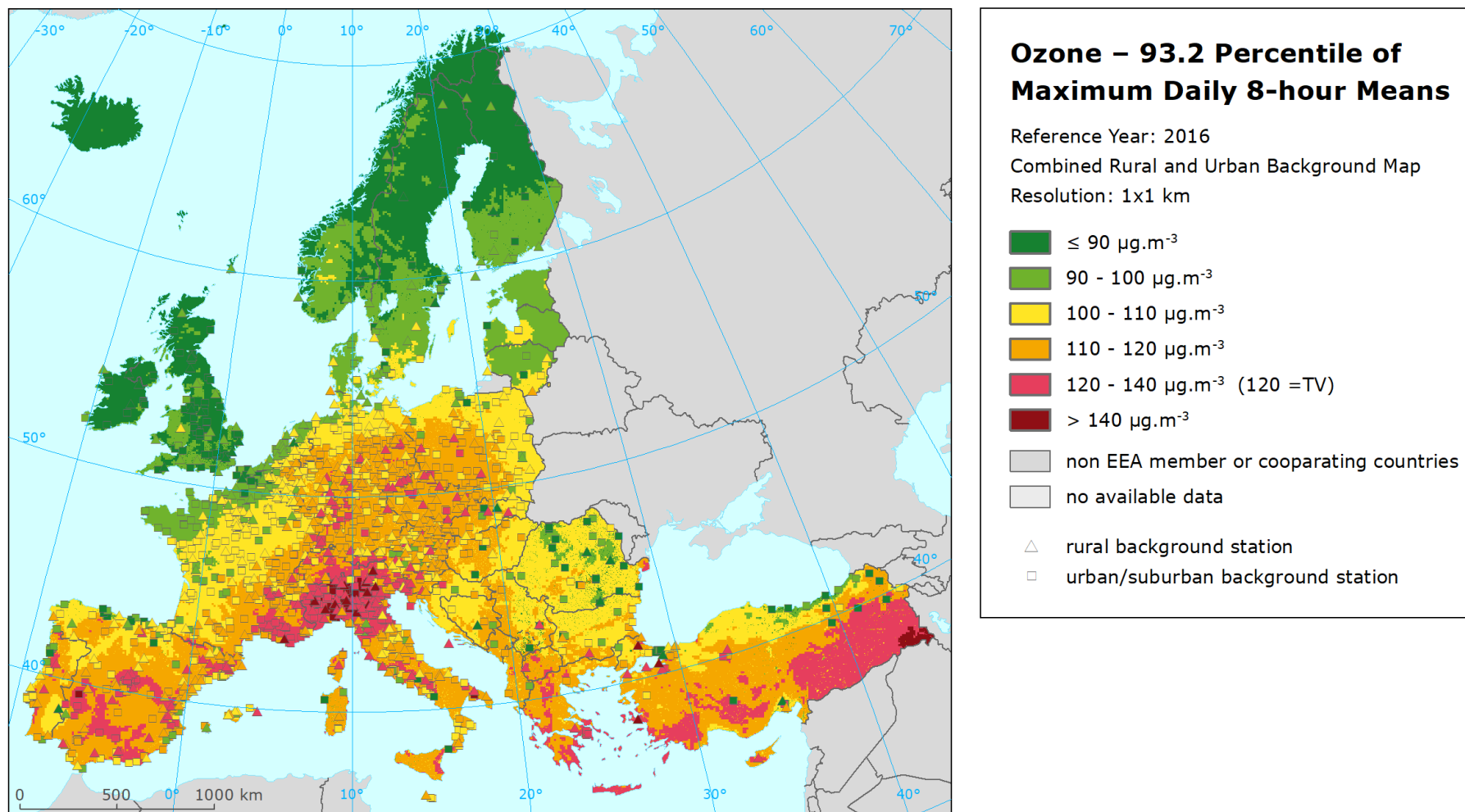


Map A5.3 Concentration map of PM<sub>2.5</sub> annual average including station points, 2016

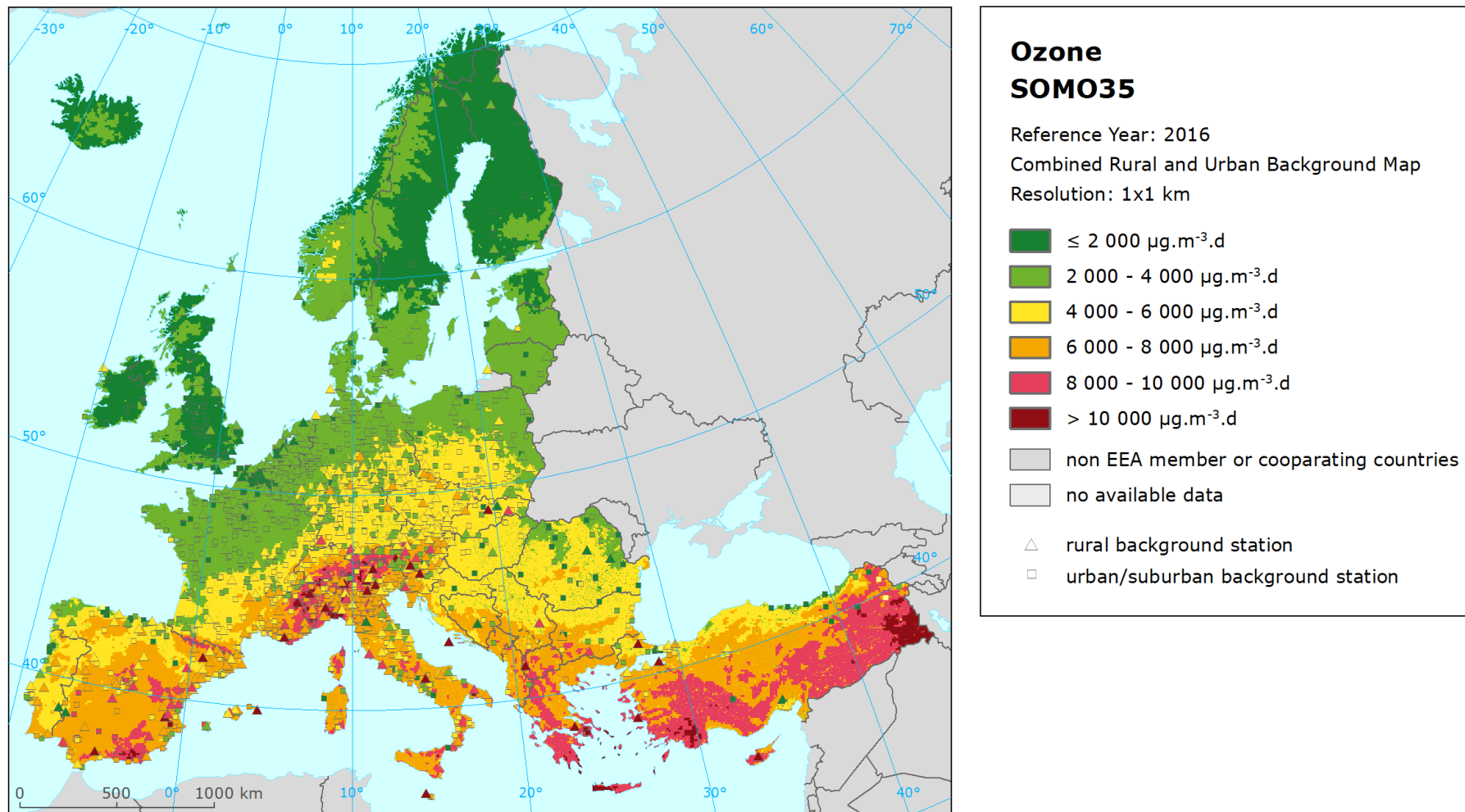




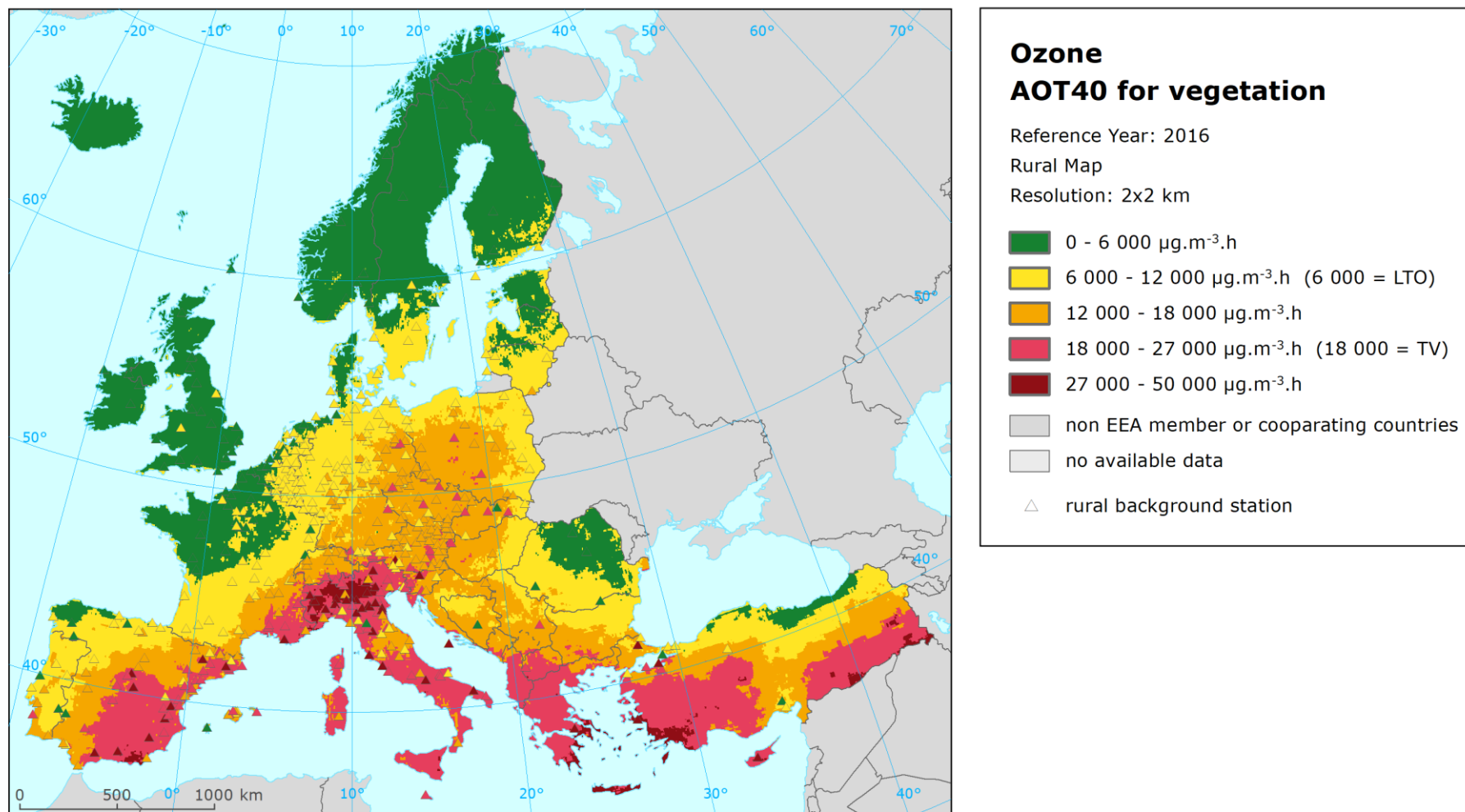
Map A5.4 Concentration map of ozone indicator 93.2 percentile of maximum daily 8-hour means including station points, 2016



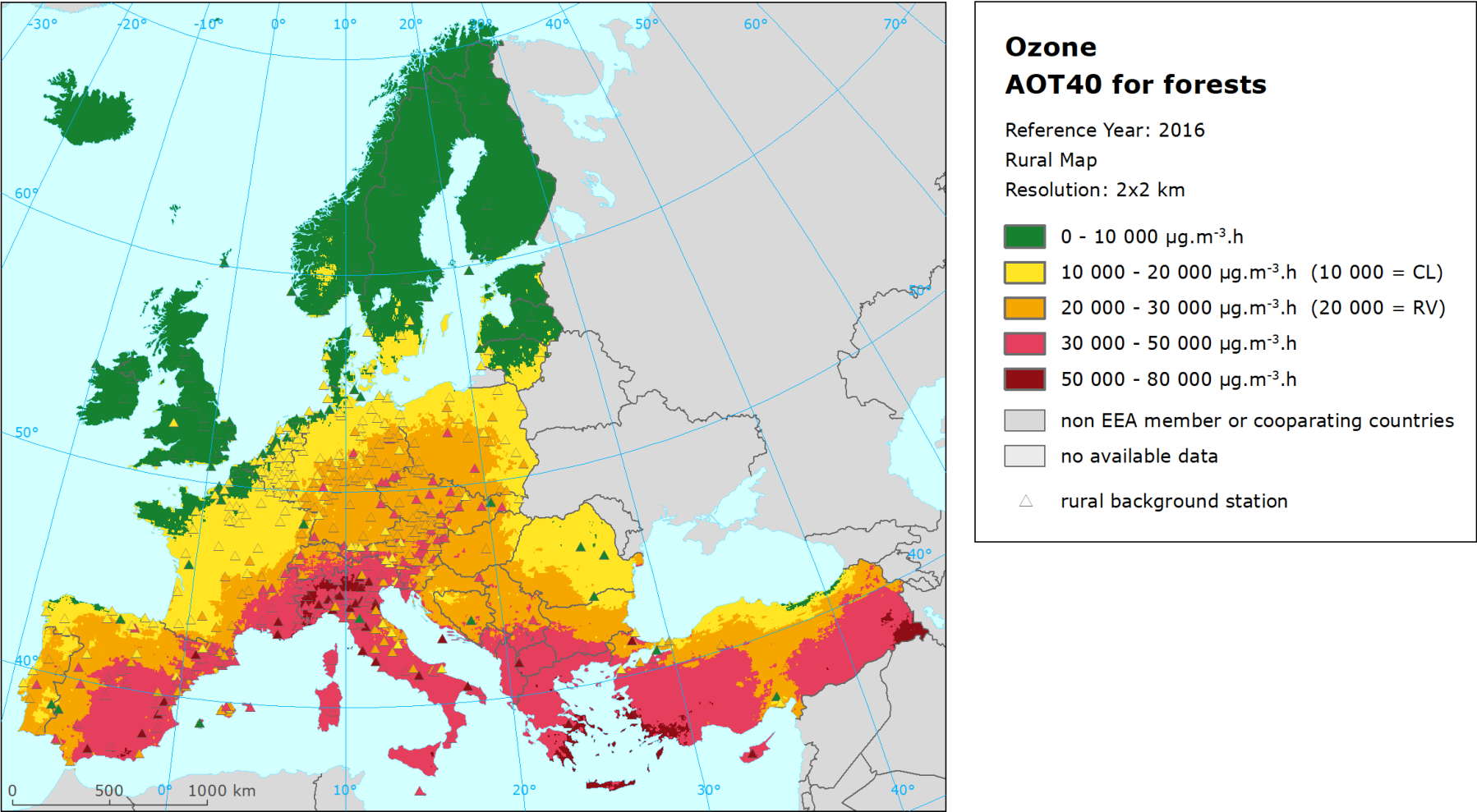
Map A5.5 Concentration map of ozone indicator SOMO35 including station points, 2016



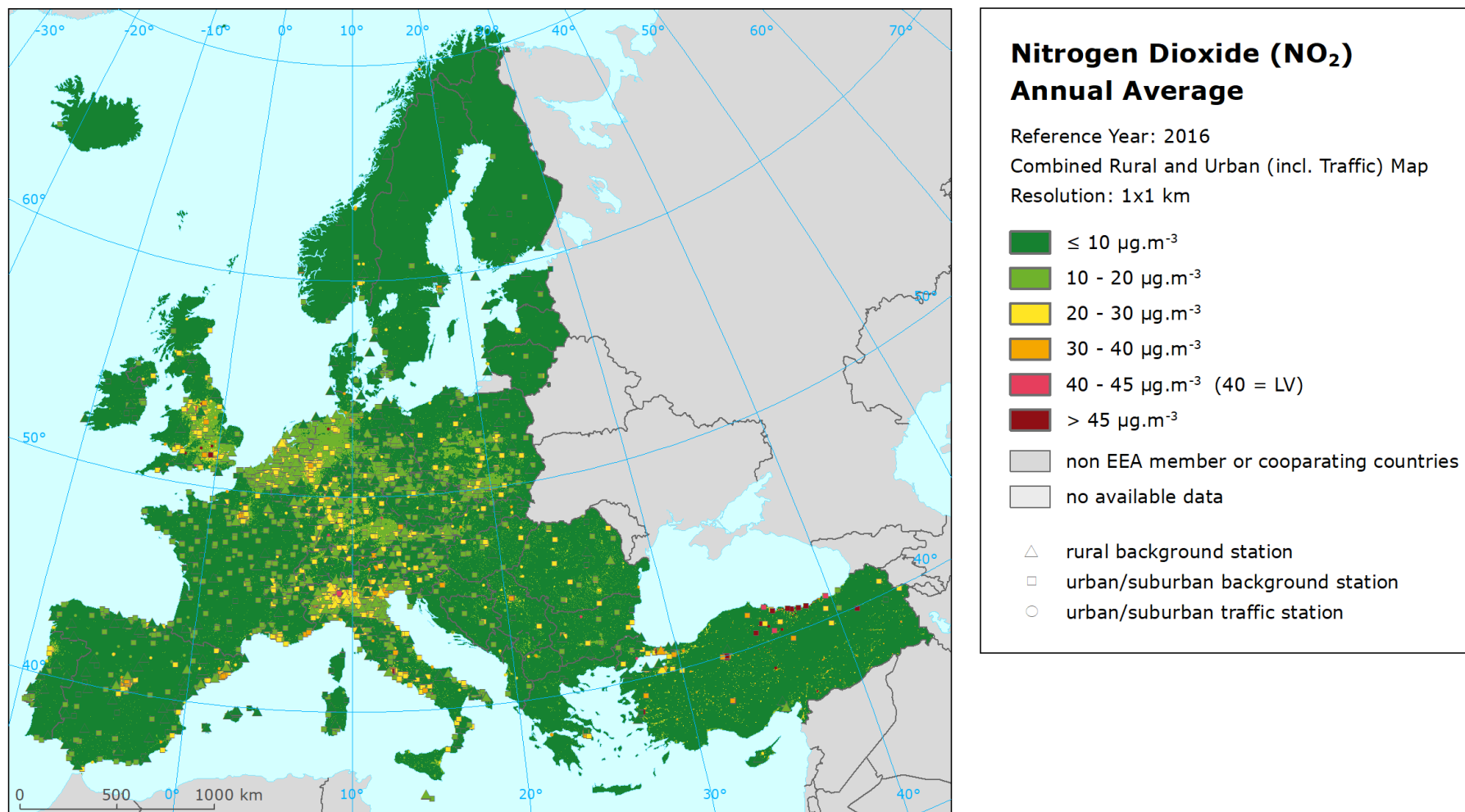
Map A5.6 Concentration map of ozone indicator AOT40 for vegetation including station points, rural air quality, 2016



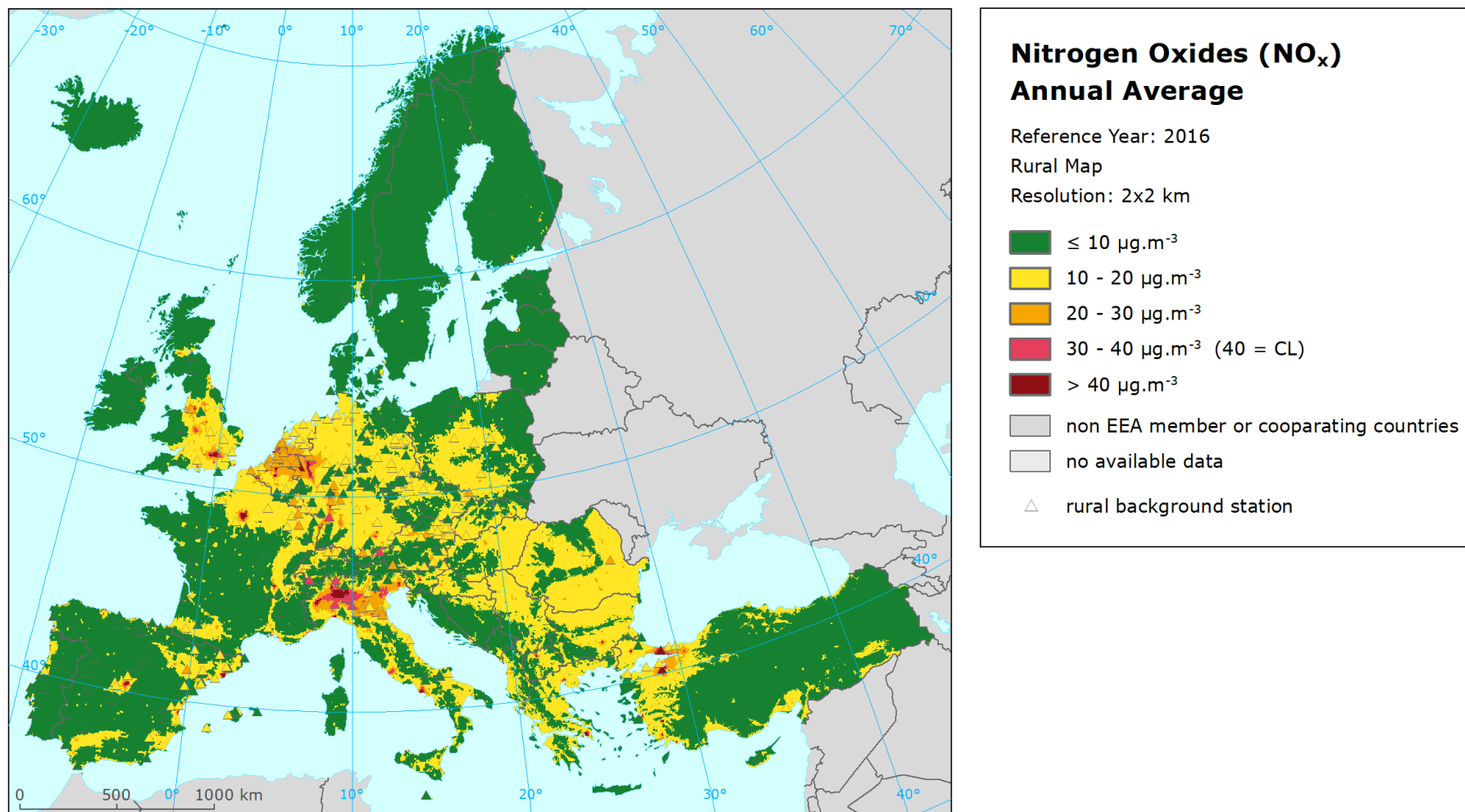
Map A5.7 Concentration map of ozone indicator AOT40 for forests including station points, rural air quality, 2016



Map A5.8 Concentration map of NO<sub>2</sub> annual average including station points, 2016



Map A5.9 Concentration map of  $\text{NO}_x$  annual average including station points, rural air quality, 2016



European Topic Centre on Air Pollution  
and Climate Change Mitigation

PO Box 1

3720 BA Bilthoven

The Netherlands

Tel.: +31 30 274 8562

Fax: +31 30 274 4433

Web: <http://acm.eionet.europa.eu>

Email: [etcacm@rivm.nl](mailto:etcacm@rivm.nl)

The European Topic Centre on Air Pollution and Climate Change Mitigation (ETC/ACM) is a consortium of European institutes under contract of the European Environment Agency.



European Topic Centre on Air Pollution  
and Climate Change Mitigation

PO Box 1  
3720 BA Bilthoven  
The Netherlands  
Tel.: +31 30 274 8562  
Fax: +31 30 274 4433  
Web: <http://acm.eionet.europa.eu>  
Email: [etcacm@rivm.nl](mailto:etcacm@rivm.nl)

The European Topic Centre on Air Pollution and  
Climate Change Mitigation (ETC/ACM) is a  
consortium of European institutes under contract of  
the European Environment Agency.

